Analysis of Soil and Land cover parameters for Flood hazard assessment;

A Case Study of the Nam Chun Watershed, Phetchabun, Thailand

Saowanee Prachansri

March, 2007

Analysis of Soil and Land cover parameters for Flood hazard assessment;

A Case Study of the Nam Chun Watershed, Phetchabun, Thailand

by

Saowanee Prachansri

Thesis submitted to the International Institute for Geo-information Science and Earth Observation in partial fulfilment of the requirements for the degree of Master of Science in Geo-information Science and Earth Observation, Specialisation: Geo-hazards

Thesis Assessment Board

Prof.Dr. V.G. Jetten (Chair)
Prof.Dr. S. de Jong (External Examiner)
Drs. D. Alkema (First Supervisor)
Dr. D. Shrestha (Second Supervisor)

Observer:
Drs. J.B. de Smeth (Programme Director)

INTERNATIONAL INSTITUTE FOR GEO-INFORMATION SCIENCE AND EARTH OBSERVATION
ENSCHEDE, THE NETHERLANDS

Disclaimer

This document describes work undertaken as part of a programme of study at the International Institute for Geo-information Science and Earth Observation. All views and opinions expressed therein remain the sole responsibility of the author, and do not necessarily represent those of the institute.

Abstract

Alterations of vegetation cover in upland catchment areas – like transformation of forest to agriculture - has an effect on the physical properties of soil, like the infiltration capacity. This influences the runoff characteristics in the catchment area which causes flooding in the down stream portion of the watershed. This study combined a physically based distributed hydrological model (LISEM) to model the catchment runoff and a one-dimensional and two-dimensional (1D2D) hydraulic model (SOBEK) to model the propagation of the flood wave on the downstream floodplain. The models were applied to assess the impacts of different land use scenarios in the Nam Chun watershed, Phetchabun province in Thailand. Soil physical properties were assessed in relation to different land cover types. In upstream catchment runoff model, model parameter which derived from the field measurement were assigned as input data in LISEM such as saturated hydraulic conductivity, initial moisture content and canopy cover. The calibration and validation of the LISEM model were done base on a visual judgement by comparing the simulated and the observed hydrograph. Sensitivity assessments were carried out to identify parameters that have the largest influence on the surface runoff models prediction. The calibrated hydrographs from LISEM were used as upstream boundary condition in SOBEK model. The flood depths of the typhoon Usagi on 2001 are used to assess the accuracy of flood depth prediction by comparing to simulated model using objective function. Analysis of the results revealed that land use change played an important role in intensifying the flood process. The impact of land cover types on the runoff generation was revealed by hydraulic conductivity measurements that show significant differences between different land cover types, especially between agricultural land use and natural vegetation. Decrease of forest areas and increase of agricultural land increased the peak-runoff and decreased the runoff confluence time. This results in an increase of the flood extent downstream. For instance for a storm with a return period 1 to 2 years and the whole catchment transformed to cornfields, the peak discharge increases six times compared to the present situation and the confluence time is reduced by 3 hours. Scenarios were generated under various land uses and coverages to estimate runoff. Under 100% forest cover, the peak discharge is reduced to approximately 76% and the confluence time increases with 2 hours. When the land cover was changed to 100% corn cultivation, the maximum flood water depth downstream increased 3 times and the spatial flood extent on the floodplain increased more than 4 times. For a storm with a return period of 1 to 2 years, there would be no flood downstream if the entire upland area became forest.

It is concluded that upstream land cover changes have a significant effect on downstream flood problems and that these kinds of studies are useful for alternative land use plans in the uplands and for floodplain management in the lowland areas.

***Keywords**: LISEM model, 1D2D hydraulic model, SOBEK, Scenarios.*

Acknowledgements

First of all I would like to express my gratitude to the Land Development Department, Thailand for granting me with this scholarship which allows me to continue with my studies. Special mention to Mr. Phitoon Kadeetum who did all efforts in bringing me here.

Speacial thanks for my supervisors Drs. Dinand Alkema and Dr. Dhruba Shrestha for their valuable support, kind advises, comments and particularly their enormous encouragement not only eased my pressure but also contributed a lot to improve the quality of the work.

Deep acknowledgement to all Earth System Analysis staff members particularly: Prof. Jetten, who advises me about LISEM model and also guidelines fieldwork methods.

Especial thanks go to all my classmates who gave me company and a lot of happiness throughout this period: PeePook, Sisay, Ephrem, Martin, Nongwaew, Maria, Alidu, Mulugata, Data, Shree, Amare and Shahjahan.

To all my friends and colleagues in Thailand who despite the distance their support loves, care and friendship were valuable and unforgettable.

Finally, most important of all, I would like to express my heartiest thanks to my parents who passed away before I got this opportunity for my MSc. but they are always in my heart. I dedicated this work to my lovely parent. Thank you for your love that you gave me all good things to make me what I am.

Table of contents

List of figures

List of tables

List of Abbreviations

1D	One-dimensional
2D	Two-dimensional
CREAMS	Chemical, Runoff and Erosion from Agricultural Management System
DEM	Digital Elevation Model
DSM	Digital Surface Model
DTM	Digital Terrain Model
EUROSEM	European Soil Erosion Model
GPS	Global Positioning System
HEC-RAS	Hydrologic Engineering Centers River Analysis System
KINEROS	KINematic Runoff and EROSion model
LDD	Land Development Department, Ministry of Agriculture and Cooperatives, Thailand
LISEM	Limburg Soil Erosion Model
USDA	United States Department of Agriculture
WEPP	Water Erosion Prediction Project

1. Introduction

1.1. Background

Floods are probably the most recurring, widespread, disastrous and natural hazard. Adverse impacts include loss of life, property damage, contamination of water supplies, loss of crops, and social dislocation and temporary homelessness. One of the causes of floods is heavy rainfall that exceeds the absorptive capacity of soil and the flow capacity of rivers. Flood disasters are often increased in intensity and severity by deforestation, poor drainage condition, and land use changes that increase agricultural activities and urbanization. All of these activities contribute to increased rates of runoff and higher flood peaks.

The frequency of flash floods seems to have increased during the past half century in many parts of the world (Wiskow and van der Ploeg, 2003). Flash floods are a major threat to human life and infrastructures and the damage is much more severe than normal floods (Foody et al., 2004). This is because flash flooding happens at much faster rates than regular floods. They are distinguished from other types of flooding by the short time scales over which flood-producing rainfall occurs within a few hour and over small spatial scales (O'Donnell, 2002). Flash floods are very short-lived floods lasting from several hours to a few days (Choudhury et al., 2004).

Flooding, both riverine floods and flash floods have damaged life and property since the earliest inhabitants settled in Thailand. Flash flooding is common during the Monsoon season (June to October). Flash flood events are usually generated by heavy convective precipitation over a relatively small area. Additional important factors that play a major role in their occurrence include catchment morphometry, initial soil moisture content and infiltration capacity of the soil. To better understand these issues, a more pragmatic look at the actual factors contributing to the flooding process is needed for instance the alteration of flow paths, sealing of soil surfaces and other human activities that alter land cover which affect the physical properties of soils. Such activities are considered to be a possible cause for changes in runoff peak flow behavior and this subsequently affects the magnitude of flooding in lowland areas. To better understand how these changes affect flood characteristics downstream, it is necessary to analyse and quantify how soil physical properties influence the volume of runoff from a catchment area and changes in land use influence the characteristics of flash flooding.

1.2. Statement of the Problem

This study focuses on The Nam Chun watershed, located in Phetchabun Province, Thailand. In this northern central province, extensive deforestation has occurred over the last decades. This mountainous area originally was characterized by dense tropical forest that has been exploited by local farmers. The primary rainforest was replaced by maize cultivation, the main crop in the area. Cultivation on steep slopes and the removal of the natural vegetation has exposed the soils to heavy

tropical rainfalls. Furthermore improper land use practices in agricultural areas have resulted in severe problems of land degradation in the watershed. Not only is the watershed losing large quantities of valuable topsoil, thereby depleting soil nutrient and reducing its agricultural yield, but the flood plain to which the watershed contributes is faced with sediment deposition and frequent problems of flooding. For example, the heavy rains of 11 August 2001 after Typhoon Usagi swept through the area, causing landslides in highland areas, and flooding in lowland areas. These floods and landslides resulted in heavy loss of human lives and destruction of property. Large landslides tore down the mountainside, uprooting vegetation and burying seven villages under two metres of water and mud. At least 120 people died and over 1,000 people made homeless (Conachy and Divjak, 2001).

Rapid alterations of vegetation cover for agricultural use have had a negative effect on the hydrological processes of the upper watershed. It is hypothesised that these changes in vegetation cover also affect the physical properties of the soils like the infiltration capacity. This in turn influences the runoff characteristics in the upper catchment. Increased runoff volumes in a short time cause severe flooding in the down stream portion of the watersheds. In order to investigate the influence of land use on runoff processes on the catchment scale, the use of hydrologic models combined with hydrodynamic modelling make it possible to predict hydrologic process and watershed behaviour under various conditions of land use. In this way different areas of watershed can be modelled separately and various scenarios can be generated and flood waves can be computed for these scenarios.

1.3. Objectives

The main objective of this research is to assess the causes of flash flood hazard at downstream areas of the Nam Chun watershed, taking into account the influence of soil and land cover parameters upstream. The specific objectives of the research are the following:

- To assess the effects of different land cover types on soil properties
- To assess the effect of soil parameters in influencing runoff
- To assess the downstream consequences in terms of flood hazard by linking the upstream catchment runoff model with a downstream 1D2D-flood model

1.4. Research Hypothesis

- Different land use/ cover types can result in different rates of infiltration due to changes in the physical properties of the soil of upstream chatchment areas
- Changes in land use/ cover characteristics of upstream catchment areas can influence the rate of runoff and flood characteristics
- An integrated modelling approach is a suitable technique to quantify the rate of runoff and flood characteristics
- Upstream land cover changes affect the downstream flood hazard

1.5. Research Questions

The general question of this research is How does land cover change affect runoff behaviour in an upstream catchment area and how does this affect downstream flood hazard? The specific questions are the following:

- Which land use/ cover types result in the generation of high surface runoff
- Which soil physical properties related to surface runoff generation change due to change in land use/cover types?
- What are the significant changes in flood behaviour in low lands if there are upstream changes in land use/cover?
- Which areas are considered hazardous for certain return period of flash flood event?
- How sensitive are the runoff models with changes in some model parameters?

1.6. Structure of the Thesis

The thesis consists of nine chapters:

Chapter one identifies the research problem emphasising on the need for this study. The objectives, hypothesis and the research questions to be answered by this study are given.

Chapter two contains explanation in research procedure on the study area and briefly description on primary and secondary data collecting during fieldwork.

Chapter three covers literature reviews discussing the background on the theoretical aspects on each topic that crucial for this study. In general, this chapter is divided into four main subtopics; runoff and surface runoff in cathment, Runoff modelling, Hydrodynamic Modelling, Flood Hazard assessment and Mapping.

Chapter four, a description of the study area is given mentioning among others its location, climate, soil characteristics and geology.

Chapter five, focus on the analysis of soil data relate to different land cover types and analyse the relationship between soil properties in order to support the modelling approach. The results are discussed in each step.

Chapter six illustrates the runoff model application in this study, discusses the procedures used in preparing the input maps and the parameterisation of the parameters required is mentioned. The analyses on the results of the model prediction are discussed. Model calibration and validation are performed in order to increase accuracy model prediction. Model sensitivity analysis and the results are discussed in this chapter.

Chapter seven deals with flood modelling aim at simulating flood behaviour in downstream under different scenarios land cover change in upstream part. Detailed explanation focuses on parameters

used in flood modelling, for instance DEM generation, boundary condition, surface roughness and etc. Moreover, the results of the model calibrations are also discussed.

Chapter eight contains analyses on the effects of land cover change in upstream catchment that influence the flood behaviour in downstream part. The impact assessments based on flood characteristics include maximum flood depth, maximum flow velocity and flood inundation areas. Finally, flood hazard map with consideration of the frequency of event is created for flood event in present situation and in each scenario.

The final chapter find conclusions on the results of the study, recommendation and limitations of the study.

2. Research Procedure

In order to meet the objectives of this study, the overall work was divided into three main phases; the pre-fieldwork phase, the fieldwork phase and the post-fieldwork phase. The overall research methodology illustrate on Figure 2-1.

2.1. Pre-fieldwork phase

In this stage of the study, the information from literatures was reviewed and research questions were formulated, methods on how to collect primary data required for the study were outlined. These included methods on soil data collection, discharge measurements, land use and land cover assessments. Alongside this, previously collected data in the area was gathered in order to avoid repetitions in primary data collection.

- The Pre-fieldwork phase of the study involved; literature review, selecting a suitable research approach, formulation of the research question.

- Fieldwork preparation involve with identification of methods and preparation of materials for field data collection, production of land cover map, data requirement assessment which includes gathering and organisation of available data from previous studies in the Nam Chun Watershed and investigation on the additional data that needs to be collected during the fieldwork. The list of the new data requirement was prepared based on this and also the research objectives and research questions.

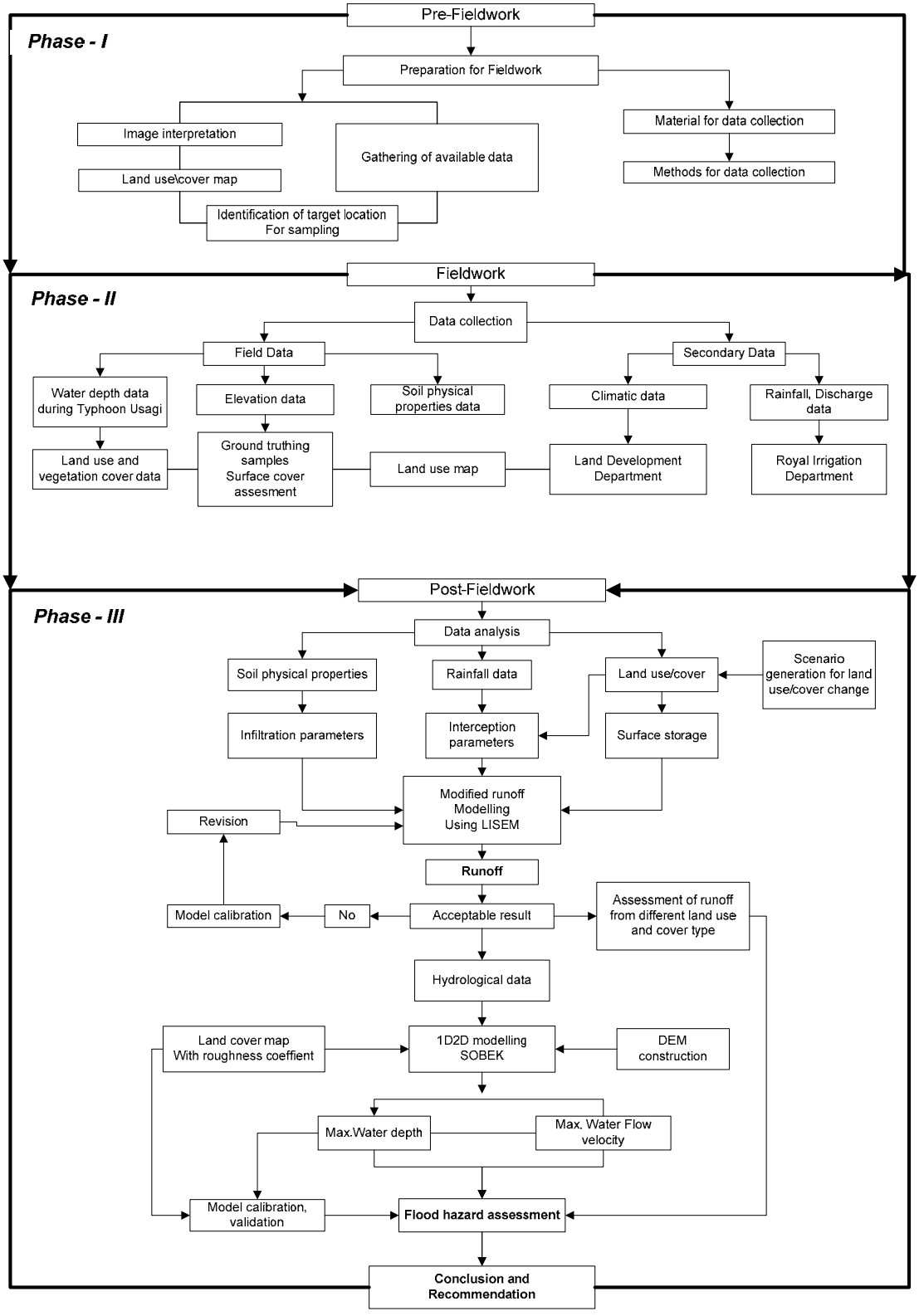

Figure 2-1: Flow chart showing the research approach of the study.

1. Available data

    a. Elevation datasets with contour interval 1 meters and height point at downstream and contour interval 10 meters at upstream were obtained from Land Development Department (LDD).
    b. A digital Land use or Land cover map for year 2004 at upstream was obtained from Land Development Department (LDD).
    c. Ortho-photo mosaic of the study area obtained from Land Development Department (LDD) with scale of 1:4000.
    d. A digital soil map based on geo-pedological approach was obtained from Solomon's research in 2004 at upstream.
    e. Climatological and daily rainfall data from Royal Irrigation Department
    f. Topographic maps of map sheets 5242I, 5242III, 5242IV, 5243II and 5243III scale 1:50,000.

2. Required data

    a. Event-based rainfall data for rainfall-runoff base simulation.
    b. Soil physical properties such as infiltration, hydraulic conductivity, soil moisture content, soil porosity, etc.
    c. Discharge and water level at upstream and downstream outlet
    d. River cross section data
    e. Water depth for flood caused by the Typhoon Usagi (2001) that useful for flood model validation

2.2. Fieldwork phase

The fieldwork phase of the study involved collection of primary and secondary data and took place in September 2006. Primary data collection included collection of manmade terrain elevation data (road network) in the watershed using GPS, physical soil properties measurement (infiltration rate, hydraulic conductivity, soil water etc.), collection of training samples for land use and land cover mapping, discharge measurements from strategic locations during rainstorms, cross sectional measurements along the river Huai Nam Chun and gathering of climatic data and hydrologic data. Secondary data collection in involved visits to various offices including the metrological station in Lom Sak, the Land Development Department (LDD) and the Royal Irrigation Department in Bangkok.

2.2.1. Primary data collections

The collected data in the field divided in 5 main groups as follow:

(a) Land use data

It was divided into two parts: the upper catchment and the downstream area. The land use map of the upper catchment was derived from Land Development Department, Thailand which is produced in 2004. In downstream area, the land use map was based on the interpretation of the orthophoto of 2002 with a scale of 1:25000. The interpretation was verified in the field using GPS and the map was updated.

(b) Event based Rainfall data and discharge data at sub-catchment

Rainfall data was colleted within the upper catchment area by using home-made raingauge with known diameter. The volume of the water collected was measured by making use of the graded measuring cylinder. The discharge of a subcatchment was derived from water depth measurements at a location with a known profile using Manning's formula.

(c) Soil physical properties

Soil samples for analysing soil physical properties such as hydraulic conductivity, bulk density, soil moisture content and particle density were taken by making use of a core sampler of known volume. A total of 59 samples were taken with undisturbed soil using a satisfied sampling method

(d) Cross section data, Boundary condition data, Embankment data, Road network elevation data

Downstream in the main valley, the cross sections of Hui Nam Chun river and embankment height were measured with measuring tape. The elevation of the road network was collected using a GPS and height difference estimates (figure 2-2).

Figure 2-2: Cross section, boundary condition, embankment, road network observation.

(e) Interviewing flood water depth

The information on floodwater depth during the typhoon Usagi(2001) was obtained by interviewing the people who live along the Namchun river in the low land area includes the villages such as Ban Nam Chun, Ban Nam Om, Ban Kok O, Ban Non Thong and Ban NamDuk. The information includes water depth, flood duration and time. About 50 points were recorded using GPS at each village along the river.

2.2.2. Secondary data collections

Besides to the data collected in the field, the existing data on discharge, water height at upstream main outlet Ban Fai Wang Bon recorded from 1998 to 2006 and rainfall recorded from 2005 to 2006 based on daily and hourly basis was obtained from the Royal Irrigation Department. In addition, the data on soil properties from previous studies was also gathered for those parts of the catchment where no sample was taken (Solomon, 2005).

2.3. Post -fieldwork phase

The final phase of the study involved the assessment of relationships between soil physical properties and land use, simulation of runoff and modeling of flood propagation in the downstream area. Different scenarios based on land use changes in the catchment were assess the flood hazard in lowland area

3. Literature review

3.1. Runoff and Surface runoff in catchment

Runoff or streamflow comprises the gravity movement of water in channels which may vary in size from the one containing the smallest ill-defined trickle to the ones containing the largest rivers. Runoff is referred to as stream or river discharge, or catchment yield, and is normally expressed as volume per unit. Runoff may also be expressed as a depth equivalent over a catchment (Ward and Robinson, 1990).

Runoff, also called overland flow, is generated by the topographic flow of water from precipitation to stream channels located at lower elevations. Runoff occurs when infiltration capacity of soil has been exceeded. It is also refered to as the water leaving an area of drainage and flowing across the land surface to points of lower elevation. Runoff characteristics can be affected by several factors including soil type, vegetation, drainage area, basin shape, elevation, slope, direction of slope orientation, drainage network patterns, presence of ponds, lakes, reservoirs, sinks, etc. in the basin, which prevent or alter runoff from continuing downstream (USGS, 2005).

Surface runoff or overland flow is that part of stream flow which originates from rain and fails to infiltrate the mineral soil surface at any point as it travels over the land surface to channels. Surface runoff usually occurs when the rainfall intensity exceeds the initial demands of interception, infiltration and surface storage (figure. 3-1). It varies during the rain storm and may cease either during its occurrence or shortly after its cessation. As surface runoff flows toward the watershed outlet, a portion of it can infiltrates into the soil or channel bed; the infiltration taking place in a channel is often referred to as transmission losses.

Surface runoff is that portion of precipitation which, during and immediately following a storm event, ultimately appears as flowing water in the drainage network of a watershed (Hann et al., 1982). During a rainstorm, the distribution of precipitation falling on the ground surface can be modified by the presence of vegetation. A portion of the rain is intercepted by the vegetation canopy. Another portion of rainwater that falls through the vegetation directly onto the soil without being intercepted is called throughfall. Some of the intercepted rainwater either evaporates from the vegetation surface or when the canopy storage capacity is exceeded, intercepted rainwater falls from the leaves through branches to the ground as leaf drainage or stemflow (Morgan, 1995; Rientjes, 2004). The amount of rainwater that is lost due to interception depends on branching structure and leaf density of the vegetation cover and the rainfall pattern (Dingman, 2002).

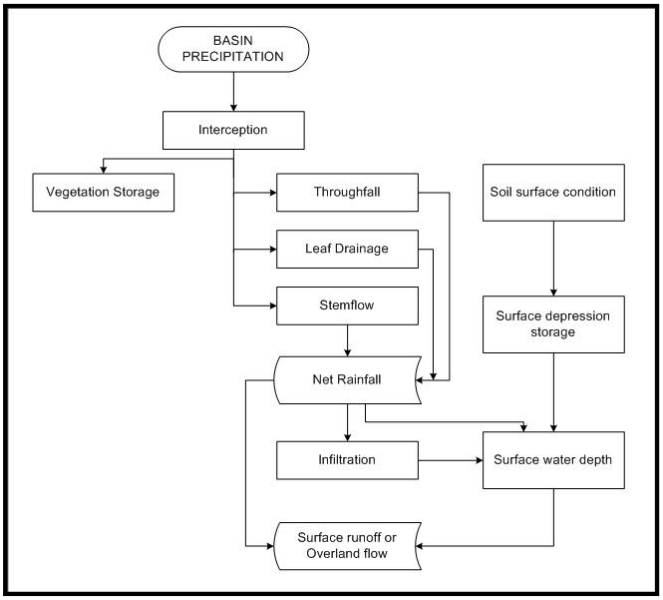

Figure 3-1: Modified diagrammatic representation of surface runoff process (Morgan et al., 1998b).

As noted above, water can arrive at the soil surface either directly as precipitation or indirectly as drip and stemflow from plants. This water can either remain as surface depression storage, or it can infiltrate into the soil. When the rate of rainfall exceeds the rate at which water can infiltrate the ground, and depression storage has been filled then, the excess water at the surface flows along its gravitational gradient as surface runoff. This process is referred to as Hortonian overland flow (infiltration excess overland flow) or unsaturated overland flow. On the other hand, when the soil is saturated, e.g. a previous rainstorm event and the rain continue to falls, infiltration capacity of the soil is full, the depression storage is filled. In this case, the rainfall will immediately result in surface runoff. This is referred to as saturation excess overland flow (Beven, 2000; Ward and Robinson, 1990). In this study was determined on rainfall excess or direct runoff, which is the water that eventually becomes flood runoff, being generated at the surface as Hortonian runoff and saturated overland flow (Maidment, 1993).

3.1.1. Soil pproperties in relation to surface runoff

Regarding the generation of surface runoff the infiltration rate is the most sensitive variable. It is a key component that significantly influences the rainfall-runoff process and plays an important role in controlling the amount of water that will be available for surface runoff after a rainstorm event (Morgan, 1995). Infiltration refers to the downward entry of water from the surface into the soil profile. It is controlled by gravitational forces, capillary action and soil porosity (Rattan, 1990; Ward and Robinson, 1990; William et al., 1991). The amount of water that infiltrates the ground varies widely from place to place. A number of factors affecting the infiltration rate include soil properties (including texture, structure, organic matter content, soil moisture content, pore size distribution), the amount and characteristics of precipitation (intensity, duration, etc.), topography or slope gradient, management factors - e.g. cropping pattern, vegetation, land or surface cover (Aimrun et al., 2004; Celik, 2005; Giertz et al., 2005; Rivas, 2005; Stolte et al., 2003; Ward and Robinson, 1990).

The soil factors influencing the rate of infiltration are: the total amount of pores (soil porosity), the particle size distribution and the structure of pores (grain size distribution), soil structure (size distribution and structure of aggregates) and organic matter content of the soil(Juo and Franzluebbers, 2003; Wischmeier et al., 1971; Yamamoto and Anderson, 1973). Coarse textured soils have large well-connected spaces between the grains and therefore allow for more water to infiltrate through it quite rapidly. Fine-grained soils dominated by clay have low infiltration rates due to their smaller sized pore spaces. Pores and fissures found in soils can be made larger through a number of factors that enhance internal soil structure. Soil containing large amount of the sand and silt tend to form crusts and become compacted, which significantly reduces the infiltration rate. The amount of organic matter found at the soil surface can also enhance infiltration because organic matter is generally more porous than mineral soil particles and it can hold much greater quantities of water (Pidwirny, 2006). Moreover, soil with low organic matter content are more easily compacted than those with high organic matter content under similar climatic condition that lead to less pores space between soil grain (Rattan, 1990)..

Infiltration during a runoff-generating rainfall event is regulated by the hydraulic conductivity, or the ability of a soil to transmit water. The hydraulic conductivity depends mainly on the geometry and distribution of the soil pore spaces. In general, sandy soils have higher saturated hydraulic conductivities than finer textured soils because of the larger pore space between the soil particles. As such, the infiltration rate of clayey soils is much lower than that of sandy soils (Maidment, 1993; Ward and Robinson, 1990). Porous soils with stable soil aggregates have higher saturated hydraulic conductivity values than soils that are compact and dense (Hillel, 1980). However, Bouma (1981) reported poor relationships between such descriptions and hydraulic properties in structured clay soils due to the complexity of soil pattern.

3.1.2. Land use changes in relation to surface runoff

Changes in land cover can result from a wide range of land management practices, including soil improvement methods, choices of crops, etc. External drivers include processes such as industrialization, urbanization, transport infrastructure development, population growth and migration and the globalization of markets and economies. The impacts of land use changes have received considerable attention from several studies, particularly with respect to effects on hydrological processes (Brath et al., 2006; Giertz et al., 2005; White and Greer, 2006).

Land use changes in a watershed can impact water supply by altering hydrological processes such as infiltration, groundwater recharge, base flow and runoff. Several studies reported that agricultural land use results in lower infiltration rates than natural vegetation, which result in higher surface runoff (Giertz and Diekkruger, 2003). Modifications of the land surface have varying effects on the runoff characteristics of a given drainage area. Deforestation followed by intensive agricultural practices particularly on mountainous sloping lands has caused degradation of watershed ecosystems. Intensified agricultural practices damage the ground cover and surface soil which resulted in decreased water infiltration capacity and leading to increase in the rate of surface runoff (Deng et al., 2003; Niehoff et al., 2002; Siriwardena et al., 2006).

Vegetation can play an important role in infiltration and can slow the movement of runoff, allowing more time for it to seep into the ground. The surface soil layer in a forest or a pasture will generally

have a far greater infiltration capacity than on a paved parking area or a compacted soil surface at a construction site. Impervious surfaces, such as parking lots, roads, and developments, act as a "fast lane" for rainfall - right into storm drains that drain directly into streams. Urbanization increases surface runoff, by creating more impervious surfaces such as pavement and buildings that do not allow percolation of the water through the soil to the aquifer (White and Greer, 2006). Agriculture and the tillage of land also change the infiltration patterns of a landscape (Takken et al., 2001).

3.1.3. Land use changes in influencing soil physical properties

Land use changes in a watershed can impact streamflow by altering hydrological processes such as infiltration. The infiltration capacity of a given soil is affected by the type and density of the vegetation cover, as demonstrated by the numerous studies reviewed by Dunn (1978), Faulkner (1990) and Ziegler (2004). Thornes (1990) proposes that infiltration capacity increases exponentially with increasing vegetation and increasing percentage of organic matter and decreases in the bulk density of the soil. Such a relationship is similar to that developed by Holtan (1961) to express the saturated hydraulic conductivity of the soil as a function of the percentage area of the vegetation.

Vegetation cover creates more porous soils by both protecting the soil from pounding rainfall, which can close natural gaps between soil particles, and loosening soil through root action. The root-system of plants may have an effect on the amount of pore space (Van Asch, 1980). It has an important role in maintaining the structure of the soil. Plant roots increase the pore space along the lines occupied by roots and dead leaves provide litter that keeps up the organic content of the soil. Loss of soil organic matter with cultivation is connected to destruction of macroaggregates (Elliott, 1986; Tisdall and Oades, 1982). Pore size distribution and connectivity together with bulk density, aggregation and aggregate stability is important soil physical property that can be influenced to great extent land degradation due to cultivation. Because of its effect on soil physical properties by decreasing soil porosity and soil aggregate stability, increasing bulk density and reduced hydraulic conductivity (Cerda, 1996).

Dense vegetation during periods of high rainfall not only protects the soil surface from the impact of raindrops and formation of surface crusts, but also encourages the activity of earthworms and protects the soil structure. Loosening up of soil crusts or avoiding their formation by keeping the soil surface covered with plant residues can greatly increase water infiltration rates. This is why forested areas have the highest infiltration rates of any vegetative types (Giertz et al., 2005; Sullivan, 2004). Clearance of forest for agricultural production reduces the effect of roots and input of organic matter into the soil which results in a reduction in the infiltration capacity of the soil (Schwab et al., 1981). Agricultural land use has a negative effect on the abundance and activity of soil organism due to the mechanical destruction of organisms and soil structure as well as a decrease in letter (Edwards and Bohlen, 1996). The reduced abundance and activity of soil fauna influence soil physical properties, mainly the permeability.

Water infiltration of a soil can be influenced to some extent by soil and crop management practices. Removal of vegetation exposes the bare soil and inappropriate tillage operations generally reduce the infiltration rate because it reduces the number of macropores and enhances surface sealing. This prevents water from passing into the soil (Hillel, 1980; Schwab et al., 1981; White, 1997).

3.2. Runoff Modelling

Runoff models can be regarded as stochastic or deterministic (Ward and Robinson, 1990). Stochastic models take into consideration the chance of incidence or probability distribution of the hydrological variables, whereas deterministic models simulate the physical processes operating in the catchment to transform precipitation into runoff.

A stochastic model treats the sequence of events that it comprehends as time-dependent. Traditionally, a stochastic model is derived from a time series analysis of the historical record. The stochastic model can then be used for the generation of long hypothetical sequence of events with the same statistical properties as the historical record (Beven, 2000).

Deterministic models focus on the simulation of physical processes involved in the transition from precipitation to runoff. It can be classified according to whether the model gives a lumped or a distributed description of the considered area, and whether the description of the hydrological processes is empirical, conceptual, or more physically-based. Most conceptual models are also lumped, and most physically-based model are distributed (Beven, 2000).

Physically-based models are mathematical models that represent the physical basis underlying the hydrological system by a series of equations (Wilby, 1997). They represent all the relevant processes in the hydrological system under consideration in a physically meaningful way. An understanding of physical processes allows the prediction of the behaviour of the system under any set of conditions. Because physically based models determine system behaviour based on physical processes and measurable system characteristics, it is theoretically possible to provide all of the input data required by the model directly from field and laboratory measurements. The disadvantage of such types of models is that they are complicated and demanding in their data requirement (Dingman, 2002; Rientjes, 2004).

In recent years there has been increasing emphasis on the development of physically based distributed models (Ward and Robinson, 1990). The rationale behind this development is that the model that treats the catchment as a spatially variable physical system has significant theoretical advantages that make it more useful, over a wider range of applications, than other type of model

In this study, the upper catchment determines the surface runoff which produces the magnitude of peak flow at the outlet. Thus, a model was used to simulate the surface runoff at catchment scale during excessive rainfall. Physics based simulation of surface runoff provides a key to quantitative modeling of peak flow and sediment at outlet. There has been much progress on this field in the previous decades. Beside some completely empirical approaches, several physically based models have been established such as WEPP (Lane and Nearing, 1989), CREAMS (Knisel, 1980), KINEROS (Woolhiser et al., 1990), EUROSEM (Morgan et al., 1998a) and LISEM (DeRoo et al., 1996). In this study LISEM is used. The model structure is described in section 6.1.

3.3. Hydrodynamic modelling-Couple 1D2D hydraulic model

Hydrodynamic models are driven by tidal, discharge, wave and meteorological forcing. Over the last decades, hydrodynamic modelling has become a frequently used tool for studies in hydraulic and environmental science and engineering (Bin Usamah, 2005). A wide range hydrodynamic modelling types are available today. The main distinction between different hydraulic model types is the number of dimensions in which physical processes are represented. This ranges from fairly simple hydraulic 1D models to complex 2D models, taking flow directions into account. Furthermore, linkage of a one-dimensional model system for open branches and closed culverts with a two-dimensional model system for inundation of rural and urban areas has been developed.

One dimensional hydrodynamic are widely applied for studying flood levels and discharges in river systems. As simple hydrological routing methods, 1D hydrodynamic model allow for rapid evaluation of distributed water levels and discharges in both dendritic and networked river system, considering effects such as backwater, advection and diffusion. In the one-dimensional models of river hydraulics are typically parameterised through a series of cross-sections of channel perpendicular to the flow direction and floodplain topography, which can be derived from ground survey at a reasonable cost. For some river reaches, such models have been shown to give good predictions of bulk flow properties and water surface elevations despite topography being limited to a small number of widely spaced cross-sections (Horritt et al., 2006). Several 1D hydraulic models are available these days such as HEC-RAS, which is described by the US Army Corps of Engineers and MIKE 11 from the Danish Hydraulic Institute (DHI). However, these models have problem in simulating water depth and water flow velocity when over-bank discharge occurs during flood events (Bin Abdul Rahman, 2006).

A wide range of two-dimensional hydraulic models have been developed for simulating distributed patterns of floodwater flow depth and depth-averaged velocity, to investigate the hydraulic characteristics of natural floodplains. Two-dimensional models consider flow directions in both horizontal directions, allowing calculation of more detailed water levels along the river, which results in better predictions of possible flooding and volumes of water leaving the main river channel. In addition, the water leaving the main channel can be routed through the levees or overbank flow based on the flow direction and changes to the flow direction. Applications of such models to natural river floodplains have varied in scale, both in terms of the length of the river reach considered and the spatial resolution of the model mesh or digital elevation model (DEM) used to represent the channel and floodplain topography (Nicholas and Mitchell, 2003). Hence, it becomes more popular in the flood modeling, especially in a complex topography of floodplain area. Among the popular 2D flood models are LISFLOOD, Telemac 2D, MIKE_21 and SOBEK model. The last 2 models are combined 1D and 2D flood models (Bin Abdul Rahman, 2006).

This combined modeling approach solves the problem of balancing the requirement for high resolution representation of main channel flow, against minimising redundancy on the floodplain. This hybrid model approach, specifically developed for modelling inundation events at the local scale (Werner, 2004) models the main channels using a one-dimensional hydrodynamic while overbank floodplain flow is modelled using a two-dimensional solution.

The couple 1D2D hydraulic model which is called "*Sobek 1D2D*" (WL-DELFT_HYDRAULIC, 2003), has been developed by WL | Delft Hydraulics. SOBEK is a fully dynamic 1D-2D hydraulic model, specifically designed for floodplain flood modelling. The floodplain area is represented by the 2D grid, either a DTM or a DSM, representing the terrain of the floodplain. The computation or solution used for the 2D floodplain modelling is based on the finite difference method. The SOBEK allows the integration between the 1D channel flows and the 2D overland flow. In the flood model the infrastructures, for instance bridge, etc. can be incorporated through the 1D module.

The SOBEK uses the full two-dimensional shallow water equations for describing floodplain flow in the main channel the flow is described using the full one-dimensional De Saint Venant equations. Both modeling systems produced implicit finite difference equations, which are also linked through an implicit formulation for joint continuity equations at locations where both modeling systems have common water level points (Asselman and Heynert, 2003), as shown in figure 3-2.

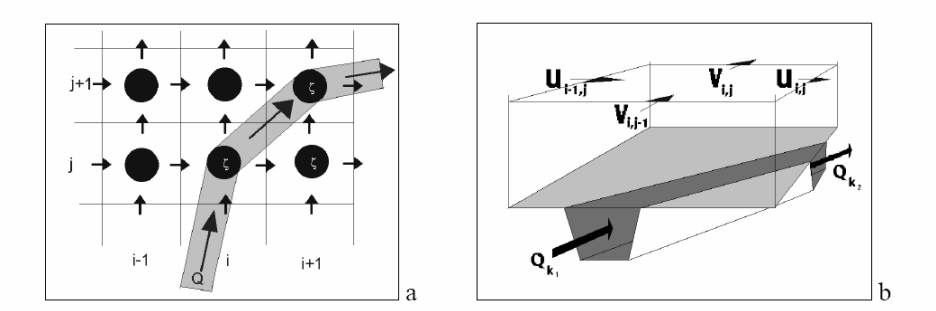

Figure 3-2: Schematisation of the Hydraulic Model: a) Combined 1D2D Staggered Grid; b) Combined Continuity Equation for 1D2D computations (www.sobek.nl).

3.4. Flood Hazard Assessment and mapping

Flooding is a natural process, which can be both beneficial to societies or cause damage. However, increasing population pressure and economic activities has led to the development of extensive infrastructures near the rivers, as the number and susceptibility of settlements increase, flooding increasingly becomes a natural hazard.

A natural hazard refers to the probability of occurrence of a potentially damaging phenomenon occurring within a given area and within a specified period of time (Alexander, 1993). It is a results from the potential for extreme geophysical events such as floods that can create an unexpected threat to human life and their environment (Smith, 1996).
Flood hazard is the threat to life and damage to properties and infrastructures. It varies in both time and space across a floodplain. "Flood result from a combination of physical exposure and human vulnerability to geophysical processes. Physical exposure reflects the type of flood events that can occur, and their statistical pattern, at a particular site, whilst human vulnerability reflects key socio-economic factors such as the number of people at risk on the floodplain or low-laying areas, the extent of any flood defence work and the ability of the population to anticipate and cope with hazard" (Smith and Ward, 1998).

Flood mapping is a widely used tool in the assessment of the types and extents of flooding over floodplains and in the development of planning instruments. The mapping of flood affected areas is a basic tool for flood hazard assessment (Casale and Margottini, 1999). The most important hydrologic and hydraulic variables relevant for flood hazard assessment are: meteorological data (rainfall depths and intensities), magnitude and frequency of flood peak discharges, characteristic of the flood wave, and location and size of the flooded areas.

The estimation of upstream area peak runoff associated with a certain return period requires runoff modelling. The output hydrograph can then be used as a boundary condition for the hydrodynamic flood model, which is used to simulate the flood inundation over the floodplain. This can be used to assess flood hazard.

4. Study area

4.1. Location

The Nam Chun watershed area, about 400kms due north of Bangkok is located mainly in the district of Lom Sak and to lesser extend in the Khoa Khor district of Petchabun province in Thailand (figure 4-1). It lies between the latitudes $16^0$40' and $16^0$50' North and between the longitudes $101^0$02' and $101^0$15' East. The watershed covers a total area of about 92 km^2 and consists of an upper catchment and lower plain. The upper Huai Nam Chun catchment consists of two sub-catchment of Huai Nam Chun Yai and Hui Nam Chun Noi streams. Both rivers are mountain streams with very high transport capacity due to the steep gradient. The confluence of these rivers is the outlet of the catchment at Ban Fai Wang Bon and becomes the Nam Chun river that passes through the lower plain and drain water flow to Pa Sak river. The Nam Chun floodplain is almost flat with slope gradient of 0 – 2%. The floodplain is usually inundated by flood when Nam Chun river overflow mostly during the rainy season from May to October (Suwanwerakamtorn, 1992). Nonetheless, the Nam Chun floodplain is affected also by the water level in the Pa Sak river may hamper the drainage of flood flow.

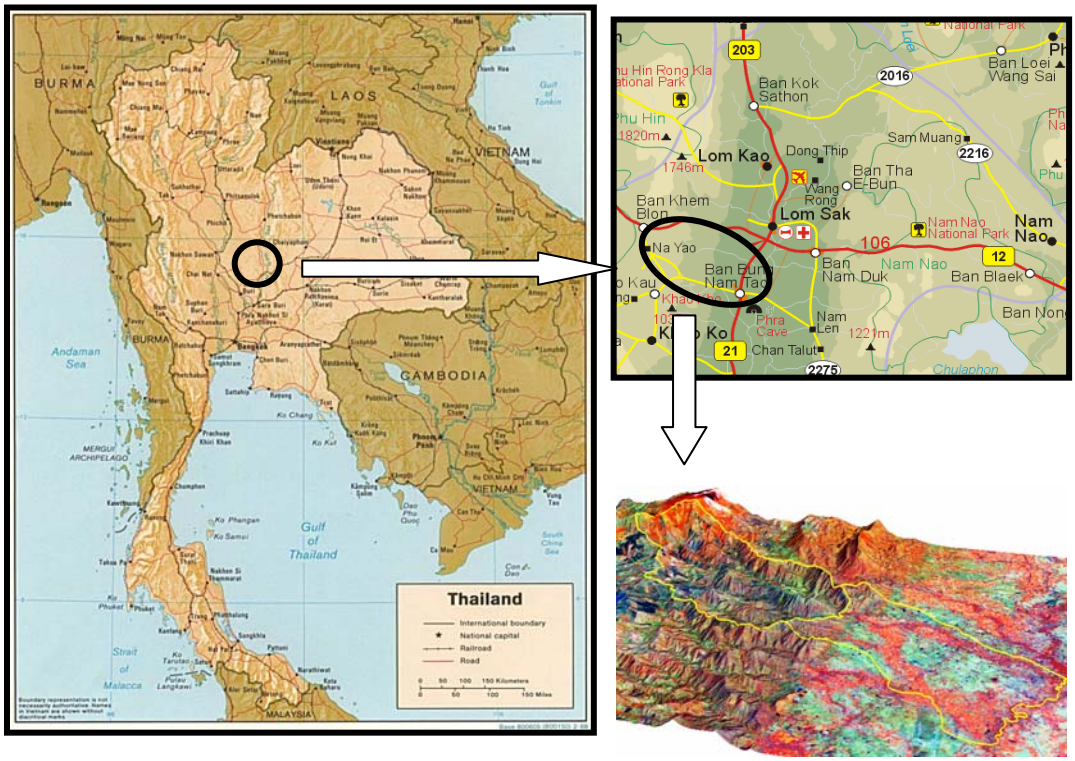

Figure 4-1: The study area in the Phetchabun Province of Thailand.

4.2. Climate

The study area is characterized by having a tropical climate that is influenced by the northeast and southwest monsoons. In general, there are three seasons in the area; a dry and cool winter, a wet hot summer and a hot rainy period. The rainy season commences from May and extends to October. In the lower plain area of Nam Chun watershed an annual average rainfall of 1066 mm is estimated from the climatic data for the period 1970 to 2005. The average number of rain days is 120 days per year.
The mean annual temperature of the area is 34^{o}C with temperature getting as high as 37^{o}C in April during the summer season and as low as 17 ^{o}C in the winter season in December. Figure 4-2 and table 4-1 show the mean monthly rainfall and temperature in Lom Sak station. This record covers a period of 35 years from 1970 to 2005.

Table 4-1: Mean monthly rainfall, rainy day and temperature period 35 years (1970 - 2005).

Month	Rainfall (mm)	Rainy day	Max Temp. (^{o}C)	Min Temp. (^{o}C)	Mean Temp. (^{o}C)
Jan.	4.6	1	32.8	17.5	25.2
Feb.	22.1	2	34.8	19.5	27.2
Mar.	45.9	5	36.6	22.0	29.3
Apr.	58.5	8	37.5	24.3	30.9
May	159.1	16	35.9	25.0	30.5
June	148.9	17	34.0	25.1	29.6
July	141.0	18	33.2	24.8	29.0
Aug.	197.5	21	32.5	24.7	28.6
Sep.	193.9	19	32.9	24.5	28.7
Oct.	75.1	10	33.2	23.3	28.3
Nov.	14.8	2	32.5	20.4	26.5
Dec.	4.9	1	31.6	17.4	24.5
Total	**1066.3**	**120**	**34.0**	**22.4**	**28.2**

Source: Lom Sak Meteological station

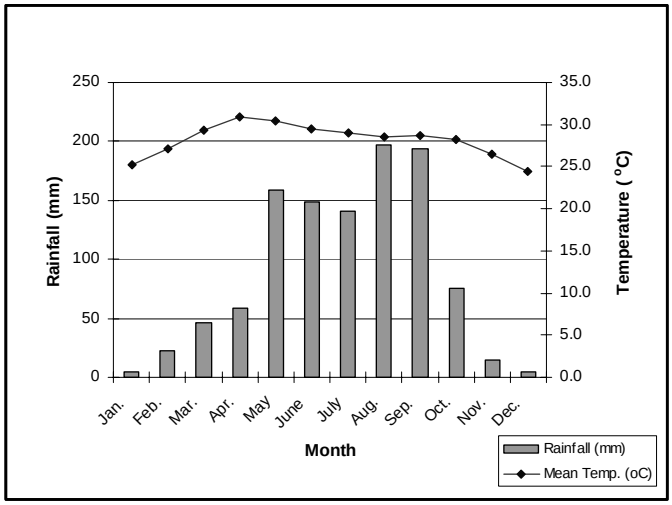

Figure 4-2: Average Annual Rainfall and Temperature of the Study Area.

4.3. Geology and Geomorphology

The area mainly composed of uplifted sedimentary rocks of the Korat group in the upper catchment area. The oldest rocks are of the Huai Hin Lat formation which consists of conglomerate, sandstone and shale, partly intercalated with andisitic tuff and aggromorate. The next formation is Nam Phong which contains raddish-brown cross-beded sandstone and conglomerate. Both formations were formed during the upper Triassic period. The formation next in age is the Phu Kradung formation which consists of shale, siltstone and sandstone. This was formed in the Jurassic period and occurs along the scarp in the study area. The youngest formation of the Korat group that occurs in the study area is Pha Wihan which consists of white and pink, cross-bedded sandstone with pebbly layers in the upper beds with some intercalations of the reddish-brown and grey shale. The lower plain consists of the Quaternary colluvial and alluvial terrace deposits.

4.4. Soils

Soils in Nam Chun watershed are mainly derived from the sedimentary rocks. The soils are characterized by having high clay content and can be categorized in the silty clay loam to silty clay textural classes. They are very shallow to moderately deep and well drained in the upper catchment. Alluvail soils in Quaternary alluvial sediments occur in the lower plain areas. The soils in the catchment are classified under the great groups such as the Haplustalfs, Palustalfs, Dystrustepts and Haplumbrepts. The soil moisture regime is mainly Ultic (Solomon, 2005).

4.5. Vegetation and Land Use

The dominant land use types in the study area include forest, agricultural land, shrub, grassland and residential area. Agricultural lands include rainfed annual crops, paddy rice fields with secondary crops, and orchard/ tree plantation areas such as tamarind, mango, litchi, etc. On the upper catchment area, the forest type is mixed deciduous. Owing to deforestation, degraded and disturbed forests are found on higher sloping areas. Most of the area is used for agricultural and human settlements. Farmers have encroached forest areas for cultivation of maize and other food crops. The major land use types are maize cultivation followed by beans or cabbage in the mountains and tamarind in the hilland. Most of the upper part of the catchment is covered by fallow grasslands which are dominated by the species *Impecata cylindica*.

At the lowland, farmers mainly grow rice in rainy season followed by various crops such as tobacco, cucumber and maize in the dry period, locally being irrigated. On the levees, coconut palm, mango and tamarind are grown, which are also occupied by settlements.

5. Analysis of soil properties in relation to land use

In order to supplement and implement the runoff modelling approach conducted in this study, certain soil properties that play key roles in the generation of runoff were assessed in relation to different land use types and in relation to one another. These soil properties are including organic matter content, porosity, bulk density, saturated hydraulic conductivity, initial soil moisture content and saturated soil moisture content. Soil physical properties are the most important factors influencing the rate of water that can infiltrate into the soil. Infiltration serves as indicators for the influence of land use on the soil (Zimmermann et al., 2006) and it has also a reducing effect on the generation of runoff volume in a catchment.

5.1. Soil physical properties data collections and measurements

To determine the influence of main land use types on soil physical properties the following investigations were carried out: a satisfied sampling technique for soil samples was employed within each soil unit in each of five land use types which included cornfields, forest areas, degraded forest, grasslands and orchard. It was assessed that each unit has similar soil textural classes and analyse those units were selected for sampling. Same slope position was also taken into consideration in the sampling procedure for each unit. A total of 59 samples were analysed for each of the properties of soil.

Undisturbed soil samples (figure 5-1) were taken by using a steel core sampler of 108-cm^3 volume (5 cm in diameter and 5.5 cm in height). The core rings were directly inserted into the soil and completely submerged in the ground, ensuring that the soil remains undisturbed. After digging around the ring, the soil together with the steel core sampler was carefully removed. Caps were placed on both sides of the soil rings and the ring was labelled. The same samples collected for determining hydraulic conductivity were also used for determining soil bulk density, soil particle density, total porosity and initial moisture content. Results of soil properties are presented in appendix 1.

Figure 5-1: Undisturbed soil core sampling.

5.1.1. Estimation of the Initial moisture content, saturated hydraulic conductivity and saturated moisture content

The initial moisture content of soil was measured from field moisture weight in the soil core samples taken in the field. Consequently, each soil core was first put into a tray to absorb water through capillary action via filter nylon for 24 hours until the soil becomes saturated. Saturated soil moisture contents were measured from saturated soil weight. The saturated hydraulic conductivity of the soil was estimated by the constant hydraulic head method (figure 5-2). The procedure is as follows; first saturated soil is packed uniformly in core ring sample. A constant height of water is maintained over the upper end of soil core and the bottom end is open to the atmosphere. Water volumes were determined using a cylinder below the core and observations were taken when the discharge began until water flow becomes constant. Stable saturated hydraulic conductivity values were calculated by averaging the last five values until the difference was less than 5 % from individual 5 min interval, then plot the amount of water volume per time to see the constant values of the water. Subsequently, the quantity of water infiltrated under saturated conditions is calculated based on Darcy's law, using equation 5-1. Those measures value were used for parameterization in runoff modeling (chapter 6).

Figure 5-2: Measuring K_{sat} values in the field.

$$K_{sat} = \frac{Q}{A} * \left(\frac{L}{\Delta H} \right) \qquad \textbf{(5-1)}$$

Where K_{sat} = saturated hydraulic conductivity (mm/hr)
Q = water volume (ml)
A = the cross sectional area of the soil core (cm^2)
L = the length of soil core (cm)
ΔH = the difference of hydraulic head (cm)

5.1.2. Estimation of bulk density, porosity and organic matter content

After measuring saturated hydraulic conductivity (K_{sat}) bulk densities were determined by oven-drying cores with soil samples at 105^o C for 24 hours. Soil organic carbon was determined using Walkley black method (FAO, 2002) on the disturbed soil samples which were sieved through a 2 mm mesh. Consequently, soil porosity was calculated based on measured bulk density as follows:

$$Porosity(\%) = \left[(W_s - W_d)/V \right] \times 100 \qquad \textbf{(5-2)}$$

Where W_s = water-saturated soil weight (gm)

W_d = dried soil weight (gm)
V = soil volume (cm^2)

5.2. Statistical analysis

Descriptive statistical approach was employed. One-way analysis of variance (ANOVA) and Student's-*t*-test were used to compare the effects of different land cover types on the soil properties. The correlations were established using a regression analysis in order to assess the relationship between soil physical properties with different land use types and within each soil physical properties itself. Data analyses were carried out using Excel and SPSS software.

5.3. Impact of land use on soil physical properties

In figure 5-3 (panel a), the box plot comparison shows a pronounced decline of the hydraulic conductivity from forested area on the top to orchard and cornfield on the bottom (table 5-1). Soil porosity appears to exhibit the same trend as well (panel b). In contrast, bulk density shows (panel c) highest values in cultivated areas (cornfield and orchard) while the lowest value shows in forested areas. Organic matter content shows (panel d) the highest values on forested areas and degraded forest where as the lowest value exhibits on cornfield, this could be due to the mechanical destruction of organisms effects on the abundance and activity of soil organism.

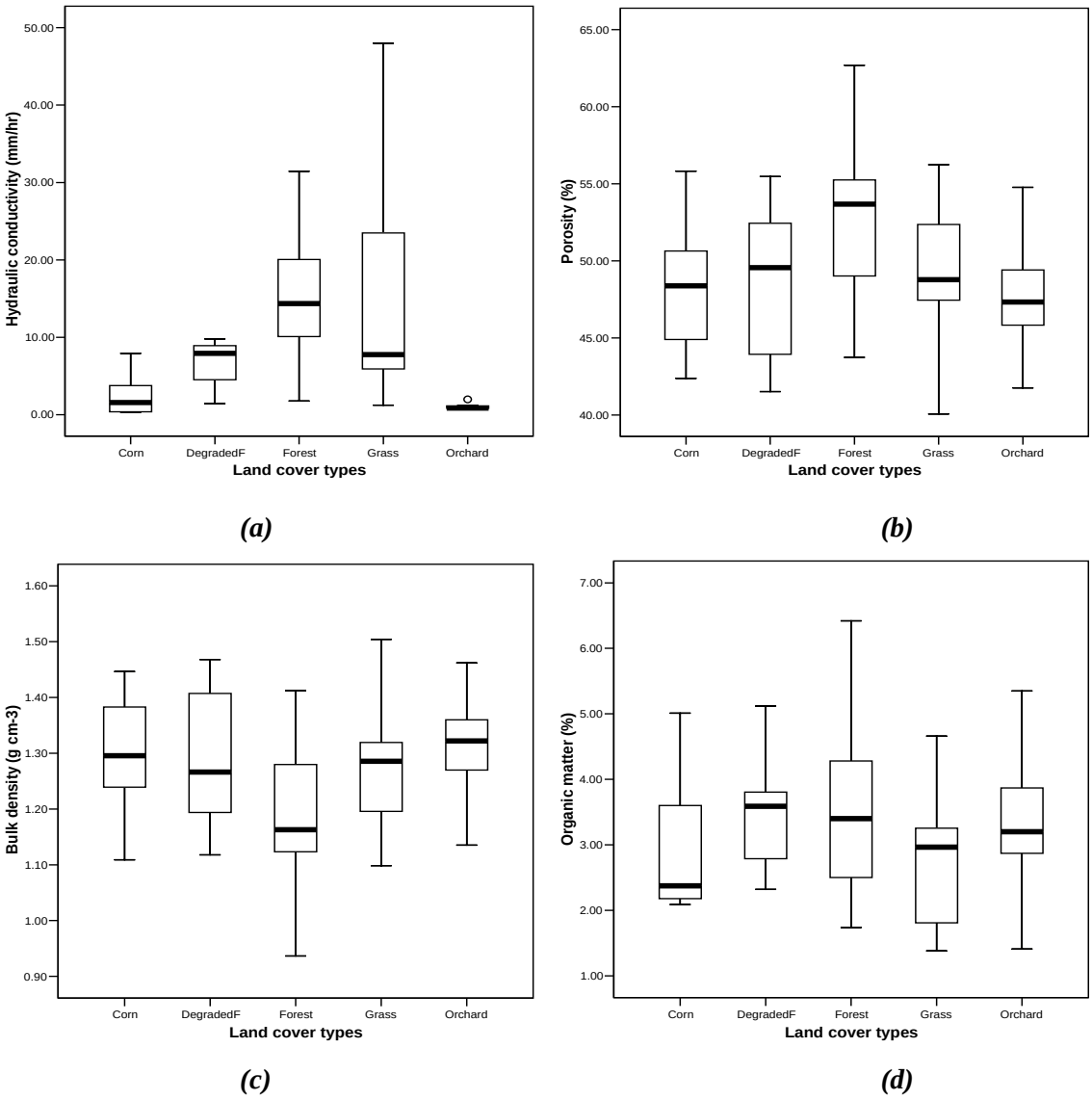

Figure 5-3: Box plots of variation of soil properties in different land cover types;(a) hydraulic conductivity, (b) porosity, (c) bulk density and (d)organic matter content.

To test the significance between the difference of the mean of each soil properties on natural vegetation (forest, degraded forest, grassland) and agricultural land uses (cornfield, orchard), a paired two-tailed Student's-*t*-test and analysis of variance (ANOVA) was performed, with the null hypotheses 'no significant difference between soil physical properties on each combination of land cover type'.

Table 5-1 summarizes the results of ANOVA performed with measuring results of each soil properties on each land cover types. The resulting level of significance of ANOVA revealed that the adjacent five land cover types significantly ($P<0.05$) differed in saturated hydraulic conductivity and not to porosity, bulk density and porosity.

Table 5-1: Mean and standard deviations of saturated hydraulic conductivity, bulk density, porosity and organic matter for different land cover types.

Land cover types	Hydraulic conductivity (mm/hr)			Bulk density (g/cm^3)		
	Mean	*n*	Std.Deviation	Mean	*n*	Std.Deviation
Forest	19.27	9	14.67	1.19	11	0.13
Grassland	15.43	11	15.70	1.26	11	0.11
DegradedForest	9.60	8	9.19	1.28	10	0.12
Cornfield	2.74	9	2.79	1.30	11	0.10
Orchard	2.31	10	3.99	1.31	12	0.09
Sig of ANOVA	0.004			0.123		
Land cover types	**Porosity (%)**			**Organic matter (%)**		
	Mean	***n***	**Std.Deviation**	**Mean**	***n***	**Std.Deviation**
Forest	52.57	11	5.36	3.62	6	1.63
Grassland	49.61	11	4.50	2.76	8	1.07
DegradedForest	49.04	10	4.95	3.46	7	0.96
Cornfield	48.12	11	4.08	2.94	6	1.16
Orchard	47.90	12	3.67	3.31	6	1.3
Sig of ANOVA	0.123			0.67		

A Student's-*t*-test (table5-2) comparing mean between two groups of land cover types consists of natural vegetation cover (forest, degradedforest and grass) and agricultural land uses (cornfield, mixedcrop, orchard) shows the significantly difference ($P<0.05$) on hydraulic conductivity, bulk density and porosity whereas organic matter was not significant.

Table 5-2: A paired two-tailed Student's-*t*-test for two groups of land cover type.

Land cover types	Hydraulic conductivity (mm/hr)			Bulk density (g/cm^3)		
	Mean	*n*	Std.Deviation	Mean	*n*	Std.Deviation
Natural vegetation	15.54	19	13.44	1.24	23	0.13
Agricultural	2.51	19	3.39	1.30	23	0.09
Sig. (2-tailed)	0.000			0.038		
Land cover types	**Porosity (%)**			**Organic matter (%)**		
	Mean	***n***	**Std.Deviation**	**Mean**	***n***	**Std.Deviation**
Natural vegetation	50.97	23	4.98	3.56	12	1.31
Agricultural	48.01	23	3.79	3.12	12	1.19
Sig. (2-tailed)	0.001			0.440		

Figure 5-4 shows the average means of each soil properties including hydraulic conductivity, soil porosity, bulk density and organic matter on different land cover types. Hydraulic conductivity (panel a) was found to be highest in the forest areas (19.27 mm/hr) and the lowest in agricultural area (2.31 mm/hr in orchard and 2.74 mm/hr in cornfield). The results revealed that hydraulic conductivity varies dramatically between forest areas and cultivated areas.

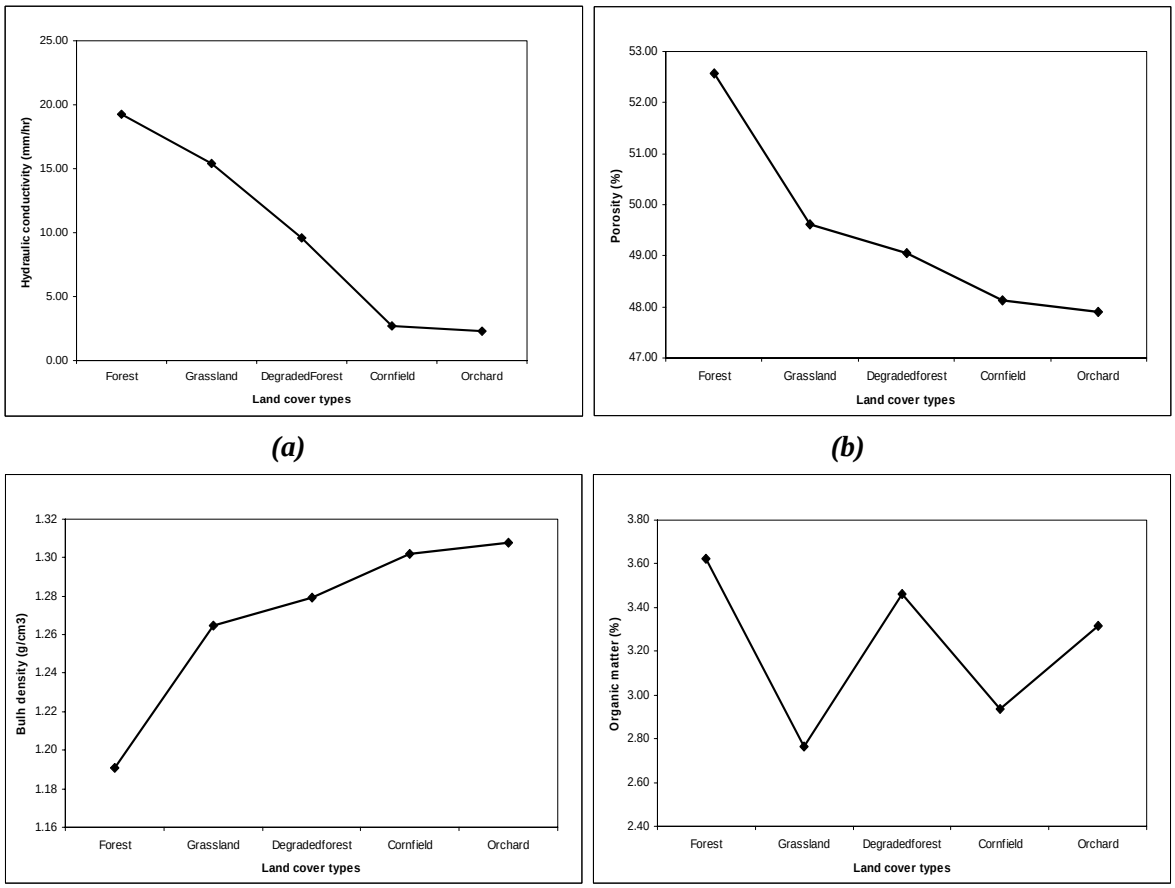

Figure 5-4: Average hydraulic conductivity (a), porosity (b), bulk density (c)and organic matter(d) in different land cover types.

The low hydraulic conductivity could be an indication that the soils in these areas are degraded as a result of human interventions. The decrease in hydraulic conductivity of the cultivated soil relative to the other land cover types may be attributed to the increase of bulk density and the mechanical disruption of pore arrangements by heavy machinery ploughing and tillage (Celik, 2005). This could be responsible for making the soil compact and negatively influencing hydraulic conductivity leading to reduced infiltration rates. Forest soils showed higher values of hydraulic conductivity. The reason for this could be the root systems and litterfalls of forest and grass land may have increased hydraulic conductivity compared to cultivated soils (Baumhardt and Lascano, 1996). The soils in these areas are undisturbed and this has allowed them to maintain good soil structure and high porosity.

Analysis of soil porosity on different land cover types also shows in a similar pattern (figure 5-4 panel b). There was a significant difference in total porosity between the cultivated soils and the uncultivated areas. For cultivated areas soil porosity was obviously lower due to mechanical compaction. This tendency was consistent with that of bulk density changes, while this reduction was not significantly different between land cover types with the highest average porosity (52.57%) in forested areas and the lowest (47.90%) in orchard. It is indicated that the proportion of macro-pore space in the soil gradually increases with development of natural vegetation and with increasing total porosity (Li and Shao, 2006).

Average soil bulk densities showed (figure 5-4 panel c) the highest values in orchard with an average value of 1.31g-cm^3 and the lowest for forest areas with an average value of 1.19 g-cm^3, which is inversely related to soil porosity. The increase in bulk density and reduction in porosity on cultivated soils could be attributed to increase compaction by humans and agricultural machines, an indication that the soils in these areas are more compacted than the soil in forest or grassland areas. Since the relationship bulk density and hydraulic conductivity are negatively related (refer to section 5.4.2), an increasing bulk density results in a reduction in hydraulic conductivity. The infiltration rate depends on the hydraulic conductivity of the soil. Reduced hydraulic conductivity leads to reduction in the amount of rainwater that can infiltrate into the soil. This implies that more water will be available at the surface after a rainstorm resulting in increased surface runoff rate.

The results of the organic matter content revealed that measured values (figure 5-4 panel d) taken from forest area were highest with an average value of 3.62%, while the lowest value was found in the grassland areas with an average value of 2.76%. Grassland areas showed relatively lower values probably because most of these areas were used for cultivation in the past, which led to soil degradation. The higher value was also shown in orchard areas probably due to management implementations such as the use of organic fertilisers in these areas.

5.4. Correlation analysis of soil physical properties

The relationship between the different soil properties was assessed using a regression analysis. The resulting level of significant revealed that the relationship between all cases assessed was statistically significant ($P<0.05$).

5.4.1. Bulk density and Porosity

Correlation analysis revealed that soil bulk density was negatively related to porosity with r = -0.867 and R^2 = 0.752 (figure 5-5). The two soil properties were found to be inversely associated. This indicated that the increase of soil bulk density reduces the porosity of the soil as a result of management practices in the watershed. A reduction in soil porosity subsequently leads to decline in hydraulic conductivity of the soil (figures 5-7).

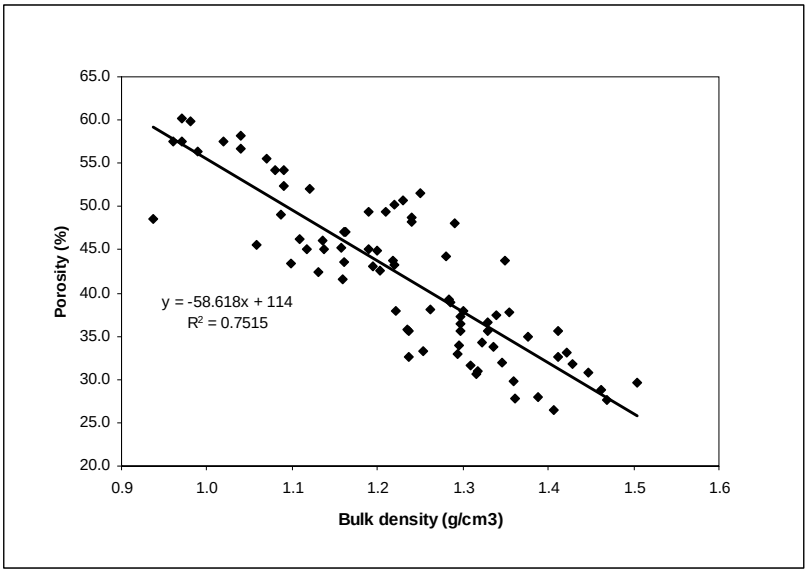

Figure 5-5: The relationship between bulk density and porosity.

5.4.2. Bulk density and hydraulic conductivity

Figure 5-6 shows the relationship between Bulk density and saturated hydraulic conductivity. The statistical significance of the relationship revealed a negative linear correlation with r= -0.712 and $R^2 = 0.507$. Increased bulk density could be attributed to increase in soil compaction due to the use of heavy machinery which is responsible for the destruction of the continuity of soil macroporosity. This leads to a significant decline in the hydraulic conductivity of the soils in these areas (Ndiaye et al., 2006; Zhang et al., 2006).

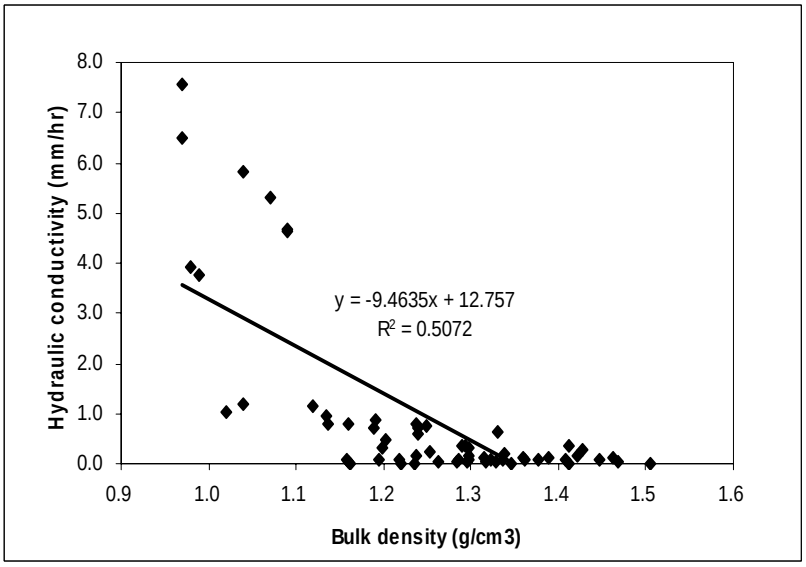

Figure 5-6: The relationship between bulk density and hydraulic conductivity.

5.4.3. Porosity and hydraulic conductivity

The relationship between soil porosity and hydraulic conductivity was significant (P<0.05). However, the results show a weak positive relationship with r=0.622 and R^2 =0.387 (figure 5-7). Increase in soil porosity was strongly related to the improvement in hydraulic conductivity. High porosity influences movement of water into the soil inline with soil hydraulic properties. Porous soils accordingly relate to infiltration rate of soil. This is reducing the amount of water that could be available for surface runoff.

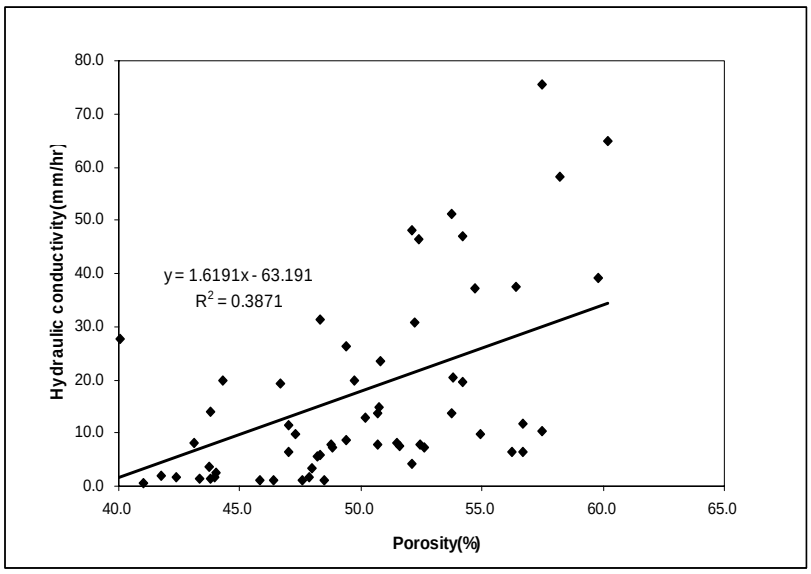

Figure 5-7: The relationship between porosity and hydraulic conductivity.

6. Surface runoff modelling

In this study, The Limburg Soil Erosion Model (LISEM) was used to quantify the amount of runoff in the upper catchment that take into account effect of land cover change and also how different factors affect surface runoff. The LISEM is constructed with the PCRater dynamic modelling language (Wesseling et al., 1996) which allows great flexibility. Moreover, on a GIS level LISEM uses a raster type representation of the catchment which allows detailed representation of the processes. In case of limited data availability, the user can also choose Green and Ampt or the Holtan equation for infiltration calculation (De Roo, 2000). The results show not only the total runoff at the outlet but also the amount of sediment.

6.1. The LISEM erosion model structure

The LISEM is a physically based hydrological and soil erosion model for simulating the hydrology and sediment transport during and immediately after a single rainfall event applied in agricultural catchment of a size ranging from 1 ha up to approximately 100 km^2 (De Roo et al., 1996). The model has been developed by Utrecht University, Department of Physical Geography, the Netherlands. LISEM is built to simulate both the effects of the current land use and the effects of soil conservation measures. Basic processes in LISEM can be divided into two parts which include a water part and an erosion part (figure 6-1). The processes incorporated in the model are rainfall, interception, surface storage in micro-depressions, infiltration, vertical movement of water in soil, overland flow, channel flow, detachment by rainfall direct throughfall, transport capacity of the flow and detachment by overland flow. The model also incorporate the influence of compaction including the influence of tractor wheeling's, small paved roads, field strips and grassed waterways on the hydrological and soil erosion processes (De Roo and Jetten, 1999). In this study, however only runoff processes are taken into account.

On the runoff process, rainfall is the basic input of the water part. Interception by crops and vegetation is simulated by regarding as a simple storage then subtracted from the rainfall. The remaining rainfall reaches the soil surface, where it can infiltrate or form a surface storage. Since LISEM is a storm-based model the infiltrated water is essentially a loss of water in the sense that infiltrated water cannot resurface. Infiltration can be simulated using one of several available equations such as the Green&Ampt and Holtan equations as well as the physically based Richards equation using the SWATRE sub model. In this study, Green and Ampt infiltration model are used. Surface storage will result in surface runoff once a certain threshold is exceeded. Flow velocity is calculated with the Manning equation and surface runoff is routed over the landscape with the kinematic wave equation. Overland flow can flow into the channel and is then routed to the catchment outlet as channel flow. For overland flow and channel flow are both routed with the kinematic wave, which is solved by a four-point finite difference solution and used together with Manning's equation. The kinematic wave is done over the Local Drain Directions that forms a network which connects cells in 8 directions (Jetten, 2002).

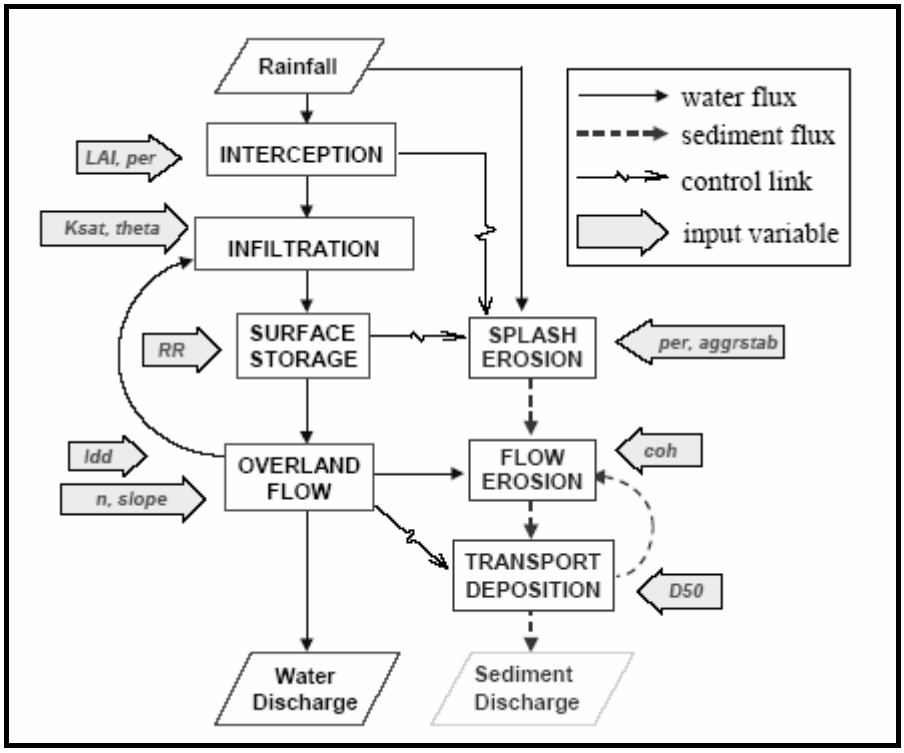

Figure 6-1: Simplified flow chart of the LISEM model (Hessel, 2002).

6.2. Model applications

6.2.1. LISEM input maps

Since LISEM is process based it requires a significant amount of input data as described by Jetten (2002). All the required input maps were derived from three basic maps which included the digital elevation model, soil unit map and land use map. Soil map which was based on geopedological approach was derived from previous study (Solomon, 2005). This map provided the basis for deriving soil parameters for all the models (appendix 2). A digital land cover map of the study area produced in 2004 by the Land Development Department of Thailand was used for this study (appendix 3). The accuracy of the map was assessed by making use of ground truth samples that were collected during the fieldwork. The overall accuracy of the map was 72% which was considered to be satisfactory for the purpose of this study. The digital elevation model (DEM) was derived using ILWIS version 3.3 by interpolating contours with 10 meters intervals. Grid size of 30 meters was chosen for the resulting map.

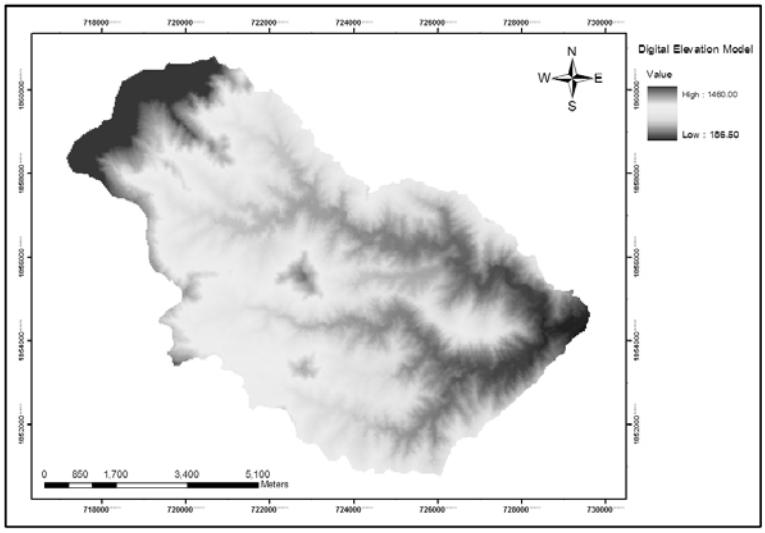

Figure 6-2: Digital Elevation Model (DEM) used in LISEM model.

As LISEM is grid-based, all input maps used in the model were converted into raster format having grid size of 30m by 30m. This resolution was selected to coincide with the spatial resolution of the input maps (land-use/cover, soil map and DEM). The choice of time step length used for model depend on the grid size, where smaller cell sizes require small time steps (Hessel, 2005). Thus, time step length of 60 seconds was used to ensures that the time step of the model is less than the time for a wave to travel the distance of a pixel (Chow et al., 1988).

Table 6-1 shows a number of parameters required for running the model were derived in the field. Since, LISEM is largely built in a mixture of PCRaster commands and C^{++} and PCRaster capabilities are used to create the input maps. Thus, a large number of input maps for different parameters are usually generated by using lookup table that assign parameter values for the different units on the land use map or soil map using the PCRaster script file (appendix 4).

Table 6-1: Input data for LISEM version 2.39, with the use of the Green and Ampt infiltration sub model.

Parameter	Name	Method	Unit
Catchment characteristic			
Local drain direction	LDD.map	derived from DEM	-
Catchment boundaries	AREA.map	derived from DEM	-
Area covered by raingauges	ID.map	mapping	-
Slope gradient (sine of slope angle)	GRAD.map	derived from DEM	-
Location of outlet and suboutlets	OUTLET.map	derived from DEM	-
Rainfall data	ASCII	derived from fieldwork	mm/hr
Vegetation			
Leaf area index	LAI.map	derived from PER.map	-
Fraction of soil covered by vegetation	PER.map	field observation	-
Vegetation height	CH.map	field observation	m
Soil surface			
Manning's n scalar	N.map	derived from literature	-
Random Roughness	RR.map	derived from literature	cm
width of impermeable roads	ROADWIDT.map	mapping	m
Green and Ampt Layer 1			
Saturated hydraulic conductivity	KSAT1.map	meaure from fieldwork	mm/hr
Saturated volumetric soil moisture content	THETAS1.map	meaure from fieldwork	-
Initial volumetric soil moisture content	THETAI1.map	meaure from fieldwork	-
Soil water tension at the wetting front	PSI1.map	derived from literature	cm
Soil depth	SOILDEP1.map	field observation	mm
Channels			
Local drain direction of channel network	LDDCHAN.map	derived from ldd.map	-
Channel gradient	CHANGRAD.map	derived from grad.map	-
Manning's n for the channel	CHANMAN.map	derived from literature	-
Width of channel scalar	CHANWIDT.map	derived from ldd.map	m
Channel cross section shape	CHANSIDE.map	field observation	-

6.2.2. Model Parameterisation

It is not possible to have all the parameters due to lack of time and resources. Some of the parameter values used in the model was derived from literature values and using information on the soil and land cover characteristics of the watershed. To quantify rate of runoff on the catchment, five types of parameters are involved in the water part of the LISEM model. The values used for each parameter are given in the following section.

6.2.2.1. Catchment characteristics parameter

The parameters required for catchment characteristics are slope gradient, local drainage direction, catchment boundary and location of outlet which were derived from digital elevation map. Rainfall data was obtained from the Royal Irrigation Department, which records the data automatically on hourly basis using a rain gauge installed in the catchment. Rainfall data was considered to be homogeneous over the catchment.

6.2.2.2. Vegetation parameter

The parameters required for modelling interception are the percentage canopy cover (PER.map), crop height (CH.map) and leaf area index (LAI.map). Values for fraction canopy cover and vegetation height were estimated in the field. Leaf area index was calculated from the fraction of canopy cover. The land cover map was used for this purpose. For each class of land cover map a representative fraction of canopy cover and crop height values was estimated as indicated in table 6-2 below. This information was entered into PCRaster table format.

Table 6-2: Fraction of canopy cover and vegetation height values used in the model.

Land cover	Fraction of canopy cover	Vegetation height (m)
Cornfield	0.60	1.84
DegradedForest	0.70	10.00
Forest	0.80	17.51
Orchard	0.20	7.09
Grassland	0.90	1.03
MixedCrop	0.40	0.50

6.2.2.3. Green and Ampt infiltration parameters

The parameters required for running the Green and Ampt infiltration model (see table 6-1) were the hydraulic conductivity (ksat1.map), soil water tension at wetting front (PSI1.map), initial soil moisture content (THETAI1.map) and saturated soil moisture content (THETAS1.map). The required values were measured during the fieldwork (see section 5.1) with the exception of values for soil water tension which was obtained from the EROSEM documentation and user guide (Morgan et al., 1998b) for different soil textural classes (table 6-3). The measured values of hydraulic conductivity showed a certain trend on different land cover types of the watershed and on the soil classes. To account for this trend the land cover map was crossed with the soil map in ILWIS to get a map with all the possible combinations between texture type and land cover class in the watershed. The table 6-4 shows the resulting combinations and the average values measured for each combination which are assigned for hydraulic conductivity, initial soil moisture and saturated soil moisture. For some combination between soil unit and land cover map it was not possible to obtain field data, the values were assigned using guide values from literature (Morgan et al., 1998b; Saxton, 2005).

Table 6-3: Wetting front suction values used in the model.

Soil texture	Wetting front suction (cm)
Clay Loam	20.80
Loam	8.90
Sandy Loam	11.00
Silty Clay	29.20
Silty Clay Loam	27.40

Table 6-4: Values used for saturated hydraulic conductivity, initial volumetric soil moisture content and saturated volumetric soil moisture content.

Land cover	Geopedologic Unit	Soil texture	Saturated hydraulic conductivity (mm/hr)	Initial volumetric soil moisture content	Saturated volumetric soil moisture content
Cornfield	HM311	Sandyloam	7.00	0.30	0.40
	P211	Siltyclay	0.50	0.34	0.40
	HM212, HM312, HM313	Clayloam	1.60	0.34	0.45
	HM211	Loam	2.00	0.33	0.45
Forest	HM311	Sandyloam	23.50	0.25	0.53
	LM212	Siltyclay	2.03	0.28	0.50
	HM212, HM312, LM112, LM212	Clayloam	6.48	0.28	0.48
	P111	Siltyclayloam	5.10	0.28	0.49
	HM211, LM211	Loam	14.92	0.26	0.50
DegradedForest	HM311	Sandyloam	21.00	0.28	0.44
	LM111, P211	Siltyclay	1.42	0.31	0.41
	HM112, HM212, HM213, HM312, LM212, LM211	Clayloam	5.00	0.29	0.42
	P111	Siltyclayloam	4.50	0.30	0.40
	HM211	Loam	9.72	0.28	0.45
Orchard	HM311	Sandyloam	7.00	0.30	0.37
	LM311	Siltyclay	0.50	0.39	0.42
	HM212, HM213, HM312, HM313	Clayloam	0.81	0.36	0.41
Grassland	P211	Siltyclay	1.23	0.31	0.46
	LM111,LM112,LM312, HM112, HM212, HM313	Clayloam	4.80	0.28	0.50
	P111	Siltyclayloam	3.75	0.31	0.50
	LM211, HM211	Loam	8.20	0.28	0.52
Mixedcrop	P211	Siltyclay	0.50	0.35	0.39
	HM112, HM212, HM213, HM312, HM313	Clayloam	1.60	0.34	0.39
	P111	Siltyclayloam	1.25	0.35	0.39
	LM211	Loam	2.00	0.33	0.44

6.2.2.4. Soil surface parameter

The random roughness of soil surface (RR.map), Manning's coefficient (N.map) and width of impermeable road (ROADWIDTH.map) were used in this parameter to determine several processes including infiltration, surface storage and velocity of overland flow. In this catchment these maps are based on the land use types. The values of random roughness were derived from the RUSLE handbook documentation (Renard et al., 2000) which is based on the type of tillage practices implemented in agricultural areas were used to estimated surface storage process. Manning's coefficient is based on land cover types found in the study area which was retrieved from the literature (table 6-6), these considered as surface flow resistance (Chow, 1959). The road width considered as impermeable which no infiltration. The random roughness values used for different land cover classes are shown in table 6-5 below

Table 6-5: Random roughness values used in the model (Renard et al., 2000).

Land cover	Random Roughness (std in cm)
Cornfield	1.80
DegradedForest	0.50
Forest	0.50
Orchard	0.50
Grassland	0.50
MixedCrop	1.80

Table 6-6: Guide values used for Manning's coefficient for different land cover types (Chow, 1959).

Land cover	Manning's coefficient
Cornfield	0.06
Urban	0.01
Road	0.01
DegradedForest	0.30
Forest	0.40
Orchard	0.06
Waterbody	0.01
Grassland	0.24
Stream	0.05
MixedCrop	0.06

6.2.2.5. Overland flow and channel flow parameter

The kinematic wave model was used to route the excess water and also in channel flow. In LISEM simulation can also be done considering a concentrated flow line, such as a thalweg, to be a channel.
All parameters for channel flow were created from channel mask map. The channel mask was created from local drainage direction using the PCRaster operation *accuflux* which is based on contributing area (see appendix 4). Channel input map required for using the model in LISEM include;

- Local drain direction of channel network (LDDCHAN.map) which was as produced using the DEM and the *lddcreate* operator in Pcraster. It was then repaired to ensure that it did not contain local pits using the PCRaster operator *lddrepair*.
- The gradient of the channel bed (CHANGRAD.map) was based on channelmask
- Manning's n for the channel (CHANMAN.map) was retrieved from literature (Chow, 1959).
- Channel width (CHANWIDT.map) was calculated from ldd.map and channelmask.map
- Channel cross section shape (CHANSIDE.map) is the tangent of the angle between the channel side and the vertical, the values 0 is rectangular channel was assigned for whole channel side

6.3. Model calibration and validation

Theoretically speaking it is not necessary to calibrate the physically based models but reality is different. Models are never fully physically based and many authors have demonstrated the need to calibrate process based models to obtain an acceptable predictive quality (Hessel, 2002). In the case of hydrological models calibrations are done using measured data at the outlet of the catchment. Differences between observations and simulated model response are basically caused by four different error sources consist of errors in meteorogical input data, errors in recorded observations, errors and simplifications inherent in the model structure and errors due to the use of non-optimal parameter values (Refsgaard and Storm, 1996). In model calibration only error source from non-optimal parameter values should be minimized. In this respects, it is important to realize that model parameters may compensate for the other error sources.

In this study, LISEM model was evaluated using 6 selected rainstorm events (table 6-7). Three events serve as a calibration set. Rainfall data are available in hourly and outlet discharge. The other three storms serve as a validation set, only rainfall data were used for simulation using calibration parameters (De Roo and Jetten, 1999).

The process was calibrated on peak discharge including time to peak and hydrograph shape to obtain the correct shape of hydrograph. The simulated hydrograph was visually compared with the measured data, after which some change in input data was selected to improve the simulation results. Two parameters were used to calibrate on peak discharge which includes:

- Saturated hydraulic conductivity (K_{sat}) which determines infiltration rate and runoff amount
- Initial soil moisture content was only used for calibration if calibration on saturated conductivity proved insufficient.

All these parameters were changed within reasonable boundaries; saturated hydraulic conductivity and initial moisture content were only allowed to vary between values measured on the samples and the values obtained from literature.

Hessel et al. (2003) reported that in LISEM calibration, separate calibration is necessary for event of different magnitudes. Therefore, in this study the calibration was calibrated for each event separately.

The three events were selected to calibrate which includes the 060905(06 September 2005), 180905 (18 September. 2005) and 260905 (26 September 2005) events. Table 6-7 gives a summary of the event characteristic showing that peak discharges were about 37.5, 13.0 and 31.45 m^3/s respectively. All events were thus of different magnitude and duration, with the 060905 and 180905 being the least rainfall intensity different.

Table 6-7: Event characteristics for 6 events.

Events	Event characteristics		
	Total rainfall (mm)	Maximum rainfall intensity(mm/hr)	Peak discharge (m^3/s)
Calibration			
60905	56.00	16.00	37.50
180905	20.00	18.00	13.00
260905	32.00	30.50	31.45
Validation			
70905	17.50	10.00	4.20
90905	15.00	8.50	1.02
120905	29.00	20.50	15.37

The results of the model were compared with discharge data measured from outlet of catchment. The simulated and measured hydrographs for three events are presented in figure 6-3 and table 6-8. As can be seen from the figure, the model slightly fit the volume of peak discharge and peak time exception for 260905 event, peak time occurs too early and over-predicted on peak discharge. The reason for this is the observed discharge at outlet were recorded every three hourly using gauge height, so that the momentary peak discharge could be missed**.**

Table 6-8: Observed and simulated peak discharge in Nam Chun catchment.

Events	Rainfall(mm)	Peak discharge	
		Obs(m^3/s)	Sim(m^3/s)
Calibration			
60905	52.58	37.5	37.90
180905	18.43	13.00	13.40
260905	29.49	31.45	32.99
Validation			
70905	16.60	4.2	4.72
90905	10.61	1.02	1.30
120905	26.74	15.37	23.81

Calibration saturated hydraulic conductivity is always much lower than the measured values about 30 % and 38% for event 060905 and event 180905 respectively. A possible explanation for this would be disturbance during sampling such as cracking of soil samples. However, calibration K_{sat} has different for different events; K_{sat} appears to increase with an increase in rainfall intensity (Hessel et al., 2003) as can seen on 260905 event (table 6-7), calibrated on K_{sat} was increased from measured values about 20%

Calibration on initial moisture content was not performed since K_{sat} calibration was sufficient and that results were satisfactory. The difference between the observed and the modelled hydrographs can be attributed to a number of error factors as mentioned above. Nevertheless, the model was successful in predicting the volume peak discharge of the observed hydrograph for all the events.

On validation process, the calibration parameters set on 060905 event was selected to simulate to validate on three storms event includes the events 070905, 090905 and 120905. The reasons are that these events have least different rainfall intensity and duration, they are also similar in condition. The results of the validation are shown in table 6-8 and figure 6-4. Two out of three validation events are simulated reasonably well, but problem arise with the 120905 event, where peak discharge is over-predicted, that results from high rainfall intensity. From validation results, the 060905 extreme event was selected for further analysis to simulate all case scenarios.

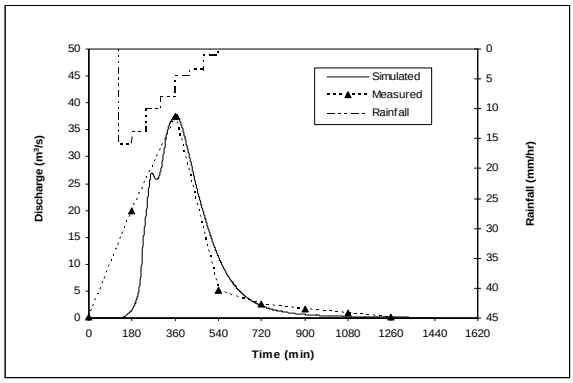

(a)

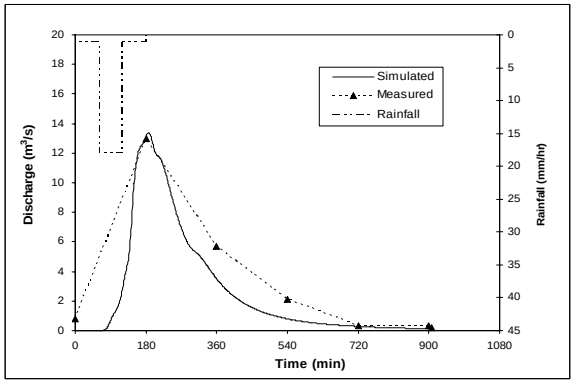

(b)

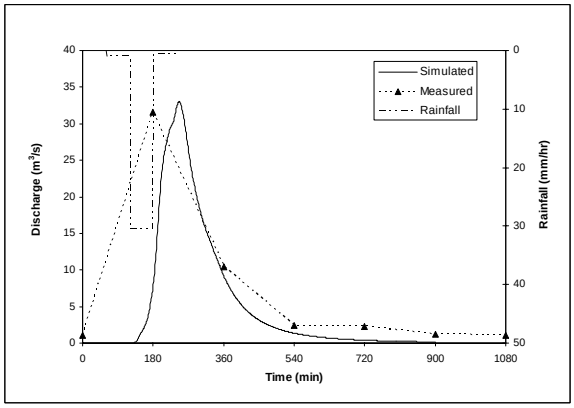

(c)

Figure 6-3: Measured and simulated discharge in Nam Chun catchment on 060905(a), 180905(b) and 260905(c) events.

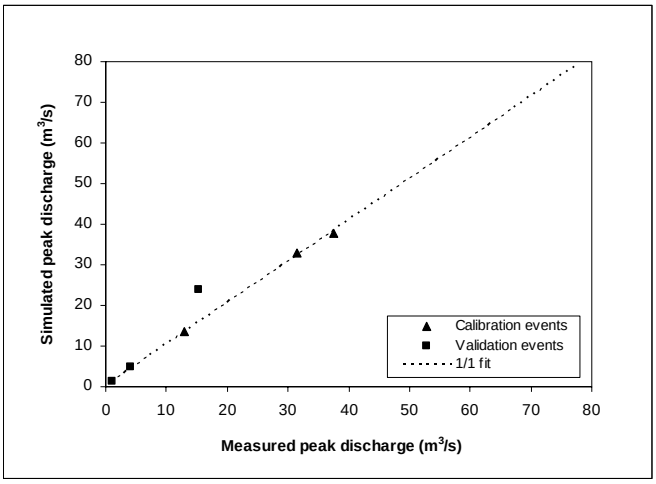

Figure 6-4: Measured and simulated discharge in Nam Chun catchment of the three calibration and three validation events.

6.4. Runoff rate for different land cover types

To study the effect of land cover on the amount of surface runoff, 18 homogenous samples areas for land cover were selected, and the total amount of runoff from these mini-catchments was modelled based on rainfall 060905 event.

The model results in table 6-9 show significant differences in predictions of average surface runoff rates for the different land cover types. The average surface runoff rate estimated for the whole area was 7.16 m^3/s. The weighted average surface runoff rates estimated per pixel for different land cover types are shown on figure 6-5. The highest volume of surface runoff was predicated for maize cultivations with an average value of 482×10^{-3} m^3/s and the lowest was predicted for forest areas with an average of 13.3×10^{-3} m^3/s. On the whole, agricultural areas includes cornfield, mixedcrop and orchard showed approximately 16 times higher values of surface runoff rates with an average of 440×10^{-3} m^3/s and non-agricultural includes forest, degradedforest and grass areas having an average surface runoff value of 27.87×10^{-3} m^3/s.

Table 6-9: Predicted average surface runoff in sub-catchment for different land cover types per pixel (rainfall event 060905).

Land cover types	Average Surface Runoff (m^3/s)		
	Sub-catchment 1	Sub-catchment 2	Sub-catchment 3
Forest	39.74 X 10^{-3}	0.13 X 10^{-3}	0.04 X 10^{-3}
DegradedForest	0.02 X 10^{-3}	63.88 X 10^{-3}	11.49 X 10^{-3}
Grass	20.80 X 10^{-3}	52.00 X 10^{-3}	62.73 X 10^{-3}
Cornfield	507.8 X 10^{-3}	463.3 X 10^{-3}	475 X 10^{-3}
MixedCrop	486.80 X 10^{-3}	118.92 X 10^{-3}	718.50 X 10^{-3}
Orchard	639.6 X 10^{-3}	333.50 X 10^{-3}	216.62 X 10^{-3}

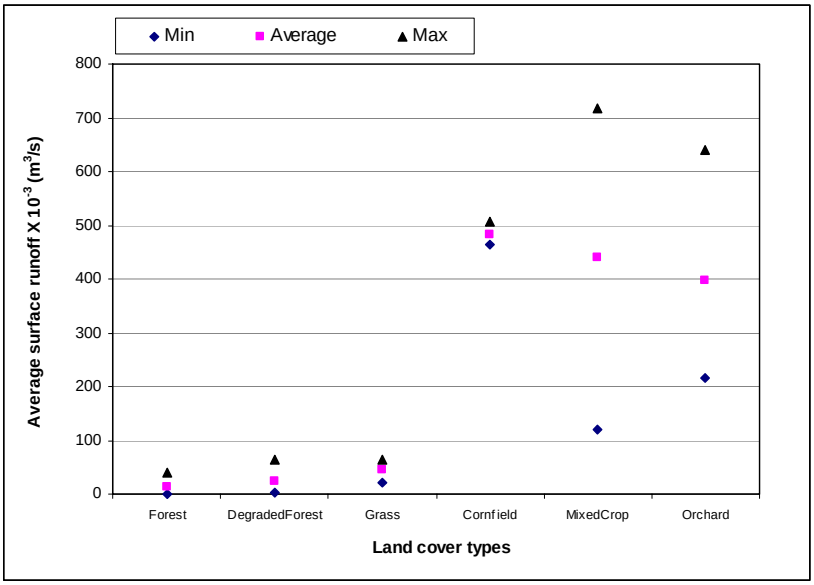

Figure 6-5: Weighted average surface runoff on different land cover types.

The relatively lower runoff level observed in non-agricultural areas can be attributed to the combination of high hydraulic conductivity, high surface cover and surface roughness values, related to high infiltration rates resulting in reduced runoff amount. The longer the water remains in the catchment by surface roughness, the more time there is for infiltration. The higher the infiltration rates the faster water moves into the soil. This means that more water can infiltrate into the soil and very less water is available for runoff. In contrast, higher runoff rates are observed in agricultural area. This can be attributed to low hydraulic conductivity in these areas that led to a decreased infiltration rate and therefore more water become available for runoff amount.

The spatial and temporal distribution of surface runoff as predicted by the calibrated model is presented in figure 6-6. The rainfall data of 060905 event, the peak of rainfall intensity was start at the first hour of the rainfall event. No runoff was estimated in the first few time steps in permeable areas, because much of the rain water was lost due to interception, infiltration and surface storage. After the initial losses were satisfied, the excess precipitation was routed over the catchment as surface runoff. The peak runoff at the outlet was observed in three hours (time step 180) after the peak rainfall occurred. In the fourth hour, the volume of surface runoff gradually declined because the rainfall intensity had significantly reduced. Although the rainfall intensity had decreased at the second hour, runoff still continued to occur because of the accumulation of rainwater from preceding time steps and because of the travel time for the water to move downstream as is calculated by the kinematic wave equation.

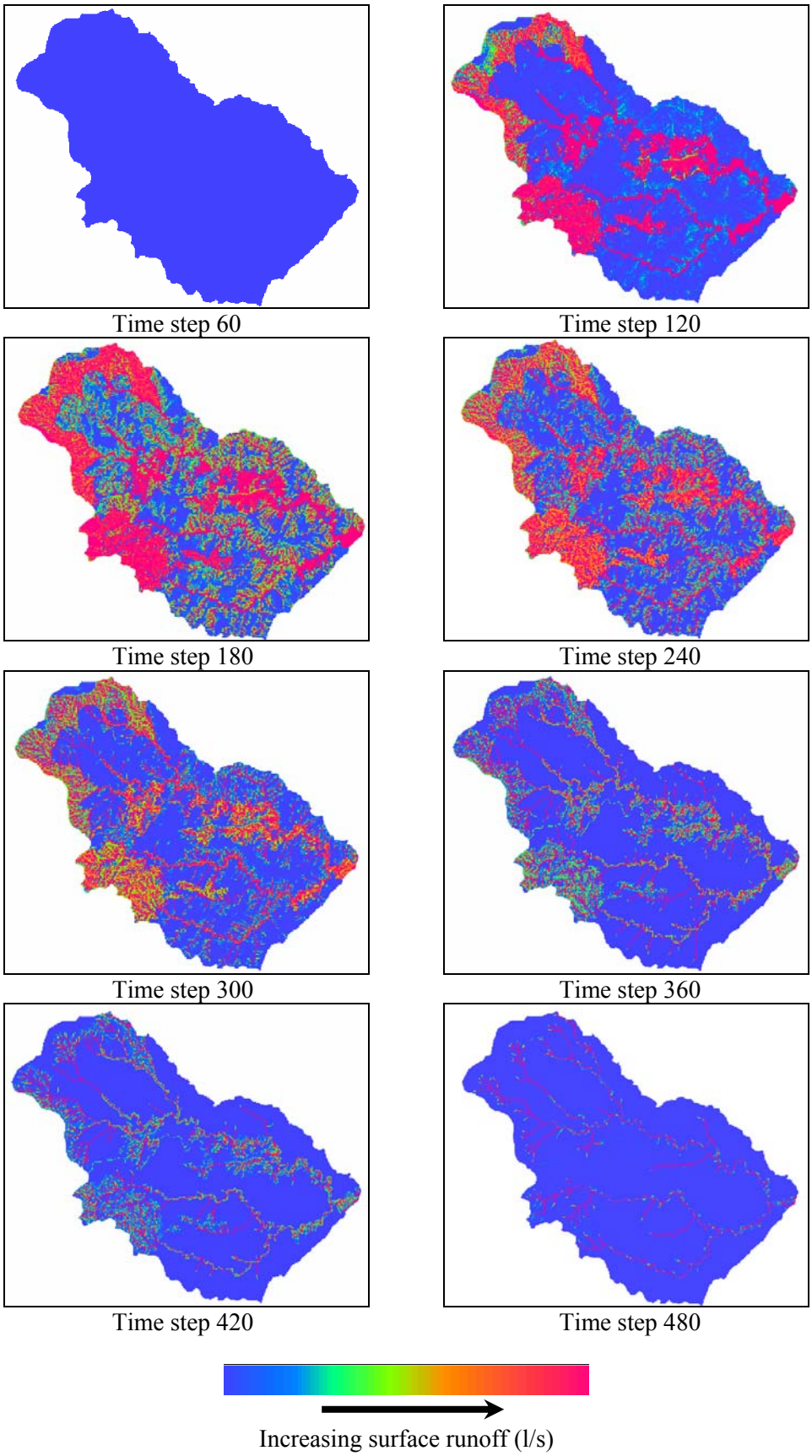

Figure 6-6: Spatial and temporal distribution of surface runoff (time step=1 min).

6.5. Sensitivity analysis

Sensitivity analysis is the act of determining the change in model behavior due to a predetermined adjustment of model parameter. A sensitivity analysis was used to find out which parameters had the largest influence on the models prediction. As can be concluded from the calibration results shown in the previous sections, these are differences between the measured and simulated discharges. A sensitivity analysis was performed on the three calibrated events to identify the most sensitive parameters of the model. Jetten et al (1998) showed that the sensitivity to certain parameters might depend on the level of other parameters. Thus model sensitivity can be more completely evaluated by changing combinations of parameters. Nonetheless, a simple sensitivity analysis in which only one parameter value is changed at a time is the easiest way to determine which individual parameters will be most important (Hessel, 2002). Therefore, in this study, simulations were carried out by symmetrically and uniformly subtracting 10% from and adding 10% to the calibration parameters including:

- Saturated hydraulic conductivity
- The initial soil moisture content
- Surface roughness (Manning's *n* and random roughness)
- Interception parameter (plant cover and crop height)

The effect of each change on the calibration runoff at the outlet was evaluated by considering the percent change in peak discharge. The results of the sensitivity of the model to parameter variation during the rainfall three events (060905, 180905 and 260905) used here are illustrated in figure 6-7.

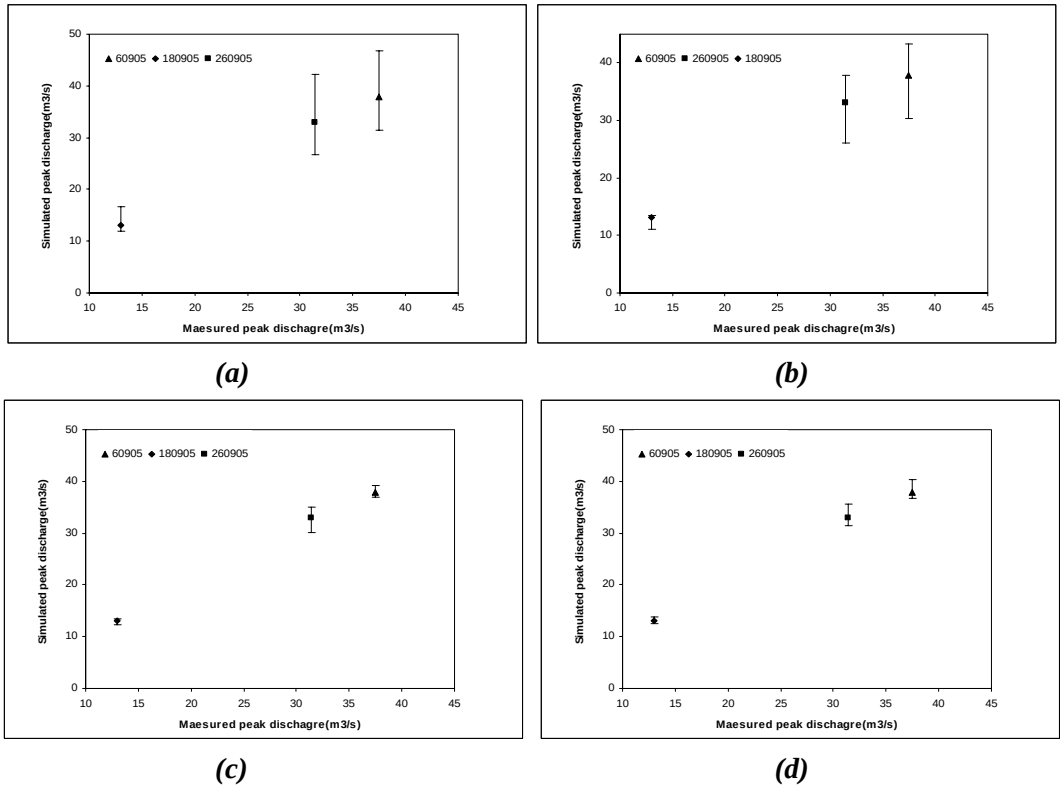

Figure 6-7: Peak discharge sensitivity to a 10% change in (a) initial soil moisture content, (b) saturated hydraulic conductivity, (c) surface roughness and (d) interception parameters.

In figure 6-7 panel a and table 6-10, the results shown the sensitivity to initial moisture content. The model predictions are much more sensitive to an increase of initial soil moisture content than to a decrease. For example, in the event 060905, the percentage changes in peak discharge prediction for adding 10% of the initial moisture content was found to increase peak discharge by 23.61%. Whereas subtracting 10% from the initial moisture content reduced peak discharge by 17.26%. Because the calibrated initial soil moisture values were close to saturation for all storms event, a 10% shift turns the soils into completely saturated. Thus very large peak discharges were simulated.

The results of changes in saturated hydraulic conductivity are shown in figure 6-7 panel b and table 6-10. The model predictions are much more sensitive to a decrease in hydraulic conductivity values than an increase. The percentage change in peak discharge from the 060905 event increased by 20.10% with subtracting 10% from hydraulic conductivity value and by the increase of 10% of hydraulic conductivity value, the peak discharge was reduced by 14.43%.

The model seems to be insensitive to changes in surface roughness and interception parameters as can be seen in table 6-10 and figure 6-7 panel c and d. The effects of increasing the interception and roughness values on the prediction of the catchment discharge results in a decrease of peak discharge of 6.67 % and 3.35 % respectively (event 060905). In contrast, decreasing 10 % of theses values was resulted in an increased peak discharge of 3.03 % and 2.79 % respectively.

Table 6-10: Model sensitivity to model variation of calibrated parameters by +10 % and -10 %.

parameters	Percent change in peak runoff (%)					
	event 060905		event 180905		event 260905	
	add 10%	subtract 10%	add 10%	subtract 10%	add 10%	subtract 10%
initial soil moisture content	23.61	-17.26	27.39	-8.57	28.04	-18.82
Saturated hydraulic conductivity	-14.43	20.10	-2.75	15.15	-14.94	20.98
interception	-6.67	3.03	-6.42	4.13	-8	4.94
Surface roughness	-3.35	2.79	-3.44	5.96	-6.34	8.69

It is concluded that the modelled is most sensitive to saturated moisture content and the initial soil moisture content, and to a lesser extent to roughness and interception.

The results of sensitivity analysis on all parameters as shown above indicate that the most important parameters and uncertainty are saturated conductivity and initial moisture content. These parameters should be measured as accurately as possible in the field to improve the model predictions. The same conclusion has been reached in other sensitivity analyses of the LISEM model. For example, DeRoo (1996) performed sensitivity analyses and found that the most sensitive variable in the prediction of

runoff is saturated conductivity and also De Roo and Jetten (1999) identified saturated conductivity and initial moisture content as being very sensitive parameters.

6.6. Senarios generation

The objective of the study was to evaluate the effects of different land use scenarios and different in rainfall magnitudes on the rate of predicted surface runoff in catchment. The scenarios that were used in the present study were designed to consist of two tasks including land use scenarios and rainfall size scenarios.

6.6.1. Land use scenarios

Although the models might not be able to accurately predict future events they may be used to simulate different land use scenarios (Hessel et al., 2003; Jetten et al., 1999). In the case of scenario, the same uncertainty in input data applies to all scenarios and one can therefore assume that the differences produced for the different simulations are in fact a consequence of the applied scenario changes. Therefore in order to evaluate the effects of the different land use scenarios, three land cover scenarios were developed:

- Scenario base: Present situation.
- Scenario A: Changing the entire catchment under forest, the values of all parameters used were converted to those used for representing forest area.
- Scenario B: Changing the land use to corn cultivation before harvest, the values of all the parameters used were converted to those used for representing cornfields before harvested.
- Scenario C: Changing the land use to corn cultivation after harvest, the values of all the parameters used were converted to those used to account for cornfields after harvest and the soil being bare.

Table 6-11: Summary of change in peak runoff and their arrival time for selected event (060905) due to different land use scenarios.

Scenarios	Peak discharge(m^3/s)	Change in peak discharge [a]	Peak arrival time different (hr)	Total discharge (m^3)
Present situation	37.90	0	0.0[b]	593,152
Entire basin forested (A)	9.27	-76%	2.0	177,042
Change from forest to cornfield before harvest (B)	184.14	5X	-2.0	2,183,872
Change from forest to cornfield after harvest (C)	193.93	6X	-3.0	2,267,746

Note: [a] Compared to present situation

[b] Peak time of present situation is 3½ hours

The results of the scenario simulation are shown in table 6-11. Converting the whole catchment into forest cover results in an overall decline in the amount of surface runoff and peak discharge from the

watershed. It also increases the peak time of runoff from the catchment. The peak runoff predictions were found to be decreased by 76%, total discharge decreased by 70% and peak arrival time was delayed by two hour from present land use. In contrast, the effects of changing to corn cultivation show the opposite results of the previous scenario. For peak runoff, the predictions of the cornfield scenario before harvest were found to be 5 times greater than that of the present land use and in the case of the after harvest scenario, the peak runoff was found to be about 6 times greater than that of the present land use. The peak time decreased to 2 hour and 3 hour under cornfield before harvest and after harvest condition respectively. In scenarios B and C, total discharges were found to be about 4 times greater than that of the present land use. This indicates that the effect of cornfield cultivation brings about an increase in the amount of surface runoff that generated large water volumes flowing out of the catchment. The extent of the overall increase in both cases shows that expanding areas of agricultural practices in the watershed could result in an extensive increase in amount of surface runoff.

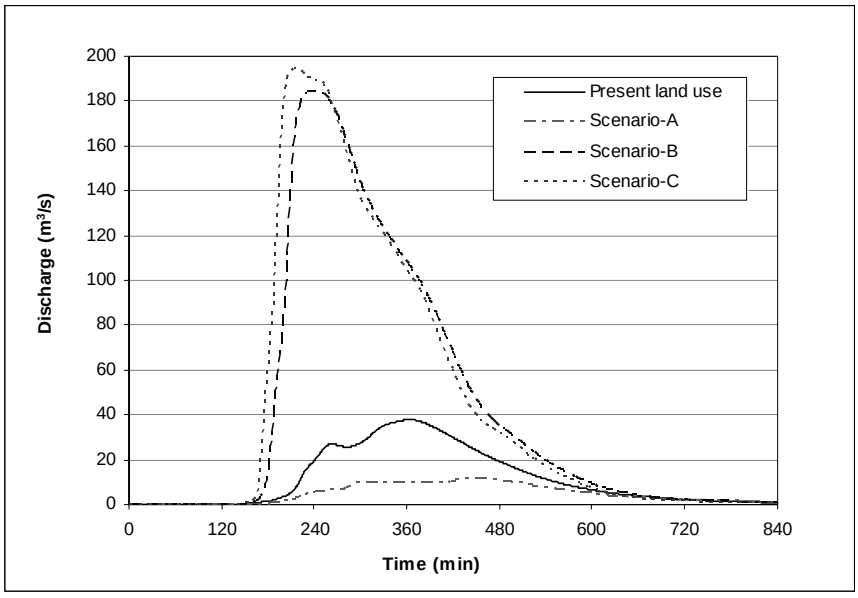

Figure 6-8: Predicted hydrograph for different land use scenarios.

The hydrographs on figure 6-8 shows the discharge pattern in the Nam Chun catchment as predicted by the present land use and the three case scenario studies. The hydrographs show significant changes on all scenarios. In forest scenario, the hydrograph reduced the peak runoff as well as the overall discharge pattern of the river. In contrast, the hydrographs show significant increase in the predictions of the scenario from the predictions of the present land use on changes to corn cultivation and also indicate a sharp increase in peak runoff.

6.6.2. Rainfall size scenarios

To understand the runoff characteristics of the study area during extreme rainfall events on the downstream portion, large historical storms should be considered. However, the historical hourly rainfall recorded data was not available. Therefore, a synthetic storm was designed based on rainfall data of 6 September 2005 by multiplying with certain factor and comparing to the maximum daily rainfall at Lom Sak station in the period 1952 to 2002. This was used to predict the event reoccurrence (return period) using Gumbel extreme values method (the results showed in appendix 5). All other setting parameters remain unchanged.

Since the storm used is only hypothetical it is not possible to assess how far its results would reflect the real situation (Hessel, 2002). The hydrographs simulated at the outlet of the catchment were used for further analysis to assess the flood hazard in lowland area (chapter 7).
The following multiplying factors were used to obtain hydrographs of predefined return periods:

- 060905 event with multiplying factor 1 (2 years return period): base simulation
- 060905 event with multiplying factor 1.5 (5 years return period)
- 060905 event with multiplying factor 2.0 (10 years return period)
- 060905 event with multiplying factor 2.5 (20 years return period)
- 060905 event with multiplying factor 3.0 (50 years return period)

In table 6-12 and figure 6-9: the results show that the influence of land-use conditions on storm runoff generation depends greatly on the rainfall event characteristics.

Table 6-12: Effect of storm size on scenarios results.

Increase rainfall*	Present land use		Scenario-A		Scenario-B		Scenario-C	
	Qp	Qtot	Qp	Qtot	Qp	Qtot	Qp	Qtot
1 (Tr 2)	37.90	593,152	9.21	177,402	184.14	2,183,872	193.93	2,267,746
1.5 (Tr 5)	162.68	1,921,274	46.18	627,268	320.93	3,997,048	336.06	4,087,745
2 (Tr 10)	303.07	3,554,639	167.86	1,903,857	461.32	5,823,994	479.99	5,916,482
2.5 (Tr 20)	441.37	5,289,931	305.22	3,427,952	603.36	7,660,082	624.44	7,753,465
3 (Tr 50)	577.33	7,067,950	445.46	5,071,631	746.43	9,507,977	769.01	9,604,245

Note: *; given as multiplication factor, Qp : peak discharge (m^3/s), Qtot : total discharge (m^3)

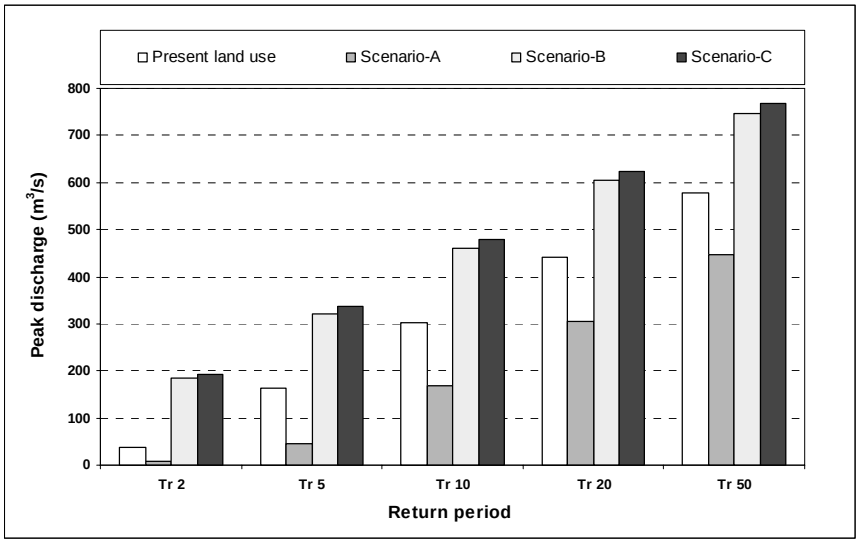

Figure 6-9: Effect of different scenarios on peak discharge with return period of 2, 5, 10, 20 and 50 years.

The prediction was very sensitive to storm size: a storm of one and a half size (multiplying factor 1.5) of the original storm produced 4 times the peak runoff from the original event (present situation). On scenario A (entire forest) also was affected by storms size. The reason for this is probably due to the fact that with increasing storm size infiltration becomes less important. However, the results showed decrease in the peak discharge and runoff amount in cases of high rainfall events therefore, the reducing effect of the catchment on the amount of runoff brought on by foresting the entire catchment could perhaps prevent the occurrence of disastrous floods downstream.

7. Flood modelling

In order to quantify the effect of the upper catchment runoff, a combined 1D2D hydraulic model is used to model the propagation of the flow over flat terrain. SOBEK 1D2D model combines one dimensional channel flow with overland flow, which is represented by a 2D-grid of elevation information. The overall methodology of the modelling is indicated in figure 7-1

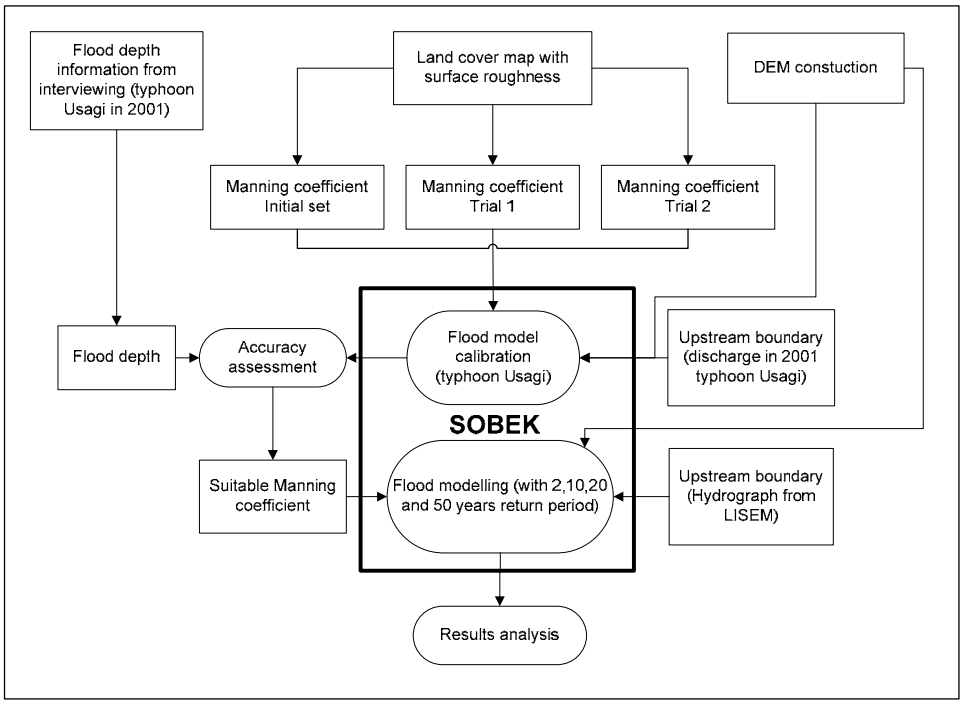

Figure 7-1: The overall methodology for flood modelling.

A 1D2D hydraulic flood model requires a digital elevation model (DEM) in order to represent the topography of the downstream floodplain and to determine the direction of water flow. In this study, a 10 m DEM resolution was created using 1 m contour lines and spot height which obtained from Mapping division, LDD. The upstream boundary conditions were derived from the hydrological modelling (LISEM) from the upstream part. The model was calibrated using the surface roughness coefficient as calibration parameter by comparing the model result (water depth and flood extent) with field observations of the 2001 flood caused by typoon Usagi. These observations were collected during the fieldwork. The output will be the Manning's coefficient to be used in the final flood scenarios modelling. In this study, the flood modelling only focuses on the flooding attributed by the Nam Chun River and not of floods caused by the Pa Sak river (see figure 7-7). The scenarios in this study will be a combination of different land covers in the upstream area and different rainfall events with known return periods (see chapter 8).

7.1. Model data input

Four main input data were used in 1D2D hydraulic modelling which included: 1) The digital elevation model which represents the natural topography and artificial structures such as embankments and the road network, 2) surface roughness data to represent the resistance of the water flow on different vegetation types along the river channel and the floodplain, 3) river cross sections that represent the shape of river and also the elevation and finally 4) boundary conditions which can be water level, discharge in time series and also the Q-H relation. The required data are described in detail below.

7.1.1. DEM construction

"A digital elevation model (DEM) is a numerical representation of topography, usually made up of equal-sized grid cells, each with value of elevation" (Chaplot et al., 2006). In many GIS applications DEM is used for basin characterization, soil distribution, geological mapping, and the hydraulic modelling of the relatively flat floodplain which requires very accurate height estimation (Maune, 2001). Hence one of the most important scientific challenges for flood modelling is the development of high resolution DEM of large areas which can represent the terrain in high accuracy in order to be close to the real flooding condition.

7.1.1.1. DEM of floodplain construction

In this study, the DEM of the lowlands of the Nam Chun downstream area was obtained from the integration of contour lines and spot heights. These data were derived from photogrammetric procedures using aerial photographs of scale 1: 4,000 and data processing was done by Mapping Division, Land Development Department, Bangkok, Thailand. Contour lines with contour intervals of 1 meters and spot height information with vertical accuracy of 0.1 meters were used (figure 7-2). The digital contour lines were converted to point data with an equivalent distance of 50 meters. Then two point data sets were combined into one file. The DEM was then created using point interpolation method following the geostatistical tool in ArcGIS. Before starting the interpolation, the spatial correlation of the data set was established. The omnidirectional method was used to investigate spatial correlation structure of input data. The lag interval was specified at 30m. The omnidirectional method determines semi-variogram values in all directions. The interpolation was done by choosing a Guassian semi-variogram model that appeared to fit the data best (assessment based on a least-square fitting method). The points were interpolated with a 10m pixel size using ordinary kriging interpolation method. This cell sizes was considered to have a suitable balance between computational time and data processing during further modelling for flood prediction.

7.1.1.2. DEM of embankment and road network construction

The embankment, road network and river network were digitized from a 1: 25,000 ortho-photo maps (LDD, 2002) in a separate layer. Segment maps, embankment and road network were converted into raster format. A heights point map was derived from survey observations and was interpolated using the nearest point interpolation method and masked with embankment and road network map. The

DEM with the embankment and road network was thus created. Apart from that, river network was converted to a raster map separately.

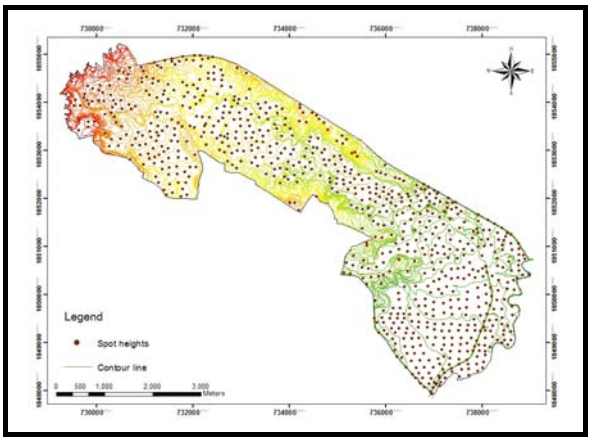

Figure 7-2: Spot heights and contour lines of the Nam Chun floodplain area.

7.1.1.3. Final DEM construction

The DEM of the floodplain, the DEM of the embankment and road network and rasterized river network were combined with each other using map calculation function in ArcGIS. The overall methodology of the final DEM creation is shown in figure 7-3, and the resulting DEM is shown in figure 7-4.

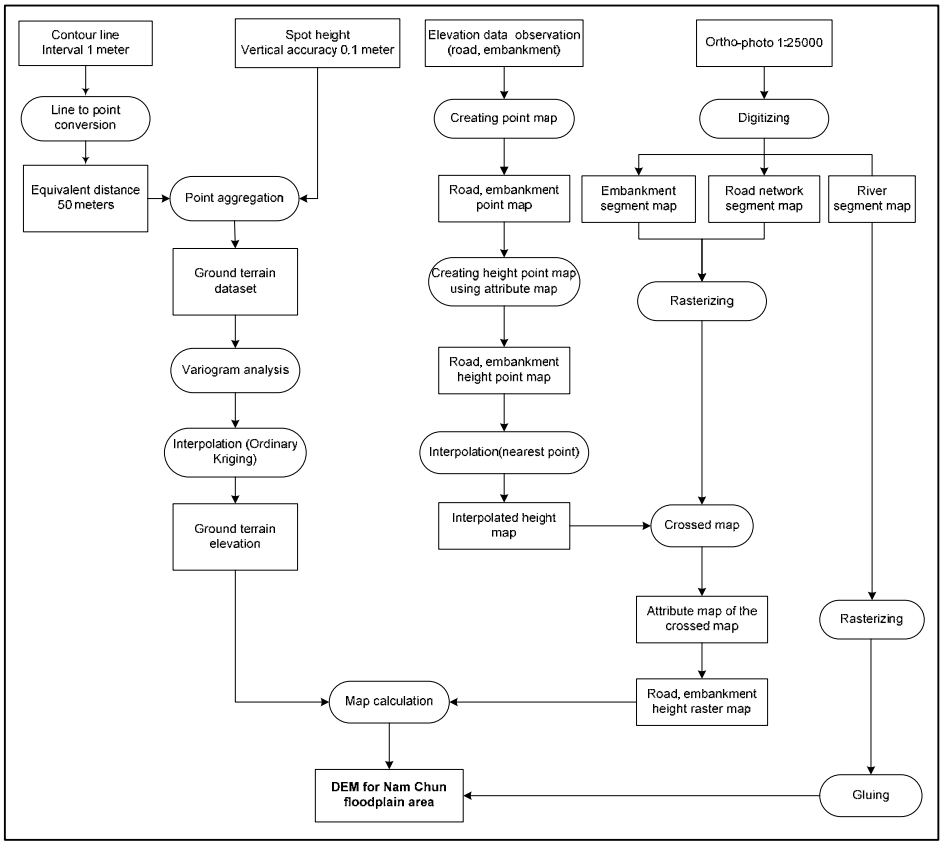

Figure 7-3: Flow chart creation of the digital elevation model of the Nam Chun floodplain area.

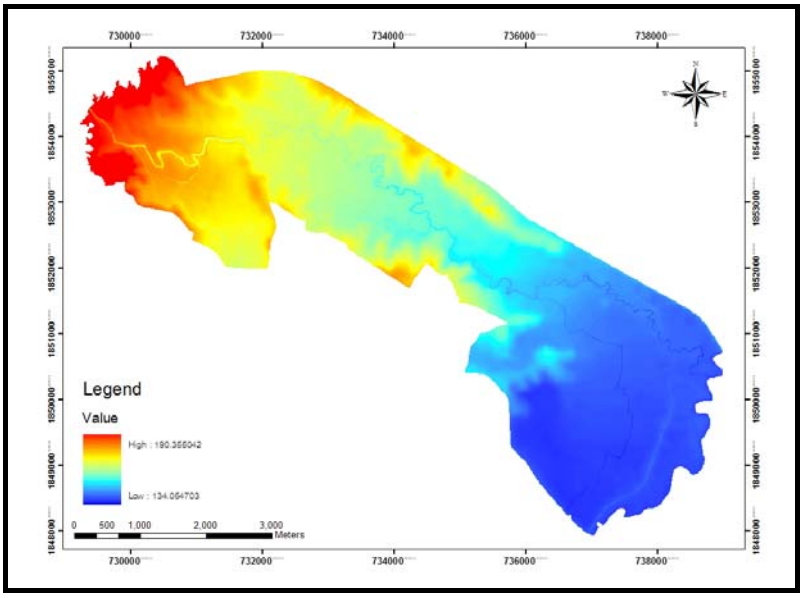

Figure 7-4: Digital Elevation Model of the Nam Chun floodplain area.

7.1.2. Boundary condition

In this study, there are four boundary condition nodes were used in the 1D2D flood modelling which include:

- One 1D node upstream boundary of Nam Chun river input data (discharge timeseries) was obtained from the output of the runoff modeling (LISEM) for flood events in three scenarios (scenario-A: entire forest, scenario-B: entire cornfield before harvest and scenario-C: entire cornfield after harvest) and the present land use for the return period of 2 years, 10 years, 20 years and 50 years. The discharge hydrograph for each scenario are illustrated in figure 7-5.
- One 2D node, the downstream boundary of this node is water level constant
- Two 1D2D internal boundaries nodes of the downstream boundary condition are defined by the daily water level of Pa Sak river. The Nam Chun river is also affected by the fluctuation of the Pa Sak river. Values for return period are derived from Royal Irrigation Department.

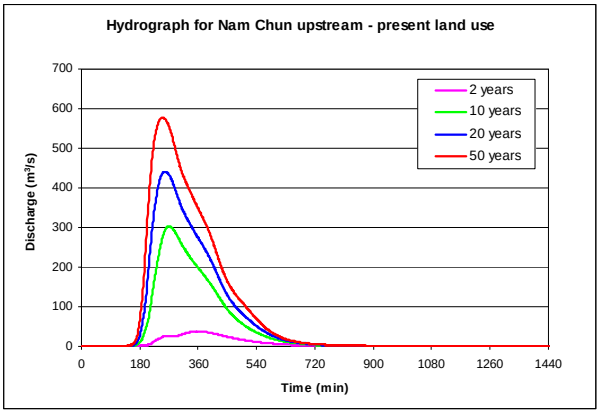

(a)

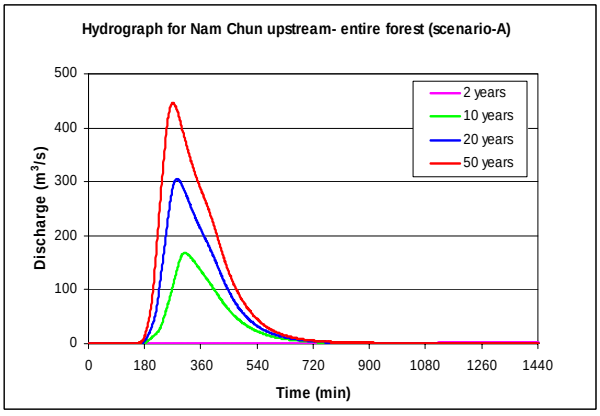

(b)

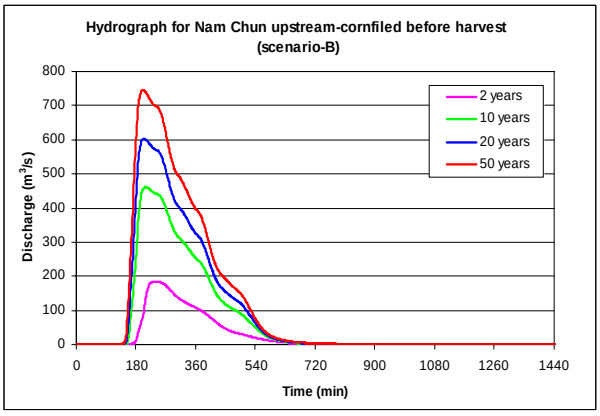

(c)

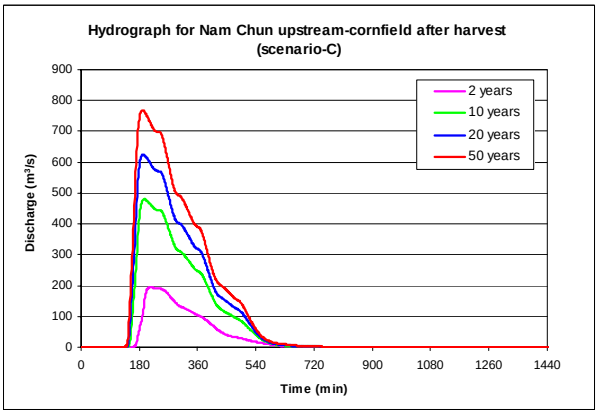

(d)

Figure 7-5: Boundary condition for Nam Chun upstream: (a) present land use, (b) scenario-A, (c) scenario-B and (d) scenario-C.

7.1.3. Surface roughness

In flood modelling, the resistance to flow is required to show the flood characteristics on floodplain. The resistance of flow is parameterized by the roughness coefficient. A roughness coefficient represents the effect of the channel bank and bed particles as well as from losses attributed to dynamic alluvial bed forms and vegetation of various types located along the banks and floodplain (Maidment, 1993).

The Land cover map was classified by visual interpretation of aerial ortho-photo at the scale of 1:25,000 (LDD, 2002). Units of uniform land cover were digitized on screen and classified according to the land use classification standard of Land Development Department of Thailand (LDD, 1999) In addition, the land cover map was created after field verifications. The land cover map is shown in figure 7-6. The classification of the land cover for the study area consists of ten classes among of which rice fields occupy 55 % of total area. The land cover map was transformed into surface roughness values according to Manning's coefficients (Chow, 1959). These coefficients were specified for different land cover classes (table 7-1).

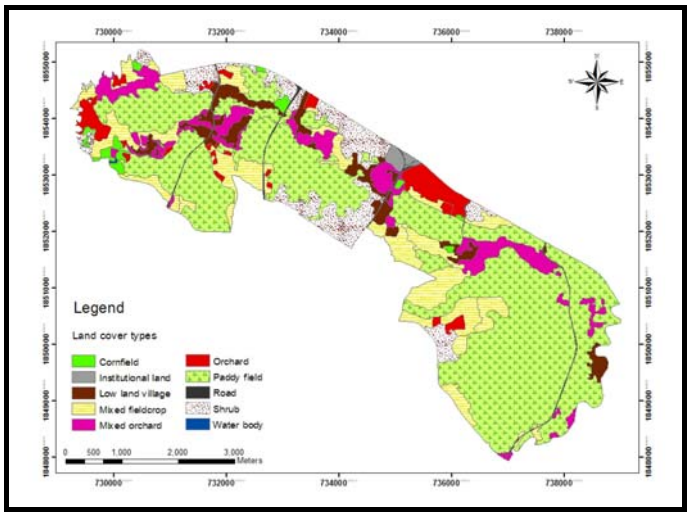

Figure 7-6: Land cover types of the Nam Chun floodplain area.

Table 7-1: Manning's roughness coefficient used for floodplain surface roughness of the model (Chow, 1959).

Land cover types	Manning's coefficient
Cornfield	0.045
Shrub	0.040
Mixed fieldcrop	0.035
Mixed orchard	0.150
Orchard	0.100
Paddy field	0.100
Institutional	0.001
Low land villages	0.150
Roads	0.001
Water body	0.033

7.1.4. Cross sections

In this study, cross sections data were derived from the DEM and by surveying during the fieldwork. The channel width and slope of river bank were measured and visually estimated. The river bed elevations were obtained directly from DEM.

7.2. Model schematization

The data input and network editing interface in SOBEK is called NETTER which allows the schematizing of all flood model components on the top of a background GIS layer map as can be seen in figure 7-7. NETTER has two editing modes including schematization and attribute edit modes. The schematization in this study consisted of boundary nodes, river cross sections, a 2D grid, connection nodes and etc, whereas their attributes are defined by the attribute editing modes.

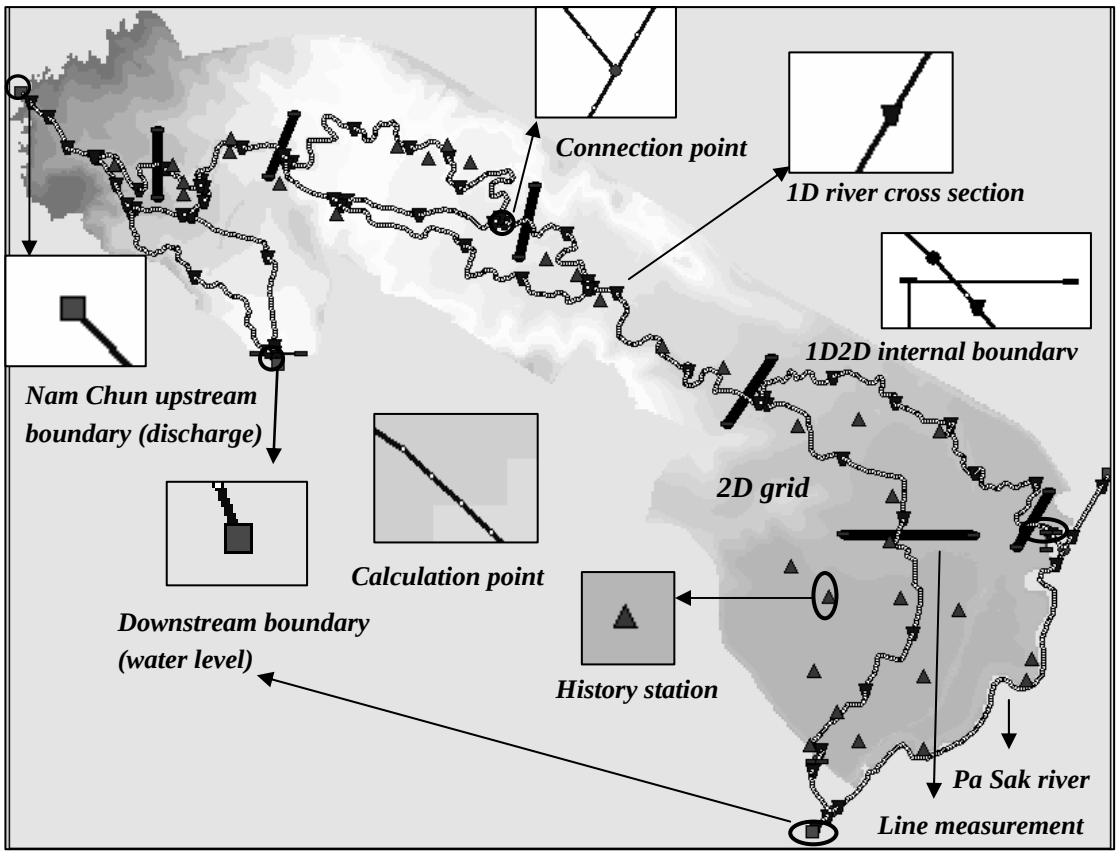

Figure 7-7: Model Schematization in SOBEK 1D2D.

7.2.1. 2D network schematization

To start the schematizing of the 2D network, the DEM that has been developed and exported into ArcGIS ASCII format file can be imported directly to the schematization using 2D grid tool. The DEM values in each cell can be edited manually based on the row and column number using grid cell editor. The surface roughness values can be defined by a single value for the whole floodplain or

spatially distributed. In this study, the roughness map was based on the land cover map (see figure 7-6). After that, the 2D schematization is continued by defining the 2D downstream flow boundary node. This node will be connected with the 1D Pa Sak river using a flow connection node. So that the water levels in the Pa Sak river form the downstream boundary condition. Furthermore, some nodes called history stations can be placed directly on 2D grid in order to generated model output of water level, water depths and water velocity variation in time at a specific location.

7.2.2. 1D network schematization

The 1D network module represents the water flow system along the river or channel. The characteristic of the river flow is determined by the characteristics of the cross section, the surface level, the river bed level and the roughness. Creating a 1D network is done by defining a reach that represent a river and connect it together by connection nodes. The results is a straight line of river networks that then has to be shaped to follow the real geometry of the river by using "edit reach vector" mode.

In 1D schematization, cross section nodes are defined that represent the river profile. The shape of the riverbed affects the discharge pattern, so each reach should contain at least one cross section. In addition, calculation nodes are added along the river reach at 10m distance interval and these were connected to underlying DEM pixels. The river bed and surface level of each cross section were obtained directly from DEM. The cross section types were defined as trapezium shaped (figure 7-8). The channel roughness is also defined for each cross section with 0.04 constant value. Then, the bed levels and hydraulic radius are interpolated for each calculation point based on the cross section data though linear interpolation (figure 7-9). This is done automatically by SOBEK.

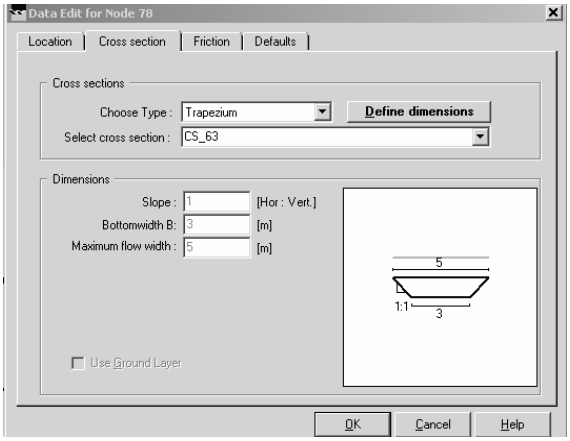

Figure 7-8: River cross section input window.

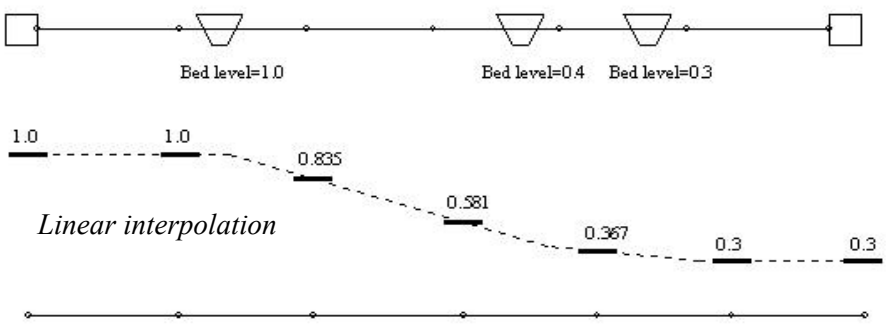

Figure 7-9: Linear interpolation method.

7.3. Model output

SOBEK generates several output files which are stored in ASCII file format which can be imported into any GIS system. The system also produces animation file which show the flooding progression. The output includes water levels, water depths, velocities, moment of flooding, flood duration and etc. These output files can be used later on to compute damage and the number of victims caused by a flooding and the risk. In this study, the maximum water depths and maximum velocity were used for flood hazard mapping.

7.4. Model calibration

There are several sources of errors which show deviations between the simulated model and recorded data as mentioned in section 6.3. Most model calibration procedures deal with finding the optimal set of parameters which result in acceptable differences between model output and observed data. For flood models, surface roughness values are usually used as the calibrating parameters. Therefore, the flood calibration was done by minimizing the deviation between the results of the flood modelling and the observed flood data, flood depth and flood extent. In this study, water depth data is obtained by interviews during the fieldwork. Information on the flood extent is not available. Thus the flood calibration is only based on flood depths. The flood depths of the typhoon Usagi on 2001 were used to assess the accuracy of flood depth prediction. During the fieldwork and interviews 50 flood depths points were collected.

The calibration process emphasizes on the different set of Manning coefficients. Three trials were decided by changing the Manning's roughness coefficient. The Manning's roughness coefficients used for each simulation are given below.

Table 7-2: Manning's roughness coefficient used for calibration of the model (Chow, 1959).

Land cover types	Initial run	Trial 1	Trial 2
Cornfield	0.045	0.040	0.050
Shrub	0.040	0.050	0.030
Mixed fieldcrop	0.035	0.450	0.250
Mixed orchard	0.150	0.200	0.110
Orchard	0.100	0.120	0.080
Paddy field	0.100	0.150	0.100
Institutional	0.001	0.011	0.001
Low land villages	0.150	0.200	0.150
Roads	0.001	0.001	0.001
Water body	0.033	0.033	0.033

The success of the model calibration were evaluated by comparing model results and observed data and by using objective functions including model biasness and root mean square error (RMSE). Brief overviews of these statistical measures are provided below.

- *Bias is calculated as follows:*

$$\frac{\sum_{i=1}^{n}(y_i - x_i)}{n} \qquad \textbf{(7-1)}$$

Where: n = total number of observations
x_i = the observed value
y_i = the model-simulated value

As can be seen from this equation, bias is calculated as the mean differences between paired observed and simulated values. Bias values closer to zero indicate better overall model performance.

- *Root Mean Square Error (RMSE)is calculate as:*

$$\sqrt{\frac{\sum_{i=1}^{n}(y_i - x_i)^2}{n-1}} \qquad \textbf{(7-2)}$$

Where: n = total number of observations
x_i = the observed value
y_i = the model-simulated value

As shown, RMSE is the square root of the average values of the squared prediction errors. This statistic is used to measure the discrepancy between modeled and observed values on an individual basis which indicates the overall predictive accuracy of a model. Due to the quadratic term, greater weight is given to larger discrepancies. With this measure, smaller values indicate better model performance.

Furthermore, the accuracy of predicted model values can be done by normality test based on skewness and kurtosis by dividing the skewness and kurtosis value by their standard errors. The normally distributed data should have skewness and kurtosis values within +2 to -2 (Bin Abdul Rahman, 2006). The statistical values for error data set are shown in table 7-3 below.

Table 7-3: Statistical measure value for error datasets of flood model with initial run, trial 1 and trial 2.

Statistics	Initial Run	Trial 1	Trial 2
Bias (unit = meter)	0.35	0.19	0.27
RMSE (unit = meter)	0.81	0.55	0.60
Skewness	0.574	-0.804	0.943
Standard error of skewness	0.343	0.343	0.343
Kurtosis	0.206	1.797	1.037
Standard error of kurtosis	0.674	0.674	0.674

As can be seen in figure 7-10, the flood water depth predictions derived from three trails neither underestimate nor overestimate the flood depth of the typhoon Usagi. These errors might be

contributed by the information on water depth derived through the interviews, which may be bias. Besides that, the DEM used may not represent the real topography.

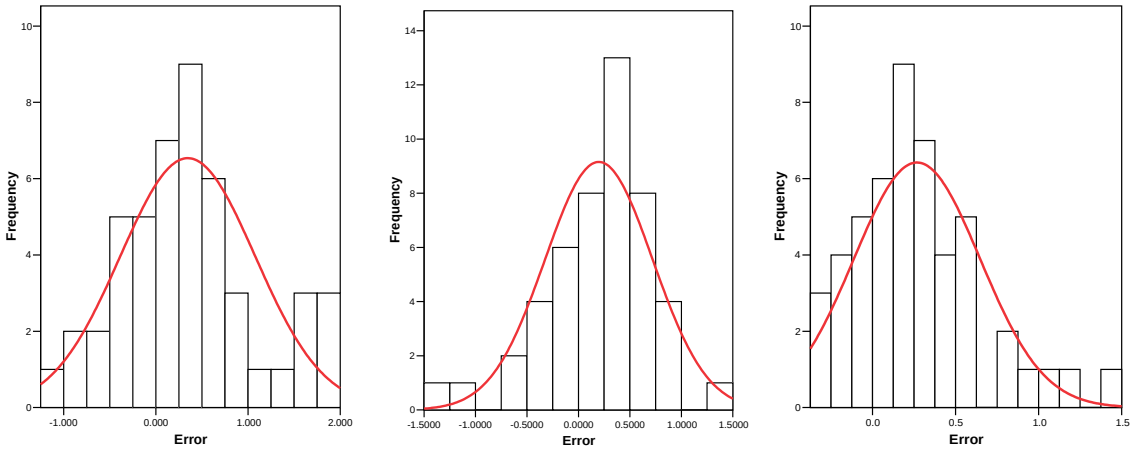

(a) ***(b)*** ***(c)***

Figure 7-10: The histogram of maximum water depth prediction error (RMSE) for flood modelling with different Manning coefficients, (a) initial Manning coefficient, (b) trial 1, (c) trial 2.

Further analysis was carried out on the comparison of prediction errors (RMSE) between 3 sets of Manning coefficient through paired-sample t-test. According to the *t*-test at 95% confidence interval, the error dataset of all Manning coefficient datasets are significantly different with exception trial 1 and initial data set (table 7-4). However, the trail 1 Manning coefficient seems to be suitable for further flood modelling.

Table 7-4: *t*- test between Manning coefficient datasets prediction error (RMSE).

	Initial Run	**Trial 1**	**Trial 2**
Initial Run	N/A	0.02	0.003
Trial 1		N/A	0.002
Trial 2			N/A

8. Analysis of effects of upstream land cover changes on downstream flood characteristics

In this chapter, a 1D2D flood model was used to quantify the effects of changing land cover on upstream catchment to flood characteristics on downstream portion of the watershed. The model simulations were carried out for three case scenarios with some design floods (storm with 2, 10, 20 and 50 years return period) as mentioned in section 6.6. The results of each scenario were analyzed to see the different flood characteristics were compared with the present situation (present land use of upstream) in each return period. Comparison was assessed based on the spatial extent, maximum water depth, maximum flow velocity and total flood volume.

8.1. Comparison of different scenarios on flood characteristics

8.1.1. 2 years return period

The results shown in table 8-1 indicated that for a storm with a return period of 2 years, under present situation (present land use on upstream), the average inundation depth was 0.35 meters but at some places a maximum depth of 0.89 was reached. Only 8% of the territory was flooded at the lower part (figure 8-1). When the whole upstream catchment was transformed to cornfields (scenarios B and C), the maximum flood water depth downstream increased 2 times and the spatial flood extent on the floodplain increased more than 3 times. There was no flood downstream in case of the entire upland area cover by forest (scenario-A). The maximum flow velocity was highest on scenario-C (the whole catchment under corn cultivation after harvest and soil condition being bare thus no vegetation cover). However, there is small different on flow characteristics between scenario-B and scenario-C. This can be explained by the shape of hydrograph from upstream which are quite similar in term of volume of water and distributions of discharge magnitudes over time.

Table 8-1: Summary of flood characteristics on different scenarios with 2 years return period.

Total area 25 km^2	**Present situation**	**Scenario-A**	**Scenario-B**	**Scenario-C**
Flood area (km^2)	1.92	0.07	7.27	7.65
Total flood volume (10^6m^3)	0.29	0.00	2.69	3.20
Average depth (m)	0.35	0.14	0.96	0.98
Maximum depth (m)	0.89	0.41	2.21	2.25
Maximum velocity (m/s)	1.11	0.12	5.51	5.8

Maximum water depth

The maximum water depth maps of scenarios B and C are quite similar except for a small inundation area at lower portion which was higher in scenario-C (figure 8-1 and table 8-2). In contrast, scenario-A shows a different result: The flood water inundated the area along the riverbed and a small portion near downstream boundary close to the Pa Sak river.

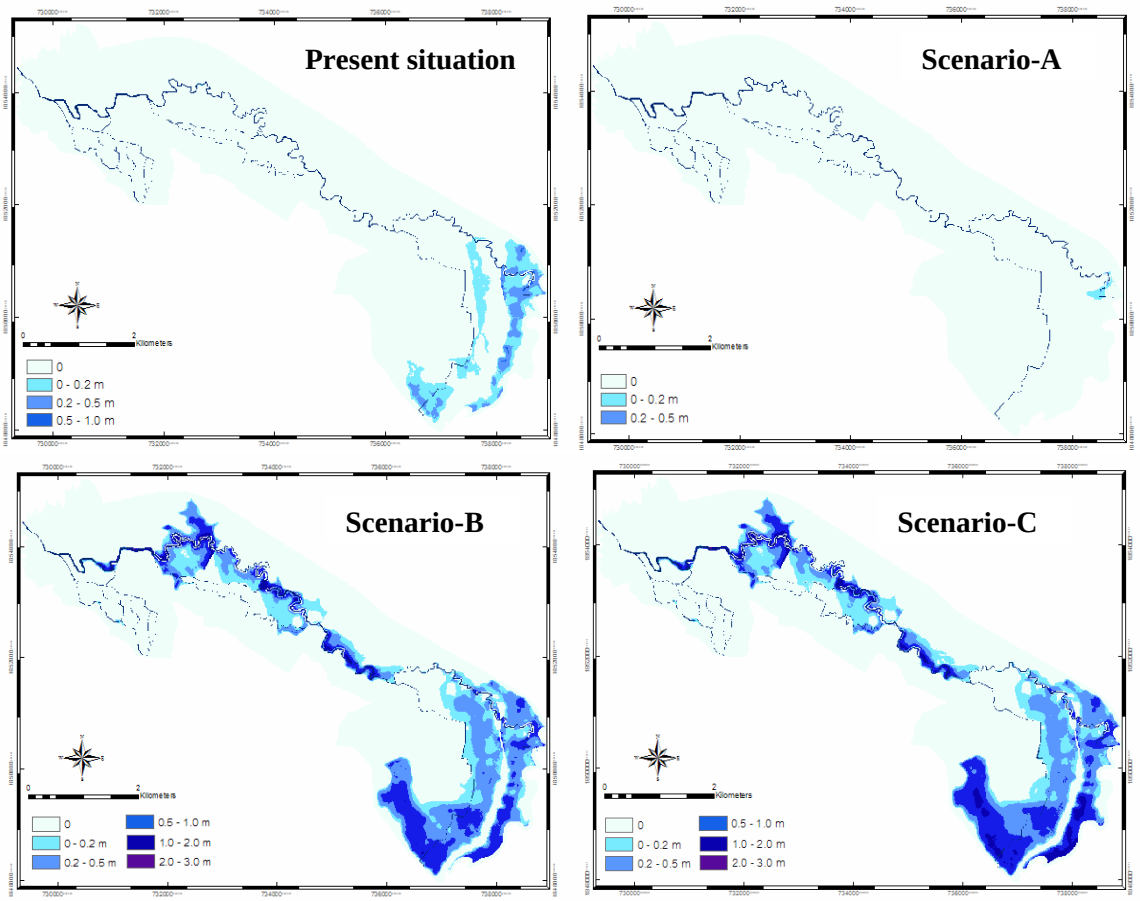

Figure 8-1: The spatial distribution of maximum water depth of the three scenarios and present land use with 2 years return period.

Table 8-2: Surface area (% of flooded area) per maximum water depth class with 2 years return period.

Water depth (m)	Present situation	Scenario-A	Scenario-B	Scenario-C
0 - 0.2	71	100	30	28
0.2 - 0.5	29	0	42	37
0.5 - 1.0	0	0	24	27
1.0 - 2.0	0	0	4	8
2.0 - 3.0	0	0	0	0
> 3.0	0	0	0	0
Total (km^2)	100 (1.92)	100 (0.07)	100 (7.27)	100 (7.65)

Maximum flow velocity

Figure 8-2 shows the distribution of the flow velocity for scenarios A, B and C. In most cases the flow velocity does not rise above 0.30 m/s. Only along the river bed and the road higher velocity are found especially in scenario-B and scenario-C.

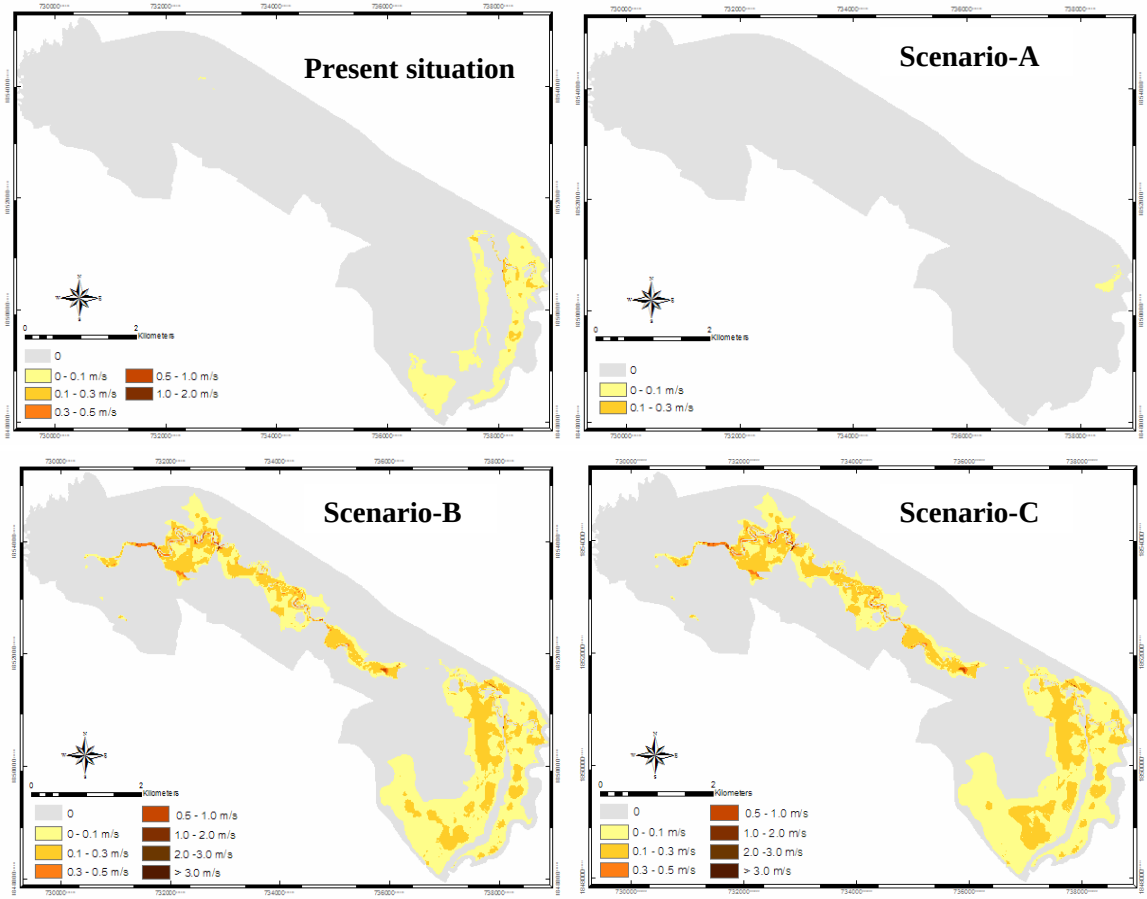

Figure 8-2: The spatial distribution of maximum flow velocity of the three scenarios and present land use with 2 years return period.

Table 8-3 shows that in scenario-C, the same flow velocity class is larger than in scenario-B and only 36% of flooded area the water flow with speed higher than 10 centimeters per second. In the present situation and scenario-A, the flow velocities are much lower than 10 centimeters per second.

Table 8-3: Surface area (% of flooded area) per maximum water velocity class with 2 years return period.

Water velocity (m/s)	Present situation	Scenario-A	Scenario-B	Scenario-C
0 - 0.1	94	100	65	64
0.1 - 0.3	6	0	34	35
0.3 - 0.5	0	0	1	1
0.5 - 1.0	0	0	0	0
1.0 - 2.0	0	0	0	0
2.0 - 3.0	0	0	0	0
> 3.0	0	0	0	0
Total (km^2)	100 (1.92)	100 (0.07)	100 (7.27)	100 (7.65)

8.1.2. 10 years return period

The results of the model simulation for a storm with a 10 year return period (table 8-4) revealed that the flood inundation covers 44% of the area, the average of maximum water depth was 1.25 meters but at some places a maximum depth of 2.96 was reached under present situation. In scenario-A, the downstream floodplain was inundated with average water height of 0.06 meter. The total of 2.28×10^6 m^3 water was stored in the flooded area in scenario-A, which is decreased to 58% from the present situation. In case of scenario-B and scenario-C, the total of flood water volume increased 2 times. The flood extent increased to 29% and 33% in scenarios B and C respectively as compared to present situation.

Table 8-4: Summary of flood characteristics on different scenarios with 10 years return period.

Total area 25 km^2	Present situation	Scenario-A	Scenario-B	Scenario-C
Area (km^2)	10.97	6.90	14.18	14.55
Total flood volume ($10^6 m^3$)	5.44	2.28	10.12	11.05
Average depth (m)	1.25	0.06	1.16	1.62
Maximum depth (m)	2.96	2.17	3.46	3.60
Maximum velocity (m/s)	5.78	5.03	6.48	6.87

Maximum water depth

Figure 8-3 shows the spatial distribution of flood extent in various scenarios: present land use, scenarios A, B and C. The flood water inundated 28%, 57%, 59% of the territory in scenario-A, scenario-B and scenario-C respectively, compared to 44% in the present land cover scenario. The flood area and water depth were larger at the lower part of floodplain due to low position. The maximum water depth of scenario-B and scenario-C higher than 1 meter covers 25% and 28% of flooded area (table 8-5). In scenario-A, the maximum depth of the flood water was lower than 50 centimeters and covers 44% of the flooded area at lower part.

Table 8-5: Surface area (% of flooded area) per maximum water depth class with 10 years return period.

Water depth (m)	Present situation	Scenario-A	Scenario-B	Scenario-C
0 - 0.2	27	34	17	15
0.2 - 0.5	32	43	27	26
0.5 - 1.0	27	20	31	31
1.0 - 2.0	13	3	23	25
2.0 - 3.0	1	0	2	3
> 3.0	0	0	0	0
Total (km^2)	100 (10.97)	100 (6.90)	100 (14.18)	100 (14.55)

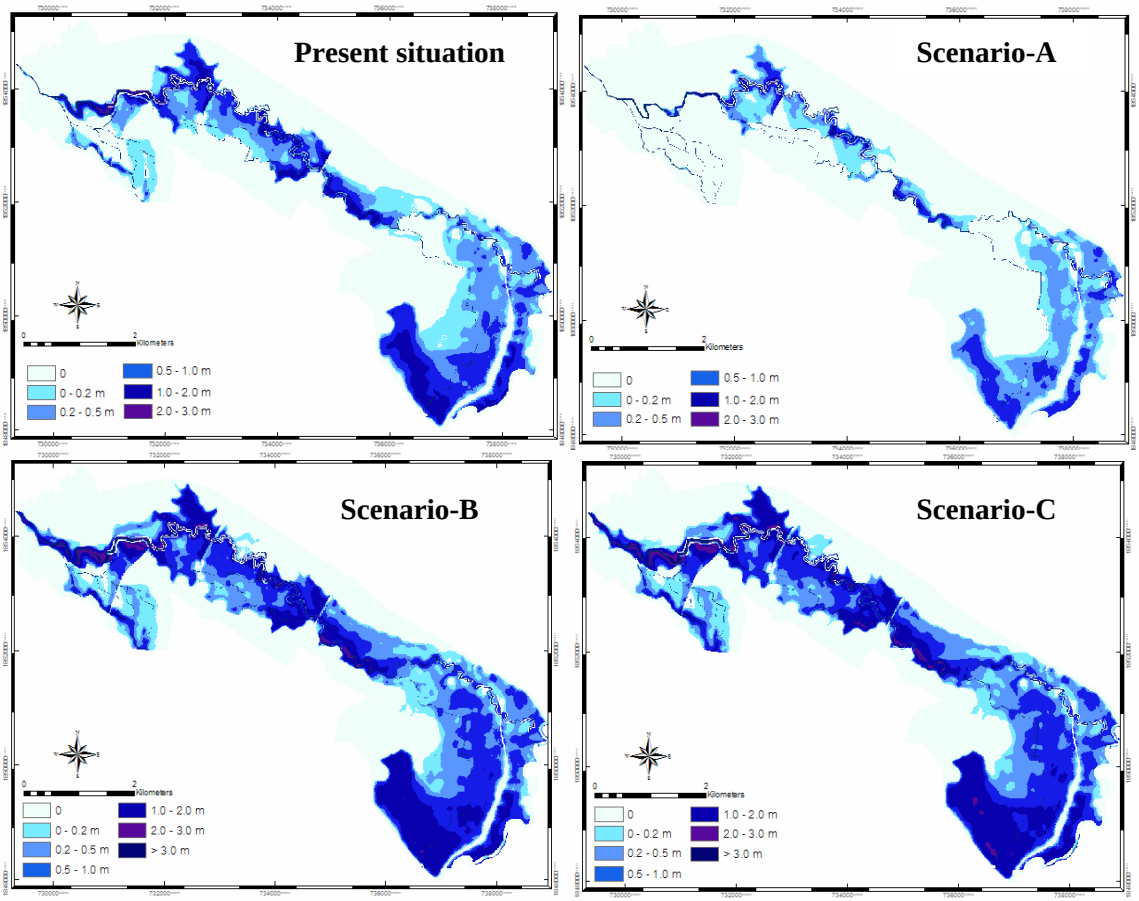

Figure 8-3: The spatial distribution of maximum water depth of the three scenarios and present land use with 10 years return period.

Maximum flow velocity

Figure 8-4 shows the distribution of the flow velocity for scenarios A, B and C. For most of inundated area the flow velocity does not rise above 0.30 m/s. For only 13% of flooded area, the speed of the water was higher than 30 centimeters per second. In scenario-B and scenario-C, the speed of the water flow is lower than 0.50 m/s but higher than 0.30 m/s covers 8% and 10% of flooded area, respectively (table 8-6). The high flow velocities are found near the apex of the stream, where the channel has the steepest gradient (see figure 8-4).

Table 8-6: Surface area (% of flooded area) per maximum water velocity class with 10 years return period.

Water velocity (m/s)	Present situation	Scenario-A	Scenario-B	Scenario-C
0 - 0.1	49	68	28	25
0.1 - 0.3	41	31	62	62
0.3 - 0.5	9	1	8	10
0.5 - 1.0	1	0	2	3
1.0 - 2.0	0	0	0	0
2.0 - 3.0	0	0	0	0
> 3.0	0	0	0	0
Total (km^2)	100 (10.97)	100 (6.90)	100 (14.18)	100 (14.55)

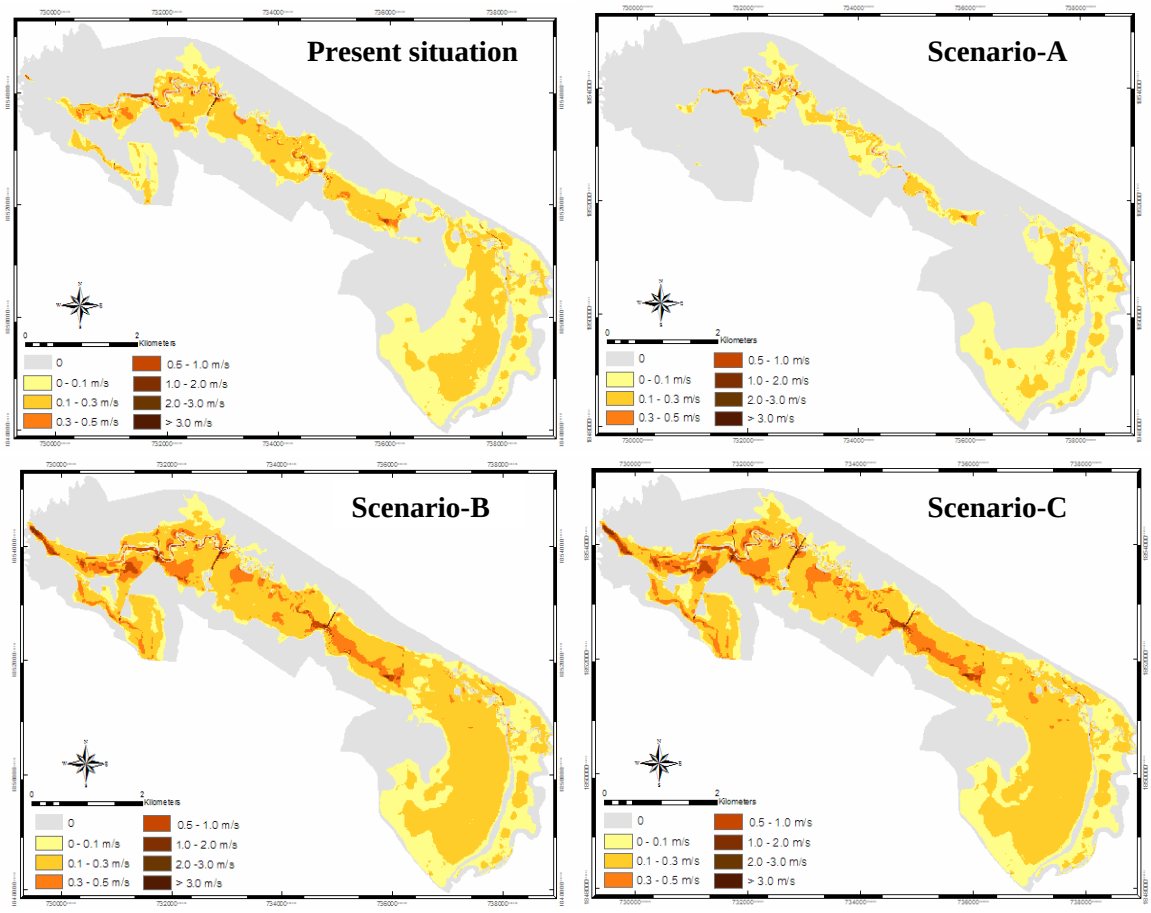

Figure 8-4: The spatial distribution of maximum flow velocity of the three scenarios and present land use with 10 years return period.

8.1.3. 20 years return period

With the 20 years return period storm event, the results of model simulation (table8-7) indicate that the inundated area of present situation cover 55% of the area. For other scenarios (A, B and C) it covers 43%, 64%, 63% respectively. In scenario-B, the total flood water volume was 19.59×10^6 m^3 which was 2 times higher than the present situation. In scenario-C, the total of flood volume was lower than scenario-B. This can be explained by the distribution of discharge over time. In scenario-C the design rain storm with a 20 year return period (annual probability of occurrence 5%), the discharge was higher at the beginning but after two hours the discharge was lower than in scenario-B (see figure 7-5). This affected the total volume of the flood water in scenario-B.

Table 8-7: Summary of flood characteristics on different scenarios with 20 years return period.

Total area 25 km^2	Present situation	Scenario-A	Scenario-B	Scenario-C
Area (km^2)	13.87	10.77	16.00	15.77
Total flood volume (10^6m^3)	9.47	5.21	19.59	14.66
Average depth (m)	1.53	1.24	1.87	1.79
Maximum depth (m)	3.40	2.96	3.90	3.97
Maximum velocity (m/s)	6.04	5.77	6.99	6.92

Maximum water depth

Figure 8-5 and table 8-8 shows that the maximum water depth maps of scenario-B and C are quite similar with only a small area at the lower part in scenario-B with higher water depth than scenario-C. In contrast, the maximum water depth (0.2 – 1.0 meter) and flood extent of scenario-C was higher and larger than in scenario-B, this are found near the apex of the stream because in scenario-C– the water propagates and inundates at the upper part then the less water drain to the lower portion. In scenario-A, most of the flood water depth did not rise up to 2 meters but in scenario-B and C found an area cover of 18% and 9% of flooded area with water depth higher than 2 meters and cover a surface area of 6% with water depth higher than 3 meters (scenario-B). 88% of flooded area in scenario-A was less than 1 meter water depth.

Table 8-8: Surface area (% of flooded area) per maximum water depth class with 20 years return period.

Water depth (m)	Present situation	Scenario-A	Scenario-B	Scenario-C
0 - 0.2	19	28	10	11
0.2 - 0.5	28	33	14	19
0.5 - 1.0	29	27	31	34
1.0 - 2.0	22	11	27	27
2.0 - 3.0	2	1	12	8
> 3.0	0	0	6	1
Total (km^2)	100 (13.87)	100 (10.77)	100 (16.00)	100 (15.77)

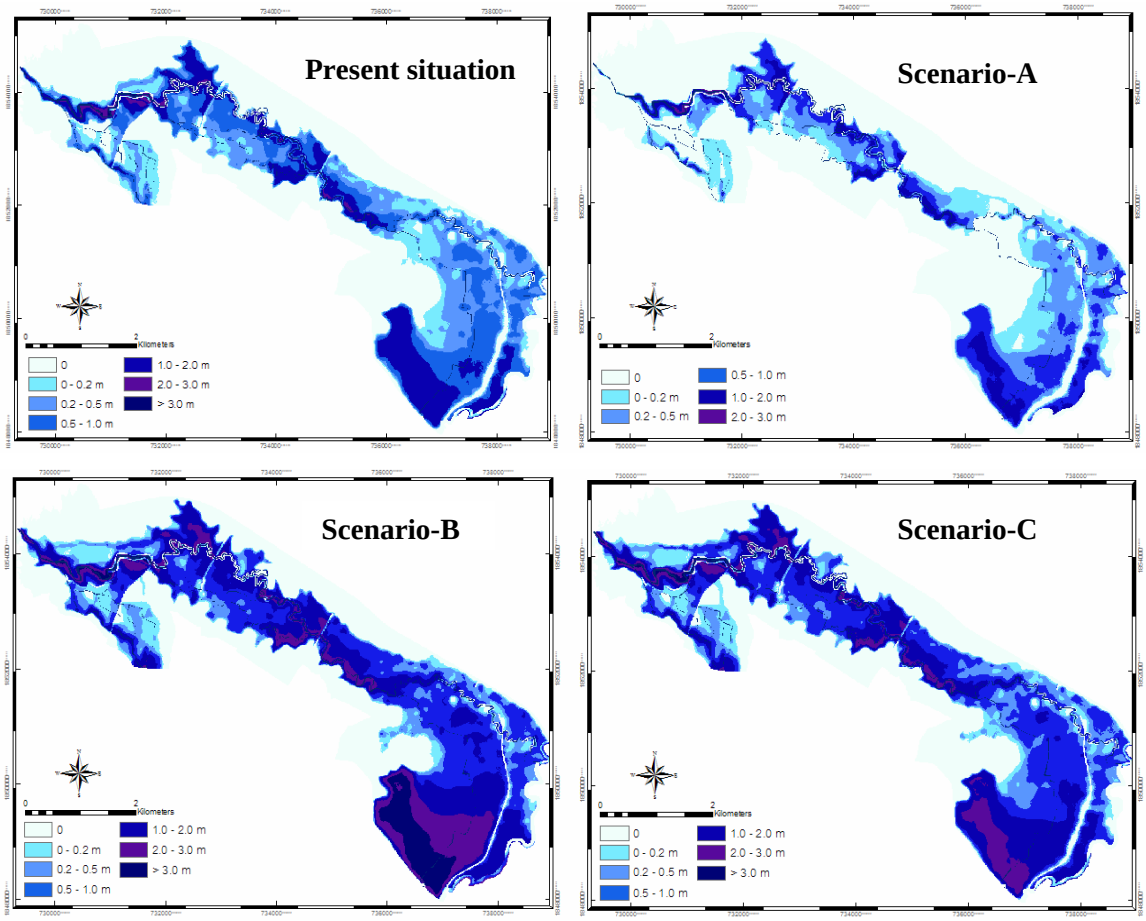

Figure 8-5: The spatial distribution of maximum water depth of the three scenarios and present land use with 20 years return period.

Maximum flow velocity

Figure 8-6 and table 8-9 show the distribution of the flow velocity for the present situation and scenarios A, B and C. For most of the inundated area the flow velocity did not rise above 0.50 m/s. In scenario-B and C, The speeds of water flow were lower than 0.50 m/s cover 97% and 96% of flooded area respectively (table 8-9) and cover 4% of the area with flow velocity higher than 50 centimeters per second. The high water flow velocities were found at the top of the downstream area (near the apex). In scenario-A, most of inundated area the flood flow velocity was lower than 30 centimeters per second. This means that, if the upland catchment became completely forest area, it will reduce the speed of the water flow in downstream area.

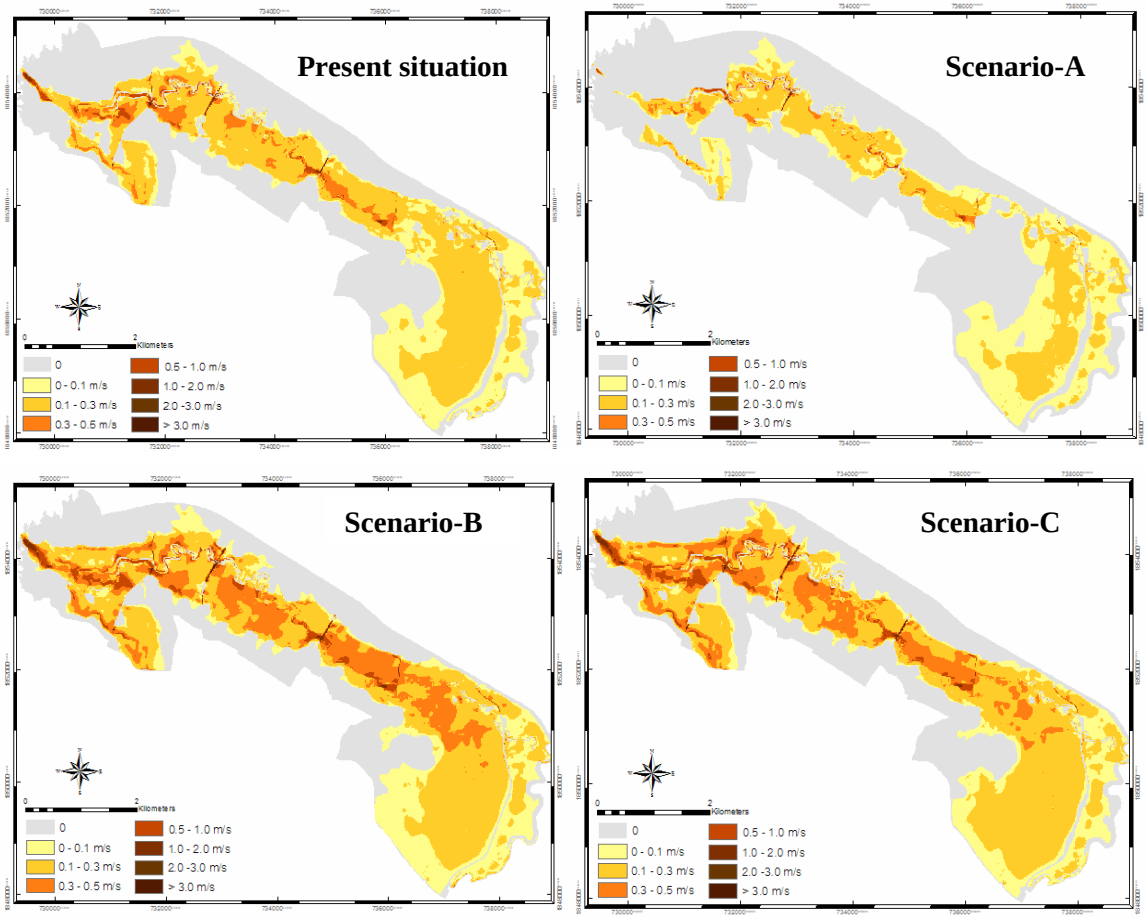

Figure 8-6: The spatial distribution of maximum flow velocity of the three scenarios and present land use with 20 years return period.

Table 8-9: Surface area (% of flooded area) per maximum water velocity class with 20 years return period.

Water velocity (m/s)	Present situation	Scenario-A	Scenario-B	Scenario-C
0 - 0.1	31	50	25	20
0.1 - 0.3	59	47	51	59
0.3 - 0.5	8	3	21	17
0.5 - 1.0	2	0	3	4
1.0 - 2.0	0	0	0	0
2.0 - 3.0	0	0	0	0
> 3.0	0	0	0	0
Total (km^2)	100 (13.87)	100 (10.77)	100 (16.00)	100 (15.77)

8.1.4. 50 years return period

The results in table 8-10 indicate that for a storm with a return period 50 years (with increased rainfall intensity and rain volume). Under present situation, the average inundation depth was 1.72 meters but at some places a maximum depth of 3.82 was reached. The inundation flood area covers 62% of the total area (figure 8-7). The average maximum flood depth was similar in all scenarios with the

exception of scenario-B which was higher. The total of flood volume was highest in scenario-B. This can be explained similarly as in section 8.1.3 for the design storm of 20 years return period. For scenario-A, the flood extent was almost similar with present situation. With intense rainfall, the downstream area trend to be flooded no matter what land cover in upstream catchment is.

Table 8-10: Summary of flood characteristics on different scenarios with 50 years return period.

Total area 25 km^2	Present situation	Scenario-A	Scenario-B	Scenario-C
Area (km^2)	15.43	13.63	16.85	17.01
Total flood volume (10^6m^3)	13.33	8.88	24.65	17.97
Average depth (m)	1.72	1.51	2.17	1.89
Maximum depth (m)	3.82	3.38	4.41	4.41
Maximum velocity (m/s)	6.94	6.12	6.99	6.90

Maximum water depth

Figure 8-7 shows the spatial distribution of the flood extent in the present land use, scenarios A, B and C. The flood water inundated 62%, 54%, 67% and 68% of the territory respectively. For the most inundated area the maximum depth of the flood water was lower than 2 meter in all scenarios. In scenario-B, the maximum flood depth was higher than 3 meters in 13% of flooded area in the lower part of floodplain. The flood depth ranges from 0.2 to 1 meter, in scenario-C which covers a larger area than in scenario-B that can be founded only at the upper part of downstream (table 8-11).

Table 8-11: Surface area (% of flooded area) per maximum water depth class with 50 years return period.

Water depth (m)	Present situation	Scenario-A	Scenario-B	Scenario-C
0 - 0.2	13	20	6	8
0.2 - 0.5	21	28	12	18
0.5 - 1.0	32	29	24	30
1.0 - 2.0	27	21	31	30
2.0 - 3.0	7	2	14	13
> 3.0	0	0	13	1
Total (km^2)	100 (15.43)	100 (13.63)	100 (16.85)	100 (17.01)

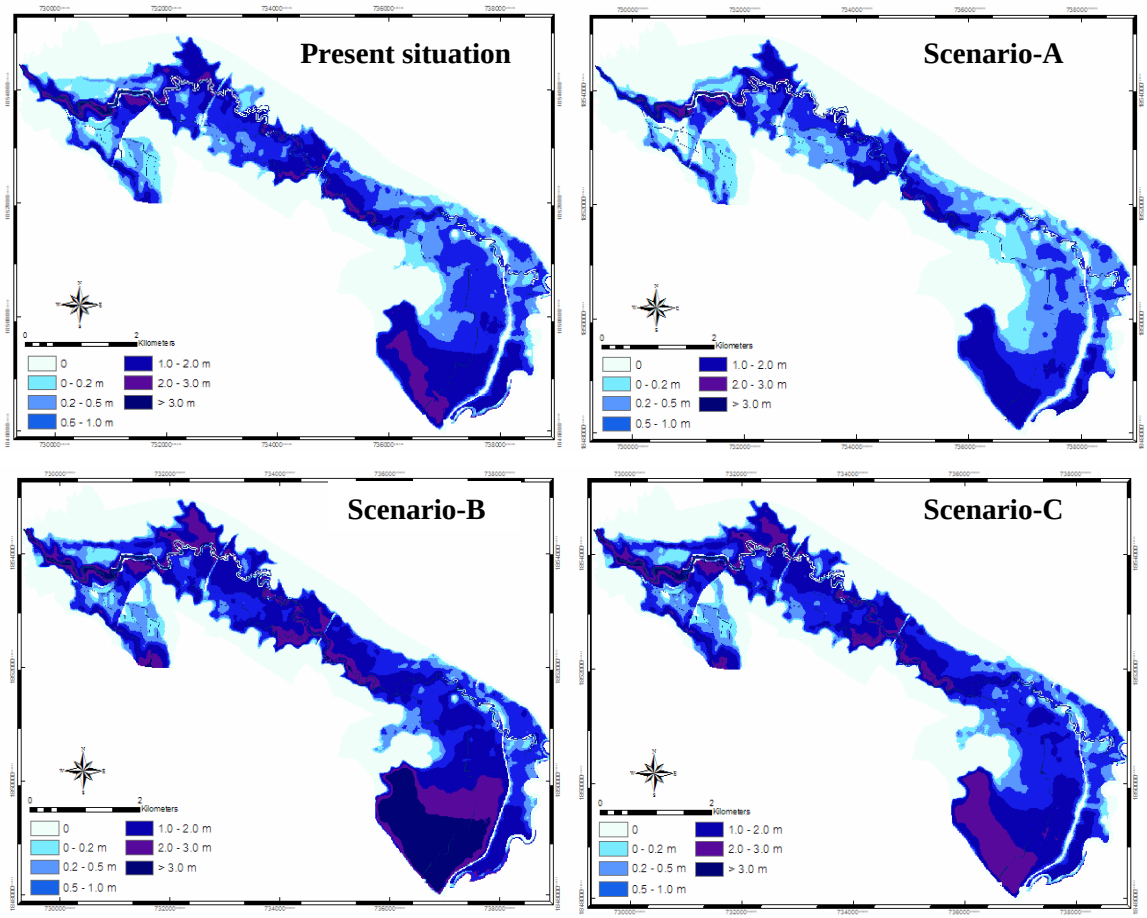

Figure 8-7: The spatial distribution of maximum water depth of the three scenarios and present land use with 50 years return period.

Maximum flow velocity

Figure 8-8 and table 8-12 show the distribution of the flow velocity for the present situation and scenarios A, B and C. For the most inundated area the flow velocity did not rise above 0.50 m/s. The speed of the water was higher than 50 centimeters per second which cover only in 7% of flooded area but not rise up above 1 meter per second. In scenario-B and C, the water speed was lower than 0.50 m/s and covers 93% of flooded area. The high water flow velocities were found at the top of downstream. In only 7% of flooded area in scenario-B and C, the speed of water flow was higher than 0.5 m/s but not rise above this stage. In scenario-A, most of inundate area the flood water velocity was lower than 30 centimeters per second. This means that- if the upstream catchment is under forest cover, it can reduce severe flash flood in the downstream territory.

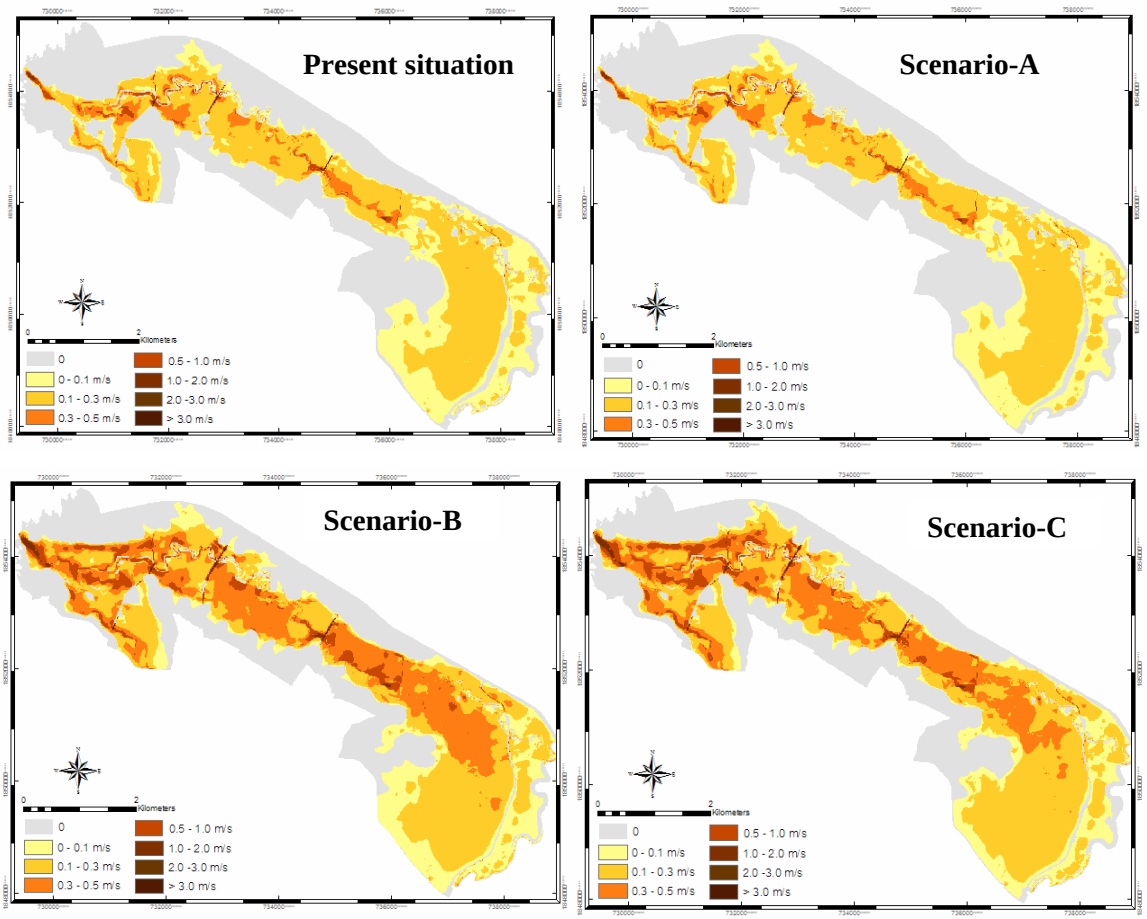

Figure 8-8: The spatial distribution of maximum flow velocity of the three scenarios and present land use with 50 years return period.

Table 8-12: Surface area (% of flooded area) per maximum water velocity class with 50 years return period.

Water velocity (m/s)	Present situation	Scenario-A	Scenario-B	Scenario-C
0 - 0.1	25	32	21	15
0.1 - 0.3	59	59	44	49
0.3 - 0.5	13	7	28	29
0.5 - 1.0	3	2	7	7
1.0 - 2.0	0	0	0	0
2.0 - 3.0	0	0	0	0
> 3.0	0	0	0	0
Total (km^2)	100 (15.43)	100 (13.63)	100 (16.85)	100 (17.01)

Summary tables for each flood characteristic are shown below:

Table 8-13: Summary for flood extent.

Scenarios	Flood extent (% of total area)			
	Tr2	Tr10	Tr20	Tr50
Present situation	8	44	55	62
Scenario-A	0	28	43	54
Scenario-B	29	57	64	67
Scenario-C	31	59	63	68

Table 8-14: Summary for flood volume.

Scenarios	Flood volume (10^6 m^3)			
	Tr2	Tr10	Tr20	Tr50
Present situation	0.29	5.44	9.47	13.33
Scenario-A	0.00	2.28	5.21	8.88
Scenario-B	2.69	10.12	19.59	24.65
Scenario-C	3.20	11.05	14.66	17.97

Table 8-15: Summary for maximum water depth.

Scenarios	Maximum water depth (m)			
	Tr2	Tr10	Tr20	Tr50
Present situation	0.89	2.96	3.40	3.82
Scenario-A	0.41	2.17	2.96	3.38
Scenario-B	2.21	3.46	3.90	4.41
Scenario-C	2.25	3.60	3.97	4.41

Table 8-16: Summary for maximum velocity.

Scenarios	Maximum velocity (m/s)			
	Tr2	Tr10	Tr20	Tr50
Present situation	1.11	5.78	6.04	6.94
Scenario-A	0.12	5.03	5.77	6.12
Scenario-B	5.51	6.48	6.99	6.99
Scenario-C	5.80	6.87	6.92	6.90

8.2. Flood hazard mapping

Flood hazard is the probability of occurrence of a potentially damaging flood event of a certain magnitude within a given time period and area (Brooks, 2003). In this chapter, flood hazard zonation maps was done from the results of flood model simulation applying rain storms of different return period. A different degree of hazard was assigned to each flood frequency. Five categories of flood hazard were established for each scenario:

- Areas with high flood hazard: high frequency floods – return period 2 years
- Areas with medium flood hazard: medium frequency floods – return period 10 years

- Areas with low flood hazard: low frequency floods – return period 20 years
- Areas with very low flood hazard: very low frequency floods – return period 50 years
- Areas without flood hazard

Figure 8-9 shows the flood hazard zonation for each scenario, for the present situation. The high flood hazard covers 31% of the area when the whole upstream catchment area is transformed into corn cultivation (scenarios B and C). In contrast, it became smaller in high flood hazard area if the upland area converted to forest.

Medium flood hazard (10 years return period) covers 36% of territory in present situation, scenarios-B and scenarios-C respectively. In scenarios-A the effect was only 28% of the area. The area under low flood hazard (20 years return period) covers only 3, 3, 2 and 1 km^2 for present situation, scenario-A, scenario-B and scenario-C respectively. This can be concluded that the flood hazard was reduced if upstream became forest. In contrast, when upland area is converted into agriculture area, the flood probability will increase and also flood hazard area.

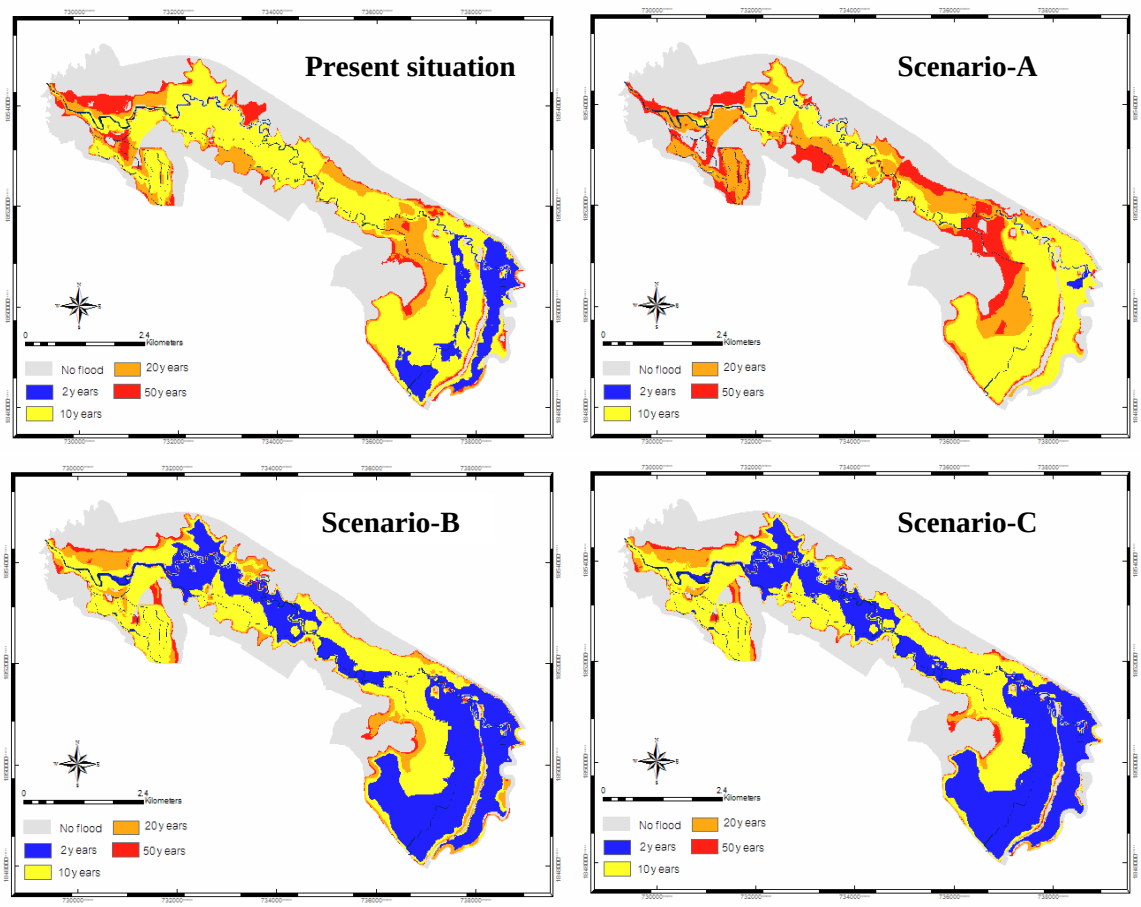

Figure 8-9: Flood hazard mapping of the three scenarios and present land use.

9. Conclusions and recommendations

9.1. Conclusions

The main objective of this research was to assess the flood hazard at downstream areas of the Nam Chun watershed, taking into account the influence of soil and land cover parameters upstream. The other objectives were to assess the effects of different land cover types on soil properties; assess the effects of soil parameters in influencing runoff and to assess the flood downstream consequence as a result of upstream land use changes by using an integrated hydrological model with a hydraulic model. Based upon the results discussed in previous section, it was possible to draw the following conclusions:

- The soil analysis results indicated that changes of land cover types have a significant effect on the physical properties of the soil. The agriculture areas show lower hydraulic conductivity, higher bulk density and less porosity than under natural vegetation. This could be an indication that the soil in agricultural areas is more compacted due to land use practices.

- The impact of land cover types on the runoff generation was revealed by hydraulic conductivity measurements that show significant differences between different land cover types, especially between agricultural land use and natural vegetation. The consequence of this was shown in the results of runoff prediction. The results revealed that there is a trend in surface runoff rate on different land cover types. The agriculture areas including corn cultivation, mixedcrop and orchard generated high rates of surface runoff than in the natural vegetation areas.

- Precipitation volume and hydraulic conductivity are of major importance for the degree to which land use can influence storm-runoff generation.

- The results of this study show the possibility to link the upstream catchment runoff model (LISEM) with a downstream 1D2D-flood model (SOBEK) for assessing the effects of upstream land use changes on downstream flood characteristics. Two models performed remarkably well when compared with real flood event data.

- The scenario studies revealed that land cover change by which natural vegetation is changed into agricultural land results in increased runoff amounts and peak discharges of river Huai Nam Chun leading to a significant change in flood characteristics in the downstream floodplain by increasing the extent, depth and velocity of the flood water.

- The results of the scenario analysis could be useful for decision making process on catchment and floodplain management for example: soil and water conservation plan, flood control measure and flood defence system focussing on the most flood susceptible areas.

9.2. Recommendations

The study revealed that land cover change influences runoff charateristics that can lead to flood problems in downstream area. The ongoing rapid land use change and expansion of agricultural area in this catchment will have negative effects on the runoff and on soil properties. To attenuate the rapid land use change, a better land management system is required, which can impede the unregulated conversion of forest for agriculture use in the study area. To avoid future flood disasters, flood management and flood mitigation plans are needed to be able to react swiftly to areas threatened by flooding. A monitoring system is required to assess, on a continuous basis, the areas affected by floods and to have emergency measures plan to reduce the damage of exceptional floods.

Land use changes in upstream catchment can increase severe flooding on downstream territory. But, not only flood disaster can occur, also large debris flows can happen and damage settlements. Further investigations should also consider the possibility of debris flow and debris floods in the area.

9.3. Limitations of study

The main limitation of this study was that the available data for applying physically based models. Especially, the rainfall data that was used for the modelling procedures was obtained from only one location in the watershed that can not represent the spatial variability of the rainfall. Rainfall gauges recorded only at an hourly interval. Furthermore, no long records of historical data were available to establish properly the rainstorm return periods. Moreover, model calibration was done based on discharge recorded only at the outlet of the catchment. For proper model calibration, at least 3 sub-cathments are needed that could lead to better estimations of the parameters but the additional discharge data was not available. In addition, in the downstream floodplain, the flood model was calibrated on only the flood depth from interviews that could lead to biasness. More data for calibrating and validating such as flood extent and discharge recorded at the downstream area, result in better model estimations. Finally, there are limitations on modeling in general, since hydrological and hydraulic models have certain degree of uncertainty. This uncertainty is due to insufficient data availability or quality and related space-time heterogeneity, insufficient knowledge on the physics and the stochastic features of the processes involved, in particular during extreme precipitation periods However, due to the large number of parameters and long computing times involved, this procedure is not easily transferable to detailed process.

References

1. Aimrun, W., Amin, M.S.M. and Eltaib, S.M., 2004. Effective porosity of paddy soils as an estimation of its saturated hydraulic conductivity. Geoderma, 121(3-4): 197-203. http://www.sciencedirect.com/science/article/B6V67-4BBVW6B-1/2/3d9d169bcd1e50b69cecd5f347fcb578
2. Alexander, D., 1993. Natural Disasters. UCL Press.
3. Asselman, N.E.M. and Heynert, K., 2003. Consequences of floods: 2D hydraulic simulations for case study area Central Holland, WL/Delft Hydraulics, Delft.
4. Baumhardt, R.L. and Lascano, R.J., 1996. Rain infiltration as affected by wheat residue amount and distribution in ridget tillage. Soil Science Society of America Journal, 60: 1908-1913.
5. Beven, K.J., 2000. Rainfall-runoff modelling: the primer. Wiley&Sons, Chichester, 360 pp.
6. Bin Abdul Rahman, M.Z., 2006. Digital Surface Model (DSM) Construction and Flood Hazard Simulation for Development Plans in Naga City, Philippines, International Institute for Geo-information Science and Earth Observation, Enschede, The Netherlands, 130 pp.
7. Bin Usamah, M., 2005. Modelling Flood Events in the Lower Bicol floodplain, International Institute for Geo-information Science and Earth Observation, Enschede, the Netherland, 127 pp.
8. Bouma, J., 1981. Soil morphology and preferential flow along macropores. Agricultural Water Management, 8: 235-250.
9. Brath, A., Montanari, A. and Moretti, G., 2006. Assessing the effect on flood frequency of land use change via hydrological simulation (with uncertainty). Journal of Hydrology, 324(1-4): 141-153. http://www.sciencedirect.com/science/article/B6V6C-4HHH640-4/2/1a90233fca4a72eece192caeb6481314
10. Brooks, N., 2003. Vulnerability, risk and adaptation: A conceptual framework, Tyndall Centre for Climate Change Research, Norwich.
11. Casale, R. and Margottini, C., 1999. Floods and Landslides: Integrated Risk Assessment. Springer, Berlin, 373 pp.
12. Celik, I., 2005. Land-use effects on organic matter and physical properties of soil in a southern Mediterranean highland of Turkey. Soil and Tillage Research, 83(2): 270-277. http://www.sciencedirect.com/science/article/B6TC6-4DDR7TB-1/2/61a3102d71ef144f721dd9b7afd460a0
13. Cerda, A., 1996. Soil aggregates stability in three Mediterranean environments. Soil Technology, 9: 133-140.
14. Chaplot, V. et al., 2006. Accuracy of interpolation techniques for the derivation of digital elevation models in relation to landform types and data density. Geomorphology, 77: 126-141.
15. Choudhury, N.Y., Paul, A. and Paul, B.K., 2004. Impact of costal embankment on the flash flood in Ban gladesh: a case study. Applied Geography. http://www.sciencedirect.com
16. Chow, V.T., 1959. Open Channel Hydraulics. McGraw-Hill, New York.
17. Chow, V.T., Maidment, D.R. and Mays, L.W., 1988. Applied hydrology. (McGraw-Hill Series in Water Resources and Environmental Engineering). McGraw-Hill, New York etc., 572 pp.
18. Conachy, J. and Divjak, C., 2001. Flood tragedy in Thailand linked to deforestation, The International committee of the Fourth International (ICFI), World socialist website. http://www.wsws.org/articles/2001/sep2001/thai-s04.shtml
19. De Roo, A.P.J., 2000. Applying the LISEM Model for investigating Flood Prevention and Soil Conservation Scenarios in South-Limburg, the Netherlands. In: J. Schmidt (Editor), Soil Erosion: Application of Physically Based Models. Springer, Heidelberge, pp. 318.
20. De Roo, A.P.J. and Jetten, V.G., 1999. Calibrating and validating the LISEM model for two data sets from the Netherlands and South Africa. CATENA, 37(3-4): 477-493. http://www.sciencedirect.com/science/article/B6VCG-3Y51V0X-H/2/c047330928040c19a8cd581e7540192b

21. De Roo, A.P.J., Wesseling, C.G. and Ritsema, C.J., 1996. LISEM: A SINGLE-EVENT PHYSICALLY BASED HYDROLOGICAL AND SOIL EROSION MODEL FOR DRAINAGE BASINS. I: THEORY, INPUT AND OUTPUT. Hydrological Processes, 10(8): 1107-1117. http://dx.doi.org/10.1002/(SICI)1099-1085(199608)10:8<1107::AID-HYP415>3.0.CO;2-4
22. Deng, H., Li, X., Chen, J., Zhang, M. and Wan, H., 2003. Simulation of hydrological response to land cover changes in the Suomo basin. Acta Geographica Sinica, 58(1): 53-62. http://www.sciencedirect.com/science/article/B6WPY-49H71BM-2X4/2/beee22cbfaa7f4c2c53e5dafe60ff397
23. DeRoo, A.P.J., 1996. LISEM: A SINGLE-EVENT, PHYSICALLY BASED HYDROLOGICAL AND SOIL EROSION MODEL FOR DRAINAGE BASINS. II: SENSITIVITY ANALYSIS, VALIDATION AND APPLICATION. Hydrological Processes, 10(8): 1119-1126. http://dx.doi.org/10.1002/(SICI)1099-1085(199608)10:8<1119::AID-HYP416>3.0.CO;2-V
24. Dingman, S.L., 2002. Physical hydrology. Prentice Hall, Upper Saddle River, 646 pp.
25. Dunne, T., 1978. Field studies of hillslope flow processes In: M.J. Kirkby (Editor), Hillslope Hydrology. Wiley, Chichester, pp. 277-293.
26. Edwards, C.A. and Bohlen, P.J., 1996. Biology and Ecology of Earth-worms. Chapman & Hall, London, 426 pp.
27. Elliott, E.T., 1986. Aggregate structure and carbon, nitrogent, and phosphorus in native and cultivated soils. Soil Science Society of America Journal, 50: 627-633.
28. FAO, 2002. Procedures for soil analysis.
29. Faulkner, H., 1990. Vegetation cover density variations and infiltration patterns on piped alkali sodic soils: implications for the modelling of overland flow in semi-arid areas. In: J.B. Thornes (Editor), Vegetation and erosion. Wiley, Chichester, pp. 317-346.
30. Foody, G.M., Ghoneim, E.M. and Arnell, N.W., 2004. Predicting locations sensitive to flash flooding in an arid environment. Journal of Hydrology, 292(1-4): 48-58. http://www.sciencedirect.com/science/article/B6V6C-4C4W52R-1/2/605833b76073b68c8ec2d56fcc4dc110
31. Giertz, S. and Diekkruger, B., 2003. Analysis of the hydrological processes in a small headwater catchment in Benin (West Africa). Physics and Chemistry of the Earth, 28(33-36): 1333-1341. http://www.sciencedirect.com/science/article/B6WPY-4BDM48F-2D0/2/f7f60bfcd1da876e9e317dc1f2bb169e
32. Giertz, S., Junge, B. and Diekkruger, B., 2005. Assessing the effects of land use change on soil physical properties and hydrological processes in the sub-humid tropical environment of West Africa. Physics and Chemistry of the Earth, Parts A/B/C, 30(8-10): 485-496. http://www.sciencedirect.com/science/article/B6X1W-4H3BM0Y-1/2/25d0047ffff3ce8616655bf544445adf
33. Hann, C.T., Johnson, H.P. and Brakensiek, D.L., 1982. Hydrologic modelling of small watersheds, 1. American Society of Agricultural Engineers, Michigan, USA, 533 pp.
34. Hessel, R., 2002. Modelling soil erosion in small catchment on the Chinese Loess Plateau; Applying LISEM to extreme conditions, Utrecht University, Utrecht, 318 pp.
35. Hessel, R., 2005. Effects of grid cell size and time step length on simulation results of the Limburg soil erosion model (LISEM). Hydrological Processes, 19(15): 3037-3049. http://dx.doi.org/10.1002/hyp.5815
36. Hessel, R., Jetten, V., Liu, B., Zhang, Y. and Stolte, J., 2003. Calibration of the LISEM model for a small Loess Plateau catchment. CATENA, 54(1-2): 235-254. http://www.sciencedirect.com/science/article/B6VCG-48SPBWM-1/2/ff6340f370a510d51967db7375eb9c66
37. Hillel, D., 1980. Fundamentals of Soil Physics. Academic Press, New York etc., 413 pp.
38. Holtan, H.N., 1961. A concept for infiltration estimates in watershed engineering. USDA Agricultural Research ServicecPublication: ARS-41-51.
39. Horritt, M.S., Bates, P.D. and Mattinson, M.J., 2006. Effects of mesh resolution and topographic representation in 2D finite volume models of shallow water fluvial flow. Journal

of Hydrology, 329(1-2): 306-314. http://www.sciencedirect.com/science/article/B6V6C-4JMKWTB-6/2/7cb844d6e8e73c5fc2ab3b9127afcd06
40. Jetten, V.G., 2002. LISEM : Limburg Soil Erosion Model User Manual Window version 2.x, Utrecht Center for Environmant and Landscape Dynamics, Utrecht.
41. Jetten, V.G., De Roo, A.P.J. and Favis-Mortlock, D., 1999. Evaluation of field-scale and catchment-scale soil erosion models. Catena, 37: 521-541.
42. Jetten, V.G., De Roo, A.P.J. and Guérif, J., 1998. Sensitivity of the model Lisem to variables related to agriculture. In: J.D.F.-M. Boardman (Editor), Modelling soil erosion by water. Springer, NATO ASI Series I 55 Berlin, pp. 339-349.
43. Juo, A.S.R. and Franzluebbers, K., 2003. Tropical soils: Properties and Management for Sustainable Agriculture. Oxford University Press, Inc., Oxford, 281 pp.
44. Knisel, W.G., 1980. CREAMS: a field scale model for chemicals, runoff and erosion from agricultural management systems, USDA-Conservation Resources Report 26, Washington, DC.
45. Lane, L.J. and Nearing, M.A., 1989. USDA-water erosion prediction project: hillslope profile model document, NSERL report 2 (USDA-ARS), West Lafayette.
46. LDD, 1999. Database structure manual for Land use planning In: L.D.D. Land Use Planning Division (Editor), pp. 72.
47. Li, Y.Y. and Shao, M.A., 2006. Change of soil physical properties under long-term natural vegetation restoration in the Loess Plateau of China. Journal of Arid Environments, 64(1): 77-96. http://www.sciencedirect.com/science/article/B6WH9-4GFV5PC-1/2/21f507f58d0cab135e7fafe6a4ae1c85
48. Maidment, D.R., 1993. Handbook of hydrology. McGraw-hill, Inc, New York, USA, 1424 pp.
49. Maune, D.F., 2001. Digital Elevation Model Technologies and Applications: The DEM Users Manual. The American Society for Photogrammetry and Remote Sensing, Bethesda, Maryland.
50. Morgan, R.P.C., 1995. Soil erosion and conservation. Longman, Harlow, 198 pp.
51. Morgan, R.P.C. et al., 1998a. The European Soil Erosion Model (EUROSEM): a dynamic approach for predicting sediment transport from fields and small catchments. Earth Surface Processes and Landforms, 23(6): 527-544. http://dx.doi.org/10.1002/(SICI)1096-9837(199806)23:6<527::AID-ESP868>3.0.CO;2-5
52. Morgan, R.P.C. et al., 1998b. The European Soil Erosion Model (EUROSEM): documentation and user guide, Cranfield University, Silsoe, Bedford. http://www.silsoe.cranfield.ac.uk/nsri/research/erosion/user_v2.pdf
53. Ndiaye, B., Molenat, J., Hallaire, V., Gascuel, C. and Hamon, Y., 2006. Effects of agricultural practices on hydraulic properties and water movement in soils in Brittany (France). Soil and Tillage Research, In Press. http://www.sciencedirect.com/science/article/B6TC6-4K42DFM-1/2/24a6079306e1f9549eccdffe1248125a
54. Nicholas, A.P. and Mitchell, C.A., 2003. Numerical simulation of overbank processes in topographically complex floodplain environments. Hydrological Processes, 17(4): 727-746. http://dx.doi.org/10.1002/hyp.1162
55. Niehoff, D., Fritsch, U. and Bronstert, A., 2002. Land-use impacts on storm-runoff generation: scenarios of land-use change and simulation of hydrological response in a meso-scale catchment in SW-Germany. Journal of Hydrology, 267(1-2): 80-93. http://www.sciencedirect.com/science/article/B6V6C-46HBKF8-2/2/e7d43db548caa8d7c0ee195052aa4e98
56. O'Donnell, S., 2002. Weather Radar Enhanced Flash Flood Forecasting, Proceedings of Open source GIS − GRASS users conference 2002, Trento, Italy.
57. Pidwirny, M., 2006. Fundamentals of Physical Geography, 2nd Edition. http://www.physicalgeography.net/fundamentals/contents.html
58. Rattan, L., 1990. Soil erosion in the tropics: Principles and management. McGraw-Hill, Inc, New York, USA, 580 pp.
59. Refsgaard, J.C. and Storm, B., 1996. Construction, calibration and validation of hydrological models. In: M.B. Abbott and J.C. Refsgaard (Editors), Distributed Hydrologial Modelling. Kluwer Academic Press, The Netherlands, pp. 41-54.

60. Renard, K.G., Foster, G.R., Weesies, G.A., McCool, D.K. and Yoder, D.C., 2000. Predicting Soil Erosion by Water: A Guide to Conservation Planning with the Revised Universal Soil Loss Equation (RUSLE). The U.S. Department of Agriculture (USDA), Washington, DC, 407 pp.
61. Rientjes, T.H.M., 2004. Inverse modelling of the rainfall-runoff relation : a multi objective model calibration approach. PhD Thesis Thesis, Delft, 371 pp.
62. Rivas, A.A., 2005. Soil hydraulic characterization and hydrologic modelling of sloping agricultural land in Uma Oya watershed, Sri Lanka, AIT, Bangkok, Thailand.
63. Saxton, K.E., 2005. SPAW: Soil-Plant-Atmosphere-Water field & Pond Hydrology The U.S. Department of Agriculture (USDA), Washington,DC.
64. Schwab, G.O., Frevert, R.K., Edminster, T.W. and K.K.Barnes, 1981. Soil and water conservation engineering. Wiley & Sons, New York etc., 525 pp.
65. Siriwardena, L., Finlayson, B.L. and McMahon, T.A., 2006. The impact of land use change on catchment hydrology in large catchments: The Comet River, Central Queensland, Australia. Journal of Hydrology, 326(1-4): 199-214. http://www.sciencedirect.com/science/article/B6V6C-4HTBMC9-3/2/553c96cceb99d06f11062215833e1b15
66. Smith, K., 1996. Environmental Hazards: Assessing Risk and Reducing Disaster, 2nd edition, Routledge, London.
67. Smith, K. and Ward, R., 1998. Floods: Physical Processes and Human Impacts. John Wiley & Sons, Chichester, 382 pp.
68. Solomon, H., 2005. GIS based surface runoff modeling and analysis of contributing factors : a case study of Nam Chun watershed, Thailand, International Institute for Geo-information Science and Earth Observation, Enschede, the Netherland, 99 p. pp. http://www.itc.nl/library/Papers_2005/msc/ereg/harssema.pdf
69. Stolte, J. et al., 2003. Land-use induced spatial heterogeneity of soil hydraulic properties on the Loess Plateau in China. CATENA, 54(1-2): 59-75. http://www.sciencedirect.com/science/article/B6VCG-48S3933-3/2/5e15fc9abb4fcda2089e14617d7283e9
70. Sullivan, P., 2004. Sustainable Soil Management: Soil System Guide http://attra.ncat.org/attra-pub/soilmgmt.html
71. Suwanwerakamtorn, R., 1992. Flood forecasting using a hydrologic model and gis: A case study in Huai Nam Chun catchment, Pa Sak watershed, Phetchabun, Thailand, ITC, Enschede, The Netherlands, 108 pp.
72. Takken, I., Jetten, V., Govers, G., Nachtergaele, J. and Steegen, A., 2001. The effect of tillage-induced roughness on runoff and erosion patterns. Geomorphology, 37(1-2): 1-14. http://www.sciencedirect.com/science/article/B6V93-428DVG5-1/2/99b52c0126f6f17608981c74941933e4
73. Thornes, J.B., 1990. The interaction of erosional and vegetational dynamics in land degradation: spatial outcomes. In: J.B. Thornes (Editor), Vegetation and Erosion Wiley, Chichester, pp. 41-53.
74. Tisdall, J.M. and Oades, J.M., 1982. Organic matter and water stable aggregates in soils. Journal of Soil Science, 33: 141-163.
75. USGS, 2005. Earth's water: Runoff. http://ga.water.usgs.gov/edu/runoff.html
76. Van Asch, T.W.J., 1980. Water erosion on slopes and landsliding in a mediterranean landscape, Utrechtse.
77. Ward, R.C. and Robinson, M., 1990. Principles of hydrology McGraw-Hill, London, 365 pp.
78. Werner, M., 2004. Spatial flood extent modelling: A performance-based comparison, Delft University Delft, 176 pp.
79. Wesseling, C.G., Karssenberg, D., Burrough, P.A. and Van Deursen, W.P.A., 1996. Integrating dynamic evironmental models in GIS: The development of the dynamic modelling language. Transactions in GIS, 1: 40-48.
80. White, M.D. and Greer, K.A., 2006. The effects of watershed urbanization on the stream hydrology and riparian vegetation of Los Penasquitos Creek, California. Landscape and Urban

Planning, 74(2): 125-138. http://www.sciencedirect.com/science/article/B6V91-4F53N6Y-1/2/33ca396f4e0d7bd0cadc490ed3959b86

81. White, R.E., 1997. Principles and practice of soil science : the soil as a natural resouces. Blackwell Science, Oxford, 348 pp.
82. Wilby, R.L., 1997. Contemporary Hydrology. Hydrological Modelling in Practice. John Wiley & Sons Ltd, Chichester, UK, 354 pp.
83. William, A.J., Wilford, R.G. and Walter, H.G., 1991. Soil Physics. John Wiley & Sons, Inc, New York, USA, 328 pp.
84. Wischmeier, W.H., Johnson, C.B. and Cross, B.V., 1971. A soil erodibility nomograph fpr farmland and construction sites. Journal of Soil and Water Conservation, 26: 189-193.
85. Wiskow, E. and van der Ploeg, R.R., 2003. Calculation of drain spacings for optimal rainstorm flood control. Journal of Hydrology, 272(1-4): 163-174. http://www.sciencedirect.com/science/article/B6V6C-46X93NF-1/2/fccde612acd57072e586273c83740056
86. WL-DELFT_HYDRAULIC, 2003. Sobek: Managing your flow.
87. Woolhiser, D.A., Smith, R.E. and D.C., G., 1990. KINEROS: a kinematic runoff and erosion model documentation and user manual, USDA-ARS-77, Washington, DC.
88. Yamamoto, T. and Anderson, W., 1973. Splash erosion related to soil erodibility indices and other forest soil properties in Hawaii. Water Resources Research, 9: 336-345.
89. Zhang, S., Grip, H. and Lovdahl, L., 2006. Effect of soil compaction on hydraulic properties of two loess soils in China. Soil and Tillage Research, 90(1-2): 117-125. http://www.sciencedirect.com/science/article/B6TC6-4H7T0DF-1/2/eef6957528f5657242d87fecfb1bc2e8
90. Ziegler, A.D. et al., 2004. Hydrological consequences of landscape fragmentation in mountainous northern Vietnam: evidence of accelerated overland flow generation. Journal of Hydrology, 287: 124-146.
91. Zimmermann, B., Elsenbeer, H. and De Moraes, J.M., 2006. The influence of land-use changes on soil hydraulic properties: Implications for runoff generation. Forest Ecology and Management, 222(1-3): 29-38. http://www.sciencedirect.com/science/article/B6T6X-4HV74J4-1/2/47e54214d2f8cfa8d8777330d2a84561

Appendices

Appendix 1: Soil physical properties measurement from soil samples collected in field.

UTM-X	UTM-Y	Bulk density (g cm-3)	Field capacity (%)	Porosity (%)	Initial soil moisture (%)	Hydraulic Conductivity (mm/hr)
726412	1856473	1.4680	21.63	51.52	17.56	73.8
726407	1856301	1.1892	34.26	52.62	27.52	7.29
726305	1856126	1.3157	33.84	47.58	30.64	1.22
726194	1856071	1.2526	35.71	50.09	33.22	2.51
725069	1855544	1.3083	32.53	47.88	31.67	0.81
724284	1855431	0.9365	54.86	52.69	38.52	13.82
724184	1855529	1.2222	36.35	51.31	33.98	-
724972	1855519	1.2973	36.72	48.32	36.49	0.84
724796	1855511	1.1090	43.19	45.82	34.15	0.32
728452	1853726	1.1990	32.82	52.23	29.07	30.83
728446	1853630	1.0868	39.56	56.70	31.37	6.48
728448	1853587	1.1613	38.10	53.73	35.53	13.70
728304	1853720	1.2956	33.02	48.38	31.04	0.33
725832	1855546	1.4123	33.19	43.73	33.55	3.76
721118	1855857	1.1628	39.43	53.67	33.91	-
725832	1855489	1.2373	36.85	50.70	27.87	7.92
725836	1855451	1.3296	33.68	47.03	29.57	6.48
719079	1856776	1.4071	31.57	43.94	32.32	1.64
723288	1857219	1.4277	27.75	43.12	27.98	8.10
723049	1857083	1.3362	32.90	46.77	27.99	0.79
718492	1857463	1.3770	32.68	45.14	34.94	0.79
723121	1857218	1.3886	31.62	44.68	32.11	13.63
718562	1857398	1.2935	39.14	48.46	40.15	1.23
724917	1856060	1.2367	40.36	50.73	30.65	14.92
725237	1856354	1.2185	45.27	51.46	38.36	8.20
721242	1855508	1.3174	34.76	47.51	36.79	0.28
725046	1856351	1.3606	35.36	45.79	33.75	0.85
724915	1856471	1.4464	27.46	42.38	22.98	1.56
727404	1855641	1.4620	28.49	41.75	28.73	1.98
722540	1856299	1.2997	36.34	48.22	35.93	5.50
723000	1856465	1.2972	31.62	48.32	31.48	31.44
722973	1856555	1.4222	30.08	43.34	31.08	1.39
727474	1855373	1.3231	32.76	47.29	32.20	9.72
727378	1855491	1.3592	29.00	45.85	27.92	1.13

Appendix 1: Soil physical properties measurement from soil samples collected in field.

UTM-X	UTM-Y	Bulk density (g cm-3)	Field capacity (%)	Porosity (%)	Initial soil moisture (%)	Hydraulic Conductivity (mm/hr)
721270	1855332	1.2857	41.29	48.78	42.90	7.76
721279	1855351	1.2831	40.38	48.88	40.92	0.46
721178	1855308	1.1597	42.56	53.80	39.64	20.30
726644	1855424	1.1352	40.65	44.77	31.53	0.96
722163	1855337	1.1367	41.57	54.71	31.48	-
722252	1855331	1.4121	30.08	43.74	28.60	51.25
719921	1855217	1.3386	37.32	46.67	37.38	19.19
722287	1852841	1.5043	26.95	40.07	27.61	27.75
722078	1852676	1.3536	33.24	46.07	33.68	0.38
722215	1852527	1.0581	48.94	47.84	39.61	1.76
721986	1852784	1.0985	53.98	56.24	37.49	6.34
721576	1853165	1.1580	44.18	43.86	40.51	0.86
726851	1855055	1.2622	35.98	49.71	32.09	19.80
726824	1855125	1.2349	37.35	50.80	35.70	1.42
726349	1855651	1.1939	39.92	52.43	33.75	7.93
718088	1857665	1.3454	39.19	46.40	38.04	1.23
718072	1857703	1.2199	43.33	41.40	41.23	0.60
722735	1853344	1.2022	40.12	52.10	32.14	47.98
722827	1853338	1.1312	45.34	54.93	36.36	9.80
727375	1855400	1.2973	34.67	48.32	31.65	-
720770	1855608	1.1177	45.04	55.47	33.47	-
727197	1855114	1.3286	34.19	47.07	28.51	-
722079	1855405	1.3131	29.17	47.69	28.05	-
726823	1855290	1.2423	32.09	50.51	27.06	-
726301	1855547	1.2408	30.88	50.57	27.21	-

Appendix 2: Geopedologic map used in LISEM model.

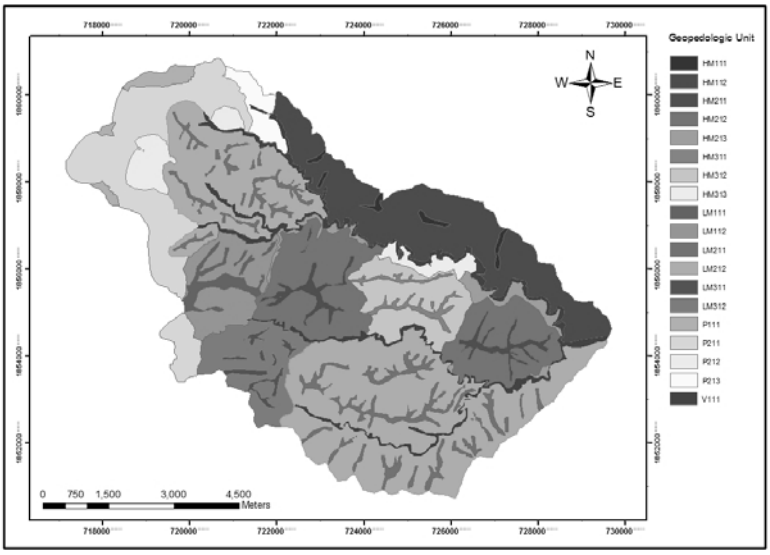

Appendix 3: Land cover map used in LISEM model.

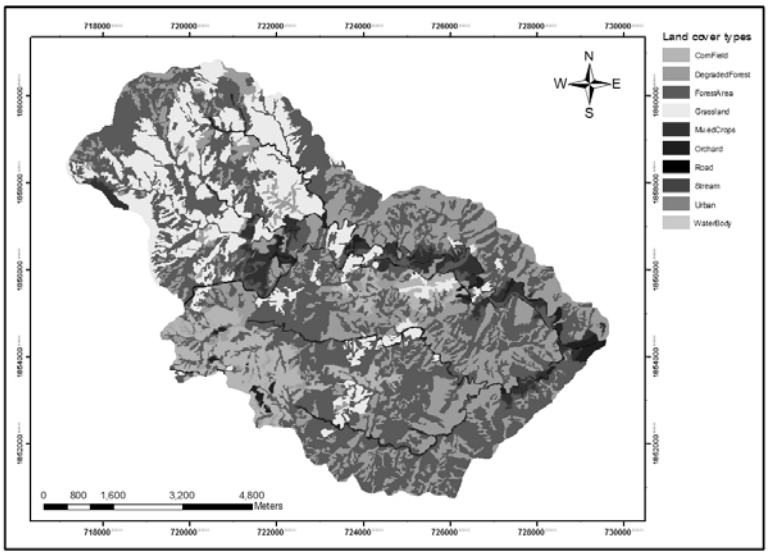

Appendix 4: PCRaster script for the generation of a LISEM input database (Jetten, 2002).

```
# PCRASTER script for the generation of a LISEM input database

binding
####################
### INPUT MAPS   ###
####################
# digital elevation model, area must be <= mask
   Dem = $NUTSHELLIN\dem.map;
# field id's
  fields = $NUTSHELLIN\landuse.map;
# texture/soil map
  texture = $NUTSHELLIN\soil.map;
# mask for channel maps
  chanmask = $NUTSHELLIN\chanmask.map;
#ksat unit map
   ks = $NUTSHELLIN\unit.map;
   lutbl = lusedata.tbl;
   lus = soildata.tbl;
   kstbl = ksat.tbl;
#######################
###INPUT CONSTANTS ###
#######################
 Soildepth = 1000;
 Chanman = 0.05; #pest runs
 Chanside = 0;
 Chanksat = 0.001; #pest runs
####################
### OUTPUT MAPS   ###
####################
# basic topography related maps
  Ldd = $NUTSHELLOUT\ldd.map;         # Local Drain Direction
  area = $NUTSHELLOUT\area.map;       # reference map for Lisem
  grad = $NUTSHELLOUT\grad.map;       # max slope
  id = $NUTSHELLOUT\id.map;           # pluviograph influence zones
  outlet = $NUTSHELLOUT\outlet.map;   # location outlets and checkpoints
# impermeable roads
  roadwidth = $NUTSHELLOUT\roadwidt.map;


# crop maps
  coverc=$NUTSHELLOUT\per.map;
  lai=$NUTSHELLOUT\lai.map;
  cropheight=$NUTSHELLOUT\ch.map;
```

```
# soil maps
  ksat=$NUTSHELLOUT\ksat1.map;
  psi=$NUTSHELLOUT\psi1.map;
  pore=$NUTSHELLOUT\thetas1.map;
  thetai=$NUTSHELLOUT\thetai1.map;
  soildep=$NUTSHELLOUT\soildep1.map;
# surface maps
  rr=$NUTSHELLOUT\rr.map;
  mann=$NUTSHELLOUT\n.map;
# channel maps
  lddchan = $NUTSHELLOUT\lddchan.map;
  chanwidth = $NUTSHELLOUT\chanwidt.map;
  changrad = $NUTSHELLOUT\changrad.map;
  chanman = $NUTSHELLOUT\chanman.map;
  chanside =$NUTSHELLOUT\chanside.map;
  chanksat = $NUTSHELLOUT\chanksat.map;

  clone=mask.map;

Areamap
# MASK
   Dem;
initial
#######################
### BASE MAPS     ###
#######################
mask=scalar(clone);

# correct topo for local depressions
   report Ldd = lddcreate(Dem*mask,1e20,1e20,1e20,1e20);
   report outlet = pit(Ldd);

# reference catchment boundaries, based on watershed from outlet
  report area = catchment(Ldd, outlet);

# sine gradient (-), make sure slope > 0.001
  report grad = max(sin(atan(slope(Dem*mask))),0.001);

########################################
### MAPS WITH RAINFALL INFLUENCE ZONE #
########################################
   report id = nominal(scalar(area));
#######################
### CROP MAPS      ###
#######################
# fraction soil cover (including residue)
```

```
  report coverc = lookupscalar(lutbl, 7, fields);
# crop height (m)
  report cropheight = lookupscalar(lutbl, 9, fields)* mask;
# LAI (m2/m2)
  report lai = ln(1-coverc)/-0.4;

################################################################
### INFILTRATION MAPS for option one layer GREEN & AMPT ###
################################################################
  report ksat = lookupscalar(kstbl, 1, ks)* mask;
  report pore = lookupscalar(kstbl, 3, ks)* mask;
  report psi =  lookupscalar(lus, 1, texture)* mask;
  report thetai = lookupscalar(kstbl, 2, ks)* mask;
  report soildep = scalar(Soildepth);

###############################
### SOIL SURFACE MAPS     ###
###############################
# micro relief, random roughness (=std dev in cm)
  report rr = lookupscalar(lutbl, 6, fields);
# Manning's n (-)
  report mann = lookupscalar(lutbl, 8, fields);

######################
### CHANNEL MAPS   ###
######################
 chanmask = chanmask/chanmask;
 report lddchan=lddcreate(Dem*chanmask,1e20,1e20,1e20,1e20);
 report changrad=max(0.001,sin(atan(slope(chanmask*windowaverage(Dem,3*celllength())))));
 report chancoh=chanmask*scalar(Chancoh);
 report chanman=chanmask*scalar(Chanman);
 report chanside=chanmask*scalar(Chanside);
 report chanwidth=max(3,chanmask*accuflux(Ldd,3.5)/10000);
 report chanksat=chanmask*scalar(Chanksat);
```

Appendix 5: Showing the Gumbel plot for Lom Sak station.